



INGENIERÍA QUÍMICA
UNIVERSIDAD DE VALLADOLID

PROYECTO FIN DE CARRERA

FOTOCATÁLISIS HETEROGÉNEA DE COLORANTES
DIRECTOS AZOICOS HIDROLIZADOS Y EFLUENTES
TEXTILES SIMULADOS SOBRE NANOPARTÍCULAS
INMOVILIZADAS DE TiO₂

LAURA DÍEZ MARTÍN
JULIO, 2012

INGENIERÍA QUÍMICA
UNIVERSIDAD DE VALLADOLID

PROYECTO FIN DE CARRERA

**TÍTULO: HETEROGENEOUS PHOTOCATALYSIS OF HYDROLYSED
DIRECT AZO DYES AND SIMULATED DYEHOUSE EFFLUENTS
ON IMMOBILIZED TiO₂ NANOPARTICLES**

ALUMNO: LAURA DíEZ MARTIN

FECHA: JULIO 2012

**CENTRO: ECOLE NATIONALE SUPERIEURE DES INDUSTRIES
CHIMIQUES (ENSIC, NANCY, FRANCIA)**

TUTOR: MARIE-NOËLLE PONS

CALIFICACIÓN LOCAL: _____

CALIFICACIÓN UVa: _____

Valladolid, 13 de julio de 2012
Coordinador Sócrates

Fdo.: Rafael Mato Chaín



Universidad de Valladolid

HETEROGENOUS PHOTOCATALYSIS OF HYDROLYSED DIRECT AZO DYES AND SIMULATED DYEHOUSE EFFLUENTS ON IMMOBILIZED TiO₂ NANOPARTICLES

July 17, 2012

By: Laura Díez Martín

Advisor at University of Valladolid: Professor Rafael Mato Chaín

Advisor at ENSIC Group of Nancy: Dr. Marie-Noëlle Pons

This report represents the final project of a student at University of Valladolid to finish Chemical Engineering studies. The work included in this report was carried out at ENSIC Group (National Polytechnical Institute of Lorraine) in Nancy (France).

FINAL PROJECT | Chemical Engineering

AUTHOR: LAURA DÍEZ MARTÍN

TITLE: HETEROGENEOUS PHOTOCATALYSIS OF HYDROLYSED DIRECT AZO DYES AND SIMULATED DYEHOUSE EFFLUENTS ON IMMOBILIZED TiO₂ NANOPARTICLES

ADVISOR (France): MARIE-NOËLLE PONS

ADVISOR (Spain): RAFAEL MATO CHAÍN

Project carried out in: ECOLE NATIONALE SUPERIEURE DES INDUSTRIES CHIMIQUES (Nancy, France)

Laboratory of research: LRGP – Sols et eaux, ENSIC – INPL

Period of performance: February 2012 – July 2012

JURORS (ENSIC-INPL):

Dr. MARIE-NOËLLE PONS

Dr. ORFAN ZAHRAA

Prof. SERGE CORBEL

Acknowledgments

I would like to thank very much to Marie-Noëlle Pons, Director of Research of CNRS, for giving me the unique opportunity to work on an innovative and interesting project such as photocatalysis and offering me guidance and advice during its development. Thank you to Steve Pontvianne for his assistance at laboratory. In addition, I would like to thank the WPI students, Rebecca and Jesse, for their first introduction to the subject. Finally I would like to express my heartfelt thanks to my parents for their support and confidence.

*“Reserve your right to think, for even to think
wrongly is better than not to think at all”*

Hypatia of Alexandria (355? – 415?),

Female, Mathematician, Astronomer and Philosopher.

INDEX

	<u>Pages</u>
Index	1
List of Figures, Tables and Equations	3
Abstract	5
CHAPTER 1: LITERATURE REVIEW	6
1.1. Sustainable development	6
1.1.1. Green chemistry	6
1.2. Concerns of water pollution	7
1.3. Legislation and characteristics of industrial wastewater	7
1.4. Technologies for industrial wastewater treatment	9
1.5. Environment and textile industry	11
1.5.1. Textile production process	11
1.5.2. Textile industry and environmental pollution	12
1.6. Textile wastewater	14
1.6.1. Characterization of industrial wastewater from textile industries	14
1.6.2. Need to treat textile wastewaters	14
1.6.3. Technologies for textile wastewater treatment	15
CHAPTER 2: BACKGROUND	17
2.1. Dyes	17
2.1.1. Azo dyes	19
2.1.2. Direct dyes	21
2.2. Titanium dioxide	22
2.3. Photocatalytic treatment	26
2.3.1. Historical perspective of catalysis	26
2.3.2. Introduction to the photochemistry	27
2.3.3. Advanced Oxidation Processes (AOPs)	29
2.3.3.1. Heterogeneous photocatalysis	34
CHAPTER 3: OBJECTIVES AND JUSTIFICATION	47

CHAPTER 4: MATERIALS AND METHODS	49
4.1. Materials	49
4.1.1. Titanium dioxide	49
4.1.2. Dyes	49
4.2. Methods	53
4.2.1. pH	53
4.2.2. UV-Visible Spectrophotometry	54
4.2.3. Ammonium	56
4.2.4. Total Organic Carbon (TOC)	58
4.2.5. Ion Chromatography for nitrates	60
4.2.6. Toxicity study	61
CHAPTER 5: INSTALLATION	68
CHAPTER 6: RESULTS AND DISCUSSIONS	70
6.1. Applied method	70
6.2. Spectrophotometry	72
6.3. Total Organic Carbon	78
6.4. Ammonium and nitrates	79
6.5. Toxicity	81
CHAPTER 7: CONCLUSIONS AND PERSPECTIVES	89
References	91
ANNEXES	
Annex I: Chemical Information about studied Direct Azo Dyes	95
Annex II: Calibration curves	97
Annex III: Summary table about studied experiences	101
Annex IV: Dye spectra	102
Annex V: Kinetic results	134
Annex VI: COT results	135
Annex VII: Ammonium and nitrates results	136
Annex VIII: Toxicity test data	137
Annex IX: Toxicity test results	139

Tables, Figures and Equations

List of Figures

Figure 1.1. Flow chart of a textile industry process	11
Figure 1.2. Pollution loads of textile wet operations.	13
Figure 2.1 .Wavelength absorbed versus colour in organic dyes.	17
Figure 2.2. Importance of a chromophore group in a conjugated system.	18
Figure 2.3 . Azo dye general structure.	19
Figure 2.4. Scheme of reduction reaction for azo dyes.	20
Figure 2.5. Crystal structure of anatase and rutile.	22
Figure 2.6 . Electromagnetic spectrum.	28
Figure 2.7. Classification of Advanced Oxidation Processes.	30
Figure 2.8. Range of application of AOPs and other treatments.	33
Figure 2.9. Bandgap for metals, semiconductors and insulators.	36
Figure 2.10. Energetic diagram of a semiconductor during photoexcitation process.	36
Figure 2.11. Global reaction in heterogeneous photocatalysis.	37
Figure 2.12 . Scheme of heterogeneous photocatalytic process.	37
Figure 2.13 .Photocatalytic reaction on TiO ₂ surface.	40
Figure 2.14. Sketch of a photocatalytic process.	41
Figure 4.1 . Amide functional group.	50
Figure 4.2. Basic hydrolysis of amides.	51
Figure 4.3.Spectrophotometer SECOMAM Anth�lie Light.	55
Figure 4.4. Spectrophotometer HACH DR 2400.	57
Figure 4.5. Calibration curve for ammonium.	57
Figure 4.6. TOC Analyzer Apollo 9000.	59
Figure 4.7. Morphology of seed and lettuce seedling.	62
Figure 5.1. Experimental installation of photocatalysis.	68
Figure 5.2. Flow diagram of photocatalytic reactor.	69
Figure 6.1 . Graph for calibrated of DV51.	70
Figure 6.2 . Calibration curve for Direct Violet 51.	71
Figure 6.3. Samples for Direct Red 23.	72
Figure 6.4. Photocatalytic decolorisation of DY50 solutions.	73
Figure 6.5. Photocatalytic decolorisation of DR81 solutions.	73
Figure 6.6. Photocatalytic decolorisation of DV51 solutions.	74
Figure 6.7. Photocatalytic decolorisation of DR23 solutions.	74
Figure 6.8. Decolorisation comparison for dye solutions.	76
Figure 6.9. Apparent rate constants for dye solutions.	77
Figure 6.10. Percentage of TOC removal for studied experiences.	79
Figure 6.11 .Comparison for ions of dye solutions.	80
Figure 6.12 . Some samples for toxicity test.	81
Figure 6.13 . Absolute germination of dye solutions.	82

Figure 6.14. Average seed length of dye solutions.	83
Figure 6.15 . Relative toxicity of dye solutions.	83
Figure 6.16. Toxicity removal of dye solutions.	84
Figure 6.17. Germination Index of dye solutions.	85
Figure 6.18. Samples of DR23 for comparison toxicity test.	87
Figure 6.19. Comparison of germination for neutral dyes.	87
Figure 6.20. Comparison of seed length for neutral dyes.	88

List of Tables

Table 1.1. Green chemistry principles.	6
Table 1.2. Limit values of discharge for industrial wastewater.	8
Table 1.3. Conventional techniques for wastewater treatment.	9
Table 1.4. Industrial sources of water pollution.	12
Table 1.5. Comparison of technologies to remove VOCs from water.	16
Table 2.1. Mainly chromophore and auxochrome groups.	18
Table 2.2. Typical physical and mechanical properties of TiO ₂ .	23
Table 2.3 . Optical properties of TiO ₂ .	24
Table 2.4.. Nobel Prizes in Catalysis or related topics.	26
Table 2.5 . Oxidation potentials for several oxidizing substances.	31
Table 2.6. Main advantages and disadvantages of photocatalytic processes.	35
Table 2.7. Semiconductors used as catalysts in photocatalytic processes.	39
Table 4.1 . Properties of MPC500 TiO ₂ nanopowder.	49
Table 4.2. Amount of nitrate that would causes health problems.	60
Table 4.3 . Plants used in germination tests.	66
Table 4.4. Characteristics and observations of plant seeds.	67
Table 6.1. Apparent constant rates and structural characteristics of neutral dyes.	75
Table 6.2. k_{app} and structural characteristics of hydrolysed dyes at pH=6.	77

List of Equations

Equation 2.1. Planck's law.	29
Equation 2.2 .Apparent rate constant.	43
Equation 2.3.Degradation rate.	43
Equation2.4 . Integrated rate equation.	43
Equation 4.1. Lambert- Beer Law.	54
Equation 4.2. Relative toxicity.	64
Equation 4.3 . Toxicity removal.	64
Equation 4.4. Germination Index.	65
Equation 6.1. Percentage of colour removal.	72

ABSTRACT

In our society, many industrial processes generate contaminated effluents which have to be treated due to their health and environmental effects.

In the case of textile wastewater, conventional physical and chemical technologies are insufficient to reach total degradation of polluted substances that contain. For this reason, the search of alternative treatments is necessary.

Heterogeneous photocatalysis is an emergent technique for air and water purifying. This technology is one of the most interesting for industrial applications, with respect to minimization of energy consumption, increasing efficiency and reducing pollution. The photocatalytic process allows the degradation of organic pollutants into CO₂ and H₂O by oxidation with hydroxyl radicals. The technique is based in the UV- visible irradiation of the pollutant substance in presence of an appropriate catalyst.

Photocatalysis is probably one of the fields with a clearly evolution in the last 30 years, mainly due to the recent developments in light technologies and materials science. In most cases, these incredible scientific and technological advances have not still be put into operation because of the high costs and the skepticism created by a new not clear technology. Currently, there is a great difficulty in understanding how the light acts like a reactant in the chemical structure of substances participants in the process.

Industrial textile wastewaters contain dyes that is require remove. In this research work, the process of heterogeneous photocatalysis with immobilized TiO₂ as photocatalyst was applied to treat four types of direct azo dyes in neutral and hydrolysed solutions and their simulated dyehouse effluents. In order to study degradation of dyes, UV-Vis spectrophotometry was used. Also, analysis of total organic carbon, ammonium and nitrate ions and toxicity were made to ensure the effectiveness of the process.

CHAPTER 1: LITERATURE REVIEW

1.1. Sustainable development

In recent years perception of a sustainable society has increased. The aim of sustainable development is to prevent or minimize pollution in industry, emerging the concept of “Green chemistry”.

1.1.1. Green chemistry

Green chemistry is based on the application of chemical engineering for sustainable development, through design, production and application of chemical processes to reduce pollution.

Referring to the issue addressed by this project, the twelve green chemistry principles are cited:

Green chemistry principle	Meaning
Prevention	It is better preventing the generation of a residue that cleaning it when it has been formed.
Atom economy	Synthesis methods must be designed to minimize generation of byproducts.
Using methodologies that generate products with reduced toxicity	If it is possible, synthesis methods must be designed to use and generate substances with low or not toxicity.
Generation of effective and not toxic products	Chemical products must be created to maintain its efficacy while its toxicity is reduced.
Reducing the use of auxiliary substances	The use of not essential substances will be avoided.
Reduce energy consumption	Methods at ambient temperature and pressure will be chosen if it is possible.
Use of renewable raw materials	The raw material has to be renewable, if it is technically and economically viable.
Avoid unnecessary derivatisation	The formation of derivative products will be avoided.
Enhancement of catalysis	Catalysts (as selective and reusable as possible) will be employed, rather than reagents.
Generation of biodegradable products	Chemicals will be designed to not persist in the environment.
Development of analytical methodologies for real-time monitoring	Analytical methodologies will be developed after process monitoring.
Minimization of chemical accidents	The substances used in process, will be selected to minimize the risk of chemical accidents.

Table 1.1. Green chemistry principles (Source: Anastas, 1998).

1.2. Concerns of water pollution

Nowadays, human activity and unbalanced development of society are the causes of water pollution. Practically, there is not any human activity that does not generate wastes, and the volume of them grows exponentially with the industrialization level of a country.

The aim to achieve a sustainable growth in water use has led to treat problems related with biological pollution, levels of heavy metals, intensive use of nutrients and organic pollutants, etc. Some of tools used to try solve these problems are water disinfection, wastewater treatment before discharge into water supplies, limitation and replacement of nitrates and phosphates in products with a massive use, and developments in analytical chemistry and ecotoxicology.

Although discharges from industry and agriculture are the main problem of water pollution, population also has a decisive role in this environmental pollution.

From the environmental point of view, besides toxic and dangerous wastes, non-biodegradable wastes are the most worrying because when they do not receive a specific treatment for destruction or inerting, they can affect the environment.

A large quantity of this type of wastes are generated in aqueous solution. The most commonly used biological treatment processes have no action on them. So if there is no additional treatment, these wastes are discharged in the environment in most cases.

1.3. Legislation and characteristics of industrial wastewater

Industrial effluents often contain substances that are not removed by conventional treatments due to their high concentrations or their chemical nature. Many organic and inorganic compounds that have been identified in industrial wastewater are subject to a special regulation owing to their toxicity or their biological effects at long term.

The control of water pollution caused by industrial activities began with the approval of "Federal Water Pollution Control Act" by United States Congress in 1972. USA legislation was completed with the "Clean Water Act" and "Water Quality Act" laws, which were adopted in 1977 and 1978 respectively (EPA, 1972).

In Europe, after the enactment of the 16/2002 Law of prevention and integrated pollution control, the pursued objectives have been to reduce the discharge of some specific pollutants and to use advanced systems of water treatment.

According to the mentioned 16/2002 Law, the main pollutants with an emission limit value into water are:

- Organo-halogenated substances and substances that may generate them in the aquatic environment.
- Substances with carcinogenic or mutagenic properties affecting reproduction in the aquatic environment.
- Persistent hydrocarbons and bioaccumulative toxic organic compounds.
- Cyanides.
- Biocides and pesticides.
- Substances which have an unfavorable influence on the oxygen balance.

These pollutants come from diverse industries and by their nature, concentration or effluent flow, and the wastewater containing them should be treated before discharge or reuse.

Table 1.2 contains limit values of discharge for industrial wastewater.

Parameter	Limit value
Temperature	40 °C
pH	6 – 10
COD	1500 mg/l
Conductivity at 20 °C	6000 µS/cm
Nitrates	500 mg/l
Ammonium	50 mg/l
Sulphates	1000 mg/l
Phenols	2 mg/l
Inhibition substances	25 equitox/m ³

Table 1.2. Limit values of discharge for industrial wastewater (Source: Ruza, 2007).

1.4. Technologies for industrial wastewater treatment

The objective of wastewater treatment is to remove pollutants present in an effluent in order to ensure certain specifications of discharge determined by a competent administration.

The first step to study the appropriate treatments that can be used to treat an effluent, is its characterization. It will be also needed information on its flow rate and its possible fluctuations.

The problems of wastewater treatment can be solved in several ways:

- Recycling water after removing of pollutants from the effluent.
- Exchanging wastes between industries. The waste of an industry sometimes may be a raw material in another process.
- Minimizing effluents through changes in product specifications or production process which generate less polluting effluents.
- Doing an individual treatment of special effluents.

The processes and technologies that are available for treatment of wastewater pollutants are very different. Currently, the treatment techniques most frequently used can be divided into three groups: physical, chemical and biological treatments.

The most common conventional technologies are listed in the table 1.3:

Physical Treatments	Chemical Treatments	Biological Treatments
Air stripping	Chemical stabilization	Activated sludge
Activated carbon adsorption	Catalysis	Aerated lagoons
Centrifugation	Chlor-alkali electrolysis	Anaerobic digestion
Steam stripping	Hydrolysis	Stabilization pond
Liquid-liquid extraction	Electrolysis	Trickling filters
Distillation	Oxidation	Enzymatic treatment
Electrodialysis	Ozonolysis	Composting
Filtration	Photolysis	
Evaporation	Microwave discharge	
Flotation	Neutralization	
Flocculation	Precipitation	
Ion exchange	Reduction	
Crystallization		
Reverse osmosis		
Sedimentation		
Ultrafiltration		

Table 1.3. Conventional techniques for wastewater treatment (Source: Hagen,1999).

Technologies for wastewater treatment are divided into the following broad groups:

- Natural treatments

These systems of treatment are not usually employed for industrial wastewater treatment because they require very specific pollution conditions. Examples of this type of treatment are aerated lagoons and green filters.

- Primary treatments

Their aim is to separation by physical means the particles from the water to be treated.

- Secondary treatments

They are biological processes used to degrade biodegradable organic matter. There are two main groups: aerobic and anaerobic processes.

- Tertiary treatments

Traditionally, tertiary processes were used to remove pollutants from water that had not been eliminated in previous treatments.

Presently these processes are used for treatment of effluents with very specific pollutants and occasionally it is the only treatment used.

Tertiary treatment includes processes such as adsorption, ion exchange, electro dialysis, ultrafiltration, membrane processes, stripping, disinfection, conventional oxidation processes and advanced oxidation processes.

For municipal wastewater treatment, pollution is greatly reduced with primary and secondary treatments, but tertiary treatments are also used to comply current regulations and to achieve a higher reclaimed water quality.

Many treatment technologies transfer toxic compounds from one medium to another, which is not be a good solution on the long term.

The aim of this project is focused on the use of a technology currently under development called "heterogeneous photocatalysis" which is included in advanced oxidation processes. Advanced oxidation processes may constitute in a nearby future one of the main technological resources used for the treatment of effluents contaminated with organic products, which are

not treatable by conventional techniques due to their high chemical stability and / or low biodegradability.

1.5. Environment and textile industry

Textile industry has had major environmental problems related mainly with water management. The environmental impact of liquid effluents is diverse due to the large variety of raw materials, reagents and methods of production.

1.5.1. Textile production process

It is necessary to know the processes which are involved in textile industry in order to understand problems about its effluent production.

The main stages in the processing of natural fibres (wool and cotton) appear in figure 1.1:

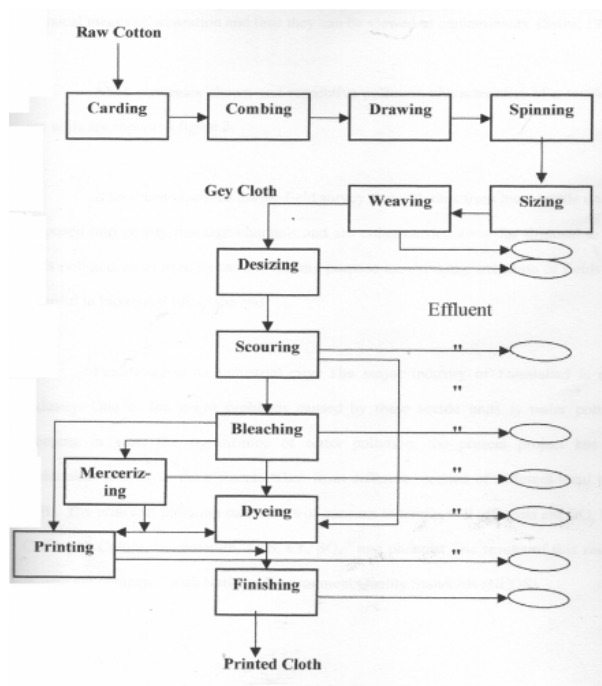


Figure 1.1. Flow chart of a textile industry process (Source: "Ullmann's Encyclopedia of Industrial Chemistry").

1.5.2. Textile industry and environmental pollution

Colored wastewater affects environment and human health if directly discharge without treatment.

Wastewater discharged from textile industry is characterised by high chemical demand (COD), low biodegradability, high salt content and is the source aesthetic pollution related to colour. Moreover, the heavy metals and salts from highly coloured wastewater are toxic to aquatic life. Also, it is noteworthy that dyes formula contain numerous auxiliary toxic compounds (Mantzavinos and Psillakis, 2004).

Serious health problems such as cancer can be caused by azo dyes and products of their degradation like aromatic amines, because there are carcinogenic. In order to achieve sustainable development, the treatment of dye before its discharge is important.

According to the report of Japan Consulting Institute (1994), textile industry is the fifth major industry that become source of environmental problem as it can be seen in table 1.4. However, textile industry is the largest industry discharging colouring effluent.

TYPE OF INDUSTRY	PERCENTAGE OF WATER POLLUTION
Food and beverage	40,5
Rubber and product	14,1
Chemical	11,8
Palm oil	11,6
Textile and leather	9,0
Raw natural rubber	8,6
Paper	4,4

Table 1.4. Industrial sources of water pollution (Source: Environmental Quality Report, 2004).

In figure 1.4. typical pollution loads of different production processes in textile industries are mentioned:

Fibre	Process	pH	BOD (mg/l)	S (mg/l)	Water use (l/kg)
Cotton	Desizing	–	1700–5200	16 000–32 000	3–9
	Scouring or kiering	10–13	50–2900	7600–17 400	26–43
	Bleaching	8.5–9.6	90–1700	2300–14 400	3 124
	Mercerising	5.5–9.5	45–65	600–1900	232–308
	Dyeing	5–10	11–1800	500–14 100	8–300
Wool	Scouring	9–14	30 000–40 000	1129–64 448	46–100
	Dyeing	4.8–8	380–2200	3855–8315	16–22
	Washing	7.3–10.3	4000–11 455	4830–19 267	334–835
	Neutralisation	1.9–9	28	1241–4830	104–131
	Bleaching	6	390	908	3–22
Nylon	Scouring	10.4	1360	1882	50 67
	Dyeing	8.4	368	641	17–33
	Scouring	9.7	2190	1874	50–67
Acrylic	Dyeing	1.5–3.7	175–2000	833–1968	17–33
	Final scour	7.1	668	1191	67–83
	Scouring	–	500–800	–	25–42
Polyester	Dyeing	–	480–27 000	–	17–33
	Final scour	–	650	–	17–33
Viscose	Scouring and Dyeing	8.5	2832	3334	17 33
	Salt bath	6.8	58	4890	4–13
Acetate	Scouring and Dyeing	9.3	2000	1778	33–50

Figure 1.2. Pollution loads of textile wet operations (Source: Cooper, 1978).

To reduce water pollution caused by textile industry, a study must be done to treat the textile effluent efficiently.

1.6. Textile wastewater

The need to manage rationally the limited water resources and environmental aggression that involves polluted waters, has given rise to more restrictive environmental laws. This fact has forced the research and development of technologies for wastewater treatment in industrial applications.

1.6.1. Characterization of industrial wastewater from textile industries

Daily, textile industries consume large amounts of water in most of their processes. The effluents generated are generally characterized by high chemical oxygen demand (COD), high temperature, unstable pH, suspended solids and chloro organic compounds. In addition, as it was explained above, these effluents are a source of pollution owing their colour.

The significant characteristic of textile effluents is their strong colour due to residual dyes. It is estimated that around 15% of the total amount of dyes is lost during synthesis and processing. Dyes concentration in wastewater is usually lower than any other chemicals, but due to their strong color they are visible even at very low concentrations, thus causing serious aesthetic and pollution problems in wastewater disposal (Zollinger, 1991).

1.6.2. Need to treat textile wastewaters

Hazards that may be due to the uncontrolled discharge of textile effluents, are:

Medium-term dangers:

- Color, turbidity and odor

The accumulation of organic matter in textile effluents provokes bacteria proliferation, foul odor generation and abnormal coloration.

- Eutrophication

Under the action of microorganisms, the dyes release nitrates and phosphates into the environment. A high amount of these ions can be toxic to aquatic life. The

consumption of these nutrients by aquatic plants increases their proliferation generating a decrease of oxygen by inhibition of photosynthesis at the deeper strata.

- Low oxygenation

When significant loads of organic matter are provided to the environment, natural processes of regulation cannot compensate the bacterial consumption of oxygen.

Long-term dangers:

- Bio - accumulation of non-biodegradable pollutants

Organic dyes are compounds impossible to treat by natural biological degradation (Pagga et Brown, 1986).

- Cancer

Some amines present or generated by reduction of azo dyes are carcinogenic.

1.6.3. Technologies for textile wastewater treatment

The treatment of textile wastewater is important due to the effects that cause in environment and human health.

Table 1.5 shows several methods of wastewater treatment from textile industry including physical, chemical, biological and emerging technologies.

Heterogeneous photocatalysis has been used only in limited applications to treat hazardous wastes. This technology presents higher capital costs than conventional air stripping or adsorption systems. However, its operating costs are lower than conventional treatment systems.

Technology	Advantages	Disadvantages
Heterogeneous photocatalysis	No air emissions, effective at all concentrations, VOCs destroyed, readily available.	High energy consumption, process mechanisms not well understood.
Air stripping	Effective at high energy concentrations; mechanically simple; relatively inexpensive.	Inefficient at low concentrations; VOCs discharged into air.
Steam stripping	Effective at all concentrations.	VOCs discharged into air; high energy consumption.
Air stripping with carbon adsorption of vapors	Effective at high concentrations.	Inefficient at low concentrations; requires disposal or regeneration of spent carbon.
Carbon adsorption	Low air emissions; effective high concentrations.	Inefficient at low concentration; requires spent carbon disposal or regeneration; relatively expensive.
Biological treatment	Low air emissions, relatively inexpensive.	Inefficient at high concentrations, slow rates of removal, sludge treatment and disposal required.

Table 1.5. Comparison of technologies to remove VOCs from water.

Biological treatments are the most used to treat liquid effluents from textile industry because they have a low cost. These are based on aerobic treatments that can be combined by one or more treatment steps (sieving, sedimentation, coagulation or other advanced physicochemical treatment).

Most of the organic matter of these effluents is not biodegradable and / or toxic, so the only application of biological treatment is inefficient.

Accordingly, the use of Advanced Oxidation Process as exclusive treatments or as pre or post biological treatment, may be a viable alternative for removing organic matter from textile effluents.

CHAPTER 2: BACKGROUND

2.1. Dyes

All aromatic compounds absorb electromagnetic energy but only those that absorb light with wavelengths in the visible range (350 – 700 nm) are coloured.

The explanation of the relationship between structure and colour depends on the basic atomic structure of the aryl ring, and the shared or delocalised electrons that this atomic arrangement has. The ability to absorb radiation is inherent in this structure.

Figure 2.1 shows the relationship between wavelength of visible and colour absorbed/observed.

Wavelength Absorbed (nm)	Colour Absorbed	Colour Observed
400–435	Violet	Yellow-Green
435–480	Blue	Yellow
480–490	Green-Blue	Orange
490–500	Blue-Green	Red
500–560	Green	Purple
560–580	Yellow-Green	Violet
580–595	Yellow	Blue
595–605	Orange	Green-Blue
605–700	Red	Blue-Green

Figure 2.1 .Wavelength absorbed versus colour in organic dye.

Dyes contain chromophore and auxochrome groups. Chromophores, which have delocalized electron systems with conjugated double bonds, are responsible of colour. Auxochromes are electron-donating substituents that cause or intensify the color of the chromophore by altering the overall energy of the electron system.

In the table 2.1, it is shown the classification of the main chromophore and auxochrome groups.

Chromophores	Auxochromes
-C=C-	-NH ₃
-C=N-	-COOH
-C=O-	-OH
-N=N-	Alkyl side chains
-NO ₂	
-SO ₃ ⁻	
Quinoid rings	

Table 2.1. Mainly chromophore and auxochrome groups.

A chromophore group generates colour in organic compounds but for that this mentioned group must be part of a conjugated system. It can be seen in the next figure:

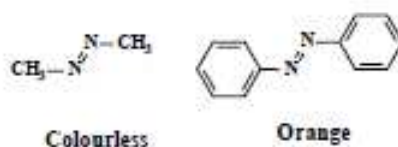


Figure 2.2. Importance of a chromophore group in a conjugated system.

An azo group between methyl groups produces a colourless compound; but when an azo group takes place between aromatic rings a yellow-orange compound is obtained (Hunger, 2011).

There are between 20 – 30 different groups of dyes according to their chemical structure.

This study is focusing on one type of dyes: the Direct Azo Dyes.

2.1.1. Azo Dyes

Azo dyes are the most widely used dyes in the industry. They represent between 60 – 70% of total dye production. They contain an azo group, $-N=N-$, as part of their structure. Often, their carbon atoms are part of aromatic systems, but not always. Most azo dyes contain only one azo group, but some contain two (disazo), three (trisazo) or more.

The aromatic groups of azo dyes helps to stabilize the $-N=N-$ group by making it part of an extended delocalized system.

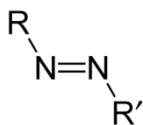


Figure 2.3. Azo dye general structure.

Properties

Azo dyes provide bright and intensity colours and they have the great advantage of their cost-effectiveness.

In theory, azo dyes can supply a complete rainbow of colours. However, commercially they tend to supply more yellows, oranges and reds than any other colours.

Depending on its application characteristics and colour, each dye has a color index generic name (C. I.).

Production

Important processes in the production of azo dyes are:

Processes involving synthesis of the azo group:

- diazotization and coupling
- condensation of nitro compounds with amines
- reduction of nitro compounds
- oxidation of amino compounds

Syntheses with compounds already containing the azo group:

- exposure of concealed or protected amino groups
- acylation of aminoazo compounds
- alkylation and acylation of phenolic hydroxyl groups
- metal-complex formation

Toxicity

According to the EU criteria for classification of dangerous substances, the acute toxicity of azo dyes is rather low.

There are three ways by which azo dyes can be toxic:

- For their structure (there are azo dyes that contain amines or other carcinogenic groups).
- By reduction reaction, azo dyes can turn into aromatic amines. Some of these amines are carcinogenic. In the following figure it is shown the reduction of an azo dye:

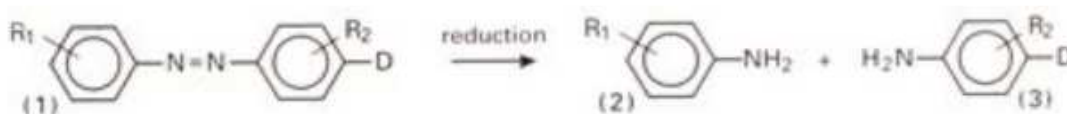


Figure 2.4. Scheme of reduction reaction for azo dyes..

- (1) Azo dye
 - (2) Original di-azo components
 - (3) Linking component with additional amine
- By direct oxidation reaction, azo dyes can be activated and highly reactive electrophilic diazonium salts can be generated.

Moreover, it is important to notice that many azo textile dyes can cause skin hypersensitivity and allergy. Some of them like tartrazine may increase allergic reactions towards other substances.

2.1.2. Direct Dyes

Direct dyes are relatively large molecules with high affinity for cellulose fibres. They are binding to the fibres by Van der Waals forces.

Direct dyes are mostly azo dyes with more than one azo bond or phthalocyanine, stilbene or oxazine compounds.

Some direct dyes have high light fastness.

In the color index, the direct dyes form the second largest dye class with respect to the amount of different dyes. Their classification refers to various planar, highly conjugated molecular structures with one or more anionic sulfonate group.

Chemically, the dyes may contain the sulphonate group ($-\text{SO}_3^-$), essential for water-solubility.

2.2. Titanium dioxide

The polycrystalline semiconductor most used as catalyst in photocatalytic processes is titanium dioxide. This is due to its photo-stability, exceptional optical and electronic properties, no high value of band gap, low cost. It also presents the advantage of being non toxic.

Chemical structure

TiO₂ exists in three crystallographic forms, anatase, rutile and brookite, but only anatase and rutile are used in photocatalysis. The non-high value of band gap of TiO₂ together with the position of the valence band holes, allows that very energetic holes are generated in the semiconductor. This situation increases the ease for oxidation reactions to occur.

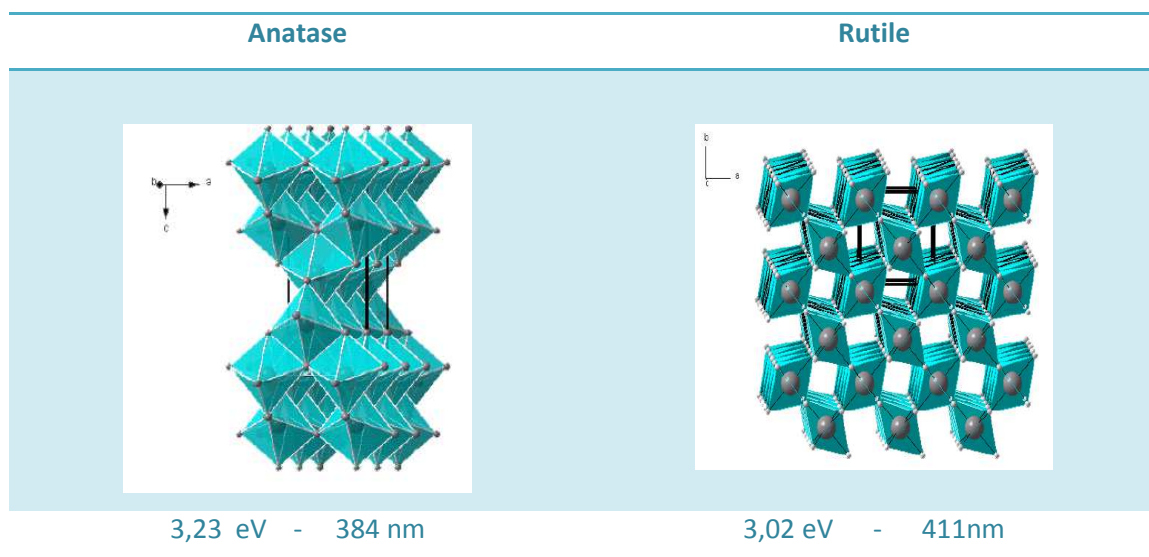


Figure 2.5. Crystal structure of anatase and rutile. (Source: Candal, 2001)

In both structures, each atom of titanium is located in the center of an octahedron of oxygen atoms. Each oxygen has three coplanar titanium atoms.

In the rutile, the oxygen atoms form a compact hexagonal lattice which is slightly distorted. The three angles Ti-O-Ti are almost equal with a value of 120°.

In anatase, an angle of Ti-O-Ti is about 180° and the other two about 90°. Oxygen atoms form a body-centered cubic lattice.

Anatase is thermodynamically less stable than rutile, but its formation is kinetically favored at lower temperatures (<600 ° C), which explains its most active area and its higher density of active sites for adsorption of substances (Epling et al, 2002a, Arslan et al, 2000)

Properties

In table 2.2 physical and mechanical properties of TiO₂ are summarized. The table 2.3 shows optical properties of TiO₂ (Source: CERAM Research Ltd, 2002).

Property	
Density	4 gcm ⁻³
Porosity	0%
Modulus of Rupture	140MPa
Compressive Strength	680MPa
Poisson's Ratio	0.27
Fracture Toughness	3.2 Mpa.m ^{-1/2}
Shear Modulus	90GPa
Modulus of Elasticity	230GPa
Microhardness (HV0.5)	880
Resistivity (25°C)	10 ¹² ohm.cm
Resistivity (700°C)	2.5×10 ⁴ ohm.cm
Dielectric Constant (1MHz)	85
Dissipation factor (1MHz)	5×10 ⁻⁴
Dielectric strength	4 kVmm ⁻¹
Thermal expansion (RT-1000°C)	9 × 10 ⁻⁶
Thermal Conductivity (25°C)	11.7 WmK ⁻¹

Table 2.2. Typical physical and mechanical properties of TiO₂.

Phase	Refractive Index	Density (g.cm ⁻³)	Crystal Structure
Anatase	2.49	3.84	Tetragonal
Rutile	2.903	4.26	Tetragonal

Table 2.3. Optical properties of TiO₂.

It has been proved that TiO₂ is the most resistant semiconductor material with respect to corrosion and photocorrosion (Neppolian et al, 2002).

A special feature of TiO₂ is the capacity to use natural UV radiation. In the photocatalytic processes with TiO₂ the area of solar spectrum utilized is small, but the study of this technology is promising, owing the abundance and low cost of this natural resource. In the last years, research and development in this field has accelerated dramatically.

Preparation technique

TiO₂ can be prepared by both liquid and gas phase processes. The sol-gel method is one of the most used liquid phase techniques to synthesize thin films, powders and membranes. Among the many advantages of this technique are ease of processing, control over composition, purity and homogeneity of the obtained materials (Hamadianian et al, 2008).

Toxicity

A study (Chung et al, 1999) found that ultrafine (less than 0,1 microns) particles of the anatase form of titanium dioxide are pathogenic or disease causing.

However, if TiO₂ particles used to act as a sunscreen are small enough, they can penetrate the cells, leading to photocatalysis within the cell, causing DNA damage after exposure to sunlight (EPA, 2009). The worry about skin cancer has appeared with this concept.

It was noted that the inhalation of titanium dioxide has not induced lung tumours in humans but it is important to note that rats are extremely sensitive species that develop tumours in the lungs.

Other studies have related that workers exposed to titanium dioxide have showed no statistically significant relationship between exposure and diseases.

It is reasonable to conclude then, that titanium dioxide is not a cancer-causing substance and is generally safe for use in photocatalytic processes.

2.3. Photocatalytic treatment

A photocatalytic process is based on the change in the rate of a chemical reaction, or its initiation under UV, visible or infrared radiation in presence of a catalyst that absorbs light and is involved in the chemical transformation of substances participating in the reaction.

2.3.1. Historical perspective of catalysis

J. J. Berzelius (1779 – 1848) coined the catalysis in 1835 in order to rationalize a number of isolated observations, such as the conversion of ethanol to acetic acid, the conversion of starch to sugar by acids, the decomposition of H_2O_2 by metals, and the reaction between H_2 and O_2 in presence of Pt. He recognized a common feature in these processes but the phenomenon was not properly understood for the next 60 years. W. Ostwald (1853 – 1932), Nobel Prize in Chemistry in 1909, established the kinetic nature of catalysis.

In the table below, scientists recognized for works in the field of catalysis are mentioned.

Year	Scientists	Research topic
1909	W. Ostwald	For his work on catalysis
1912	P. Sabatier	Catalytic hydrogenation
1918	F. Haber	Synthesis of ammonia
1931	C. Bosch, F. Bergius	High pressure methods
1932	I. Langmuir	Surface chemistry
1963	K. Ziegler, G. Natta	Stereospecific polymerization
2001	W.S. Knowles, R. Noyori, K.B. Sharpless	Chiral catalysis
2005	Y. Chauvin, R.H. Grubbs, R.R. Schrock	Olefin metathesis
2007	G. Ertl	Catalytic reactions on surfaces

Table 2.4. Nobel Prizes in Catalysis or related topics (Source: Hagen, 1999)

The development of the chemical industry in the 20th century was parallel with the evolution of catalysis. Up to about 1940, catalysts were mostly used for the production of basic chemicals and liquid fuels. Significant concepts were introduced by Sabatier (the reactants

form unstable intermediates with the catalyst) and by Taylor (there are active sites on the catalyst surface, where chemical adsorption occurs) in this period. The basis of catalytic reaction mechanisms was established by Langmuir adsorption isotherm.

During the period from 1940 to 1970, the development of hydrocarbon refining and petrochemical industry increased. Catalysts were utilized in synthesis gas, fuel production and selective oxidation processes.

In the 1970s years, the legislation about environmental pollution arose promoting the area of catalysis in this field. Important progress was made in the preparation of catalysts and in the understanding of the mechanisms of catalyst deactivation. Moreover, new fields of application emerged, such as photocatalysis and electrocatalysis.

In the 1990s, due to the major concern of sustainable development, the concept of "Green Chemistry" appeared.

2.3.2. Introduction to the photochemistry

Photochemistry is the discipline that deals with the study of interactions between atoms, small molecules and light (or electromagnetic radiation).

The first law of photochemistry, known as the law of Grotthus-Draper, states that light must be absorbed by a chemical substance to generate a photochemical reaction.

The second law of photochemistry, the Stark-Einstein law, states that for each photon of light absorbed by a chemical system, only one molecule is activated to produce a photochemical reaction.

A chemical reaction required the absorption of electromagnetic radiation with appropriate length by a molecule.

When a polychromatic light is passed through an object, it absorbs some wavelengths and transmits the wavelengths that are not absorbed as colours.

The wavelength absorbed and the efficiency of absorption will depend on the structure of the molecule and the medium in which it is found.

In the absorption spectroscopy, the sample absorbs electromagnetic radiation of a suitable source and the amount absorbed can be related with the concentration of the substance that wants to be analyzed in solution.

The photochemistry usually works in the following regions of electromagnetic spectrum:

- Ultraviolet: 100 – 400 nm
- Visible light: 400 – 700 nm
- Near infrared: 700 – 1000 nm
- Far infrared: 15 – 1000 μm

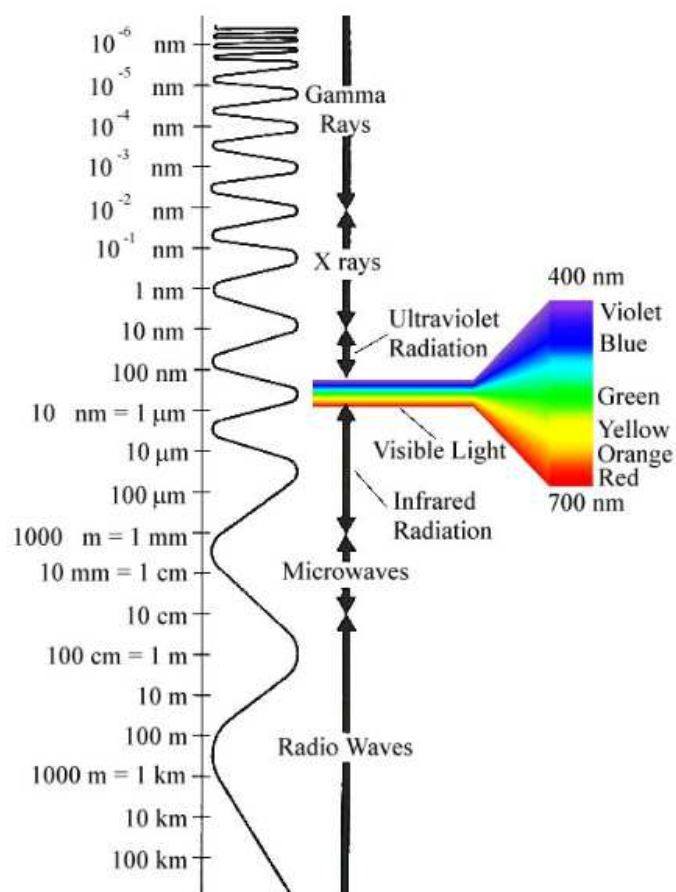


Figure 2.6 . Electromagnetic spectrum (Source: University of Arizona)

Photochemistry has numerous applications in air and water purification due to the possibility of degrade chemically pollutants with the presence of light. These reactions of degradation

take place at low temperatures when photons transfer their energy to transform the reactants directly or through photocatalysts which are not consumed by them.

Planck's law calculates the energy carried by the light to convert the molecules:

$$E = hc/\lambda \quad \text{Equation 2.1. Planck's law.}$$

h : Planck constant ($6,624 \cdot 10^{-34}$ J·s)

c: speed of light ($3 \cdot 10^8$ m·s⁻¹)

λ : wavelength of the radiation

2.3.3. Advanced Oxidation Processes (AOPs)

Advanced Oxidation Processes (AOPs) have been proposed in recent years basically as effective alternatives in the purification of air and contaminated waters.

The presence of toxic and / or refractory compounds is a major problem for the conventional biological treatments. In addition, the typical separation technologies transfer contamination from one phase to another or create a more concentrated effluent. Furthermore, in recent years, the occurrence of so-called "emerging contaminants" (pesticides, pharmaceuticals ...) creates an additional problem due to the limited information available about its effects on the environment and its interference in the biological processes.

For their ability to degrade these pollutants, the AOPs are an attractive option to perform this type of treatment.

The AOPs are based on physicochemical processes capable of producing profound changes in the chemical structure of the contaminants. These processes involve the generation of a hydroxyl radical in sufficient amount to interact with the remainder of organic compounds. This radical can be generated by photochemical means (including sunlight) or other forms of energy, and has a high efficiency for the oxidation of the organic matter.

AOPs use the high oxidative capacity of hydroxyl radical (HO°) which has very short reaction time. There are several methods depending on the way that generates these radicals. The most common methods use combinations of ozone (O₃), hydrogen peroxide (H₂O₂), ultraviolet

radiation and photocatalysis. It is possible to observe the classification of AOPs in the figure that is attached.

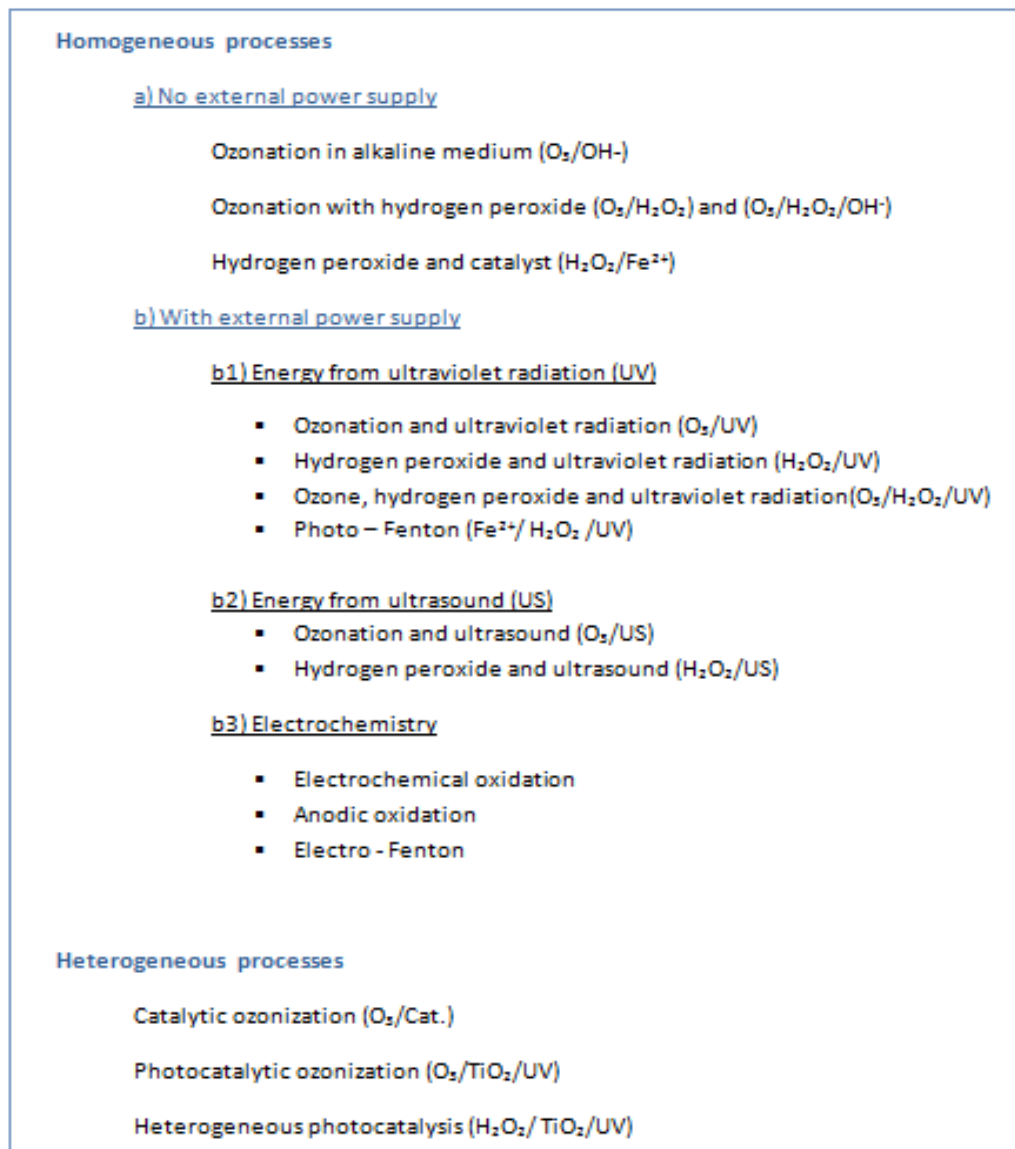


Figure 2.7. Classification of Advanced Oxidation Processes (Source: Rodríguez et al, 2006).

The aim of AOPs is to remove non-biodegradable soluble compounds that are present in wastewater. The process involves a chemical oxidation under mild conditions of temperature and pressure, until that the complete mineralization of contaminants has been produced. AOPs can be used for the degradation of pollutants like volatile organic compounds (VOCs), semivolatile organic compounds (SVOC), phenol, chlorophenols, pesticides, herbicides, cyanides, dioxins and furans.

Due to the high reactivity of hydroxyl radical it is possible to remove organic and inorganic compounds achieving a reduction of COD, TOC and toxicity in the treated wastewater. Also, the generation of radicals is made with oxygen, hydrogen peroxide and supported catalysts, so the reaction byproducts are only water and carbon dioxide.

One consequence of the high reactivity of the oxidizing agent is that AOPs are also characterized by their low selectivity; but what can be a disadvantage in a production process, is nevertheless a desirable characteristic in the case of removing contaminants from wastewater.

Thanks to radiation of sun / UV, radical production can occur spontaneously in the wild or can be caused by different combinations of the radiation UV / solar and oxidants. In the table 2.5, oxidation potentials are given for several oxidizing substances. As it can be seen, the hydroxyl radical is the strongest oxidant after fluorine.

Oxidizing substance	Oxidation potential (V)
Fluorine	3,03
Hydroxyl radical	2,8
Atomic oxygen	2,42
Ozone	2,07
Hydrogen peroxide	1,78
Perhydroxyl radical	1,7
Permanganate	1,68
Hypobromous acid	1,59
Chlorine dioxide	1,57
Hypochlorous acid	1,49
Hypoiodous acid	1,45
Chlorine	1,36
Bromine	1,09
Iodine	0,54

Table 2.5. Oxidation potentials for several oxidizing substances (Hager, 1990).

The AOPs are considered the "best available technology" for the purification of recalcitrant compounds, toxics and non-biodegradable soluble contaminants (Rashed et al, 2005).

Furthermore, some processes use expensive reagents such as hydrogen peroxide or ozone, so their use should be restricted to situations in which no other cheaper process, such as biological treatment, is impossible. Their maximum potential is exploited when they get integrated with other treatments, such as adsorption or biological treatment, in order to achieve maximum economy of the oxidant.

The main problem of the AOPs is the high cost of reagents and energy as ultraviolet light.

Regarding the latter, the use of solar radiation as an energy source would reduce costs.

Below, are mentioned the most important advantages of the AOPs:

- It changed the phase of contaminant (as in the air stripping or in the treatment with activated carbon) and even it is transformed chemically.
- Generally, it achieved the complete mineralization of the contaminant; in contrast to conventional technologies which do not use very strong oxidizing species and cannot oxidize completely the organic matter.
- Usually, sludge is not generated.
- They are very useful for refractory pollutants that resist other methods of treatment (mainly biological).
- They are valid for the treatment of contaminants with a very low concentration.
- Color removal and/or odor.
- Reaction byproducts are not formed, or they are formed in low concentration.
- Generally, the organoleptic properties of treated water are improved.

- In many cases, they consume much less energy than other methods.
- They allow the transformation of refractory pollutants into biodegradable matter.
- Disinfection.

It is worth mentioning that the quality of the final effluent may allow its reuse in the industry, solving the problem of dumping in an economically and environmentally viable way.

In the next figure 2.8 we can see the range of application of different AOPs and other treatments depending on the wastewater flow and the concentration of total organic carbon (TOC).

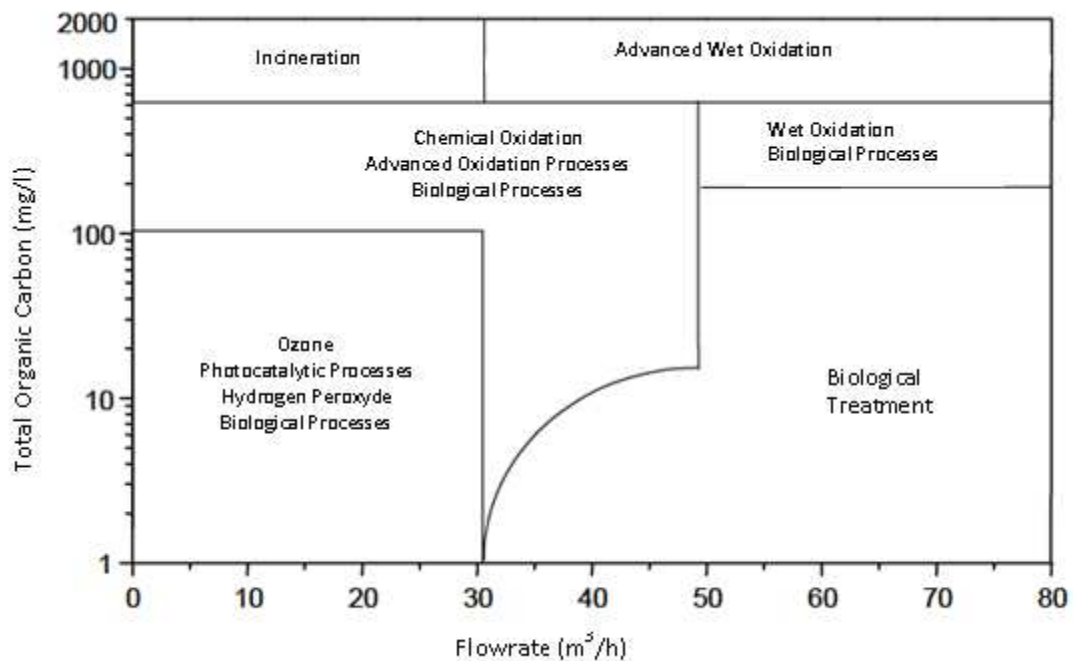


Figure 2.8. Range of application of AOPs and other treatments (Source: adapted from Forero et al, 2005).

2.3.3.1. Heterogeneous photocatalysis

Introduction

Nowadays, the treatment process and / or purification of water by heterogeneous photocatalysis with titanium dioxide as a catalyst is one of the photochemical applications that has aroused interest in the international scientific community. Heterogeneous photocatalysis, unlike most of the photochemical processes, is not selective and it may be used to treat complex mixtures of pollutants. Moreover, the possibility of using solar radiation as primary energy source, gives an important and significant environmental value; the process is a clear example of sustainable technology.

The heterogeneous photocatalysis is based on the use of the most energetic area of the electromagnetic spectrum (area of ultraviolet radiation) to promote an energetic reaction. This reaction takes place when the ultraviolet radiation activates a semiconductor catalyst in presence of oxygen. Under these circumstances, any substance found in the same medium simultaneously is subjected to an energetic oxidation process.

History of photocatalysis

In 1930, Plotnikov provided the first mention of photo catalysis in his book “Allgemeine photochemie”. Kinetic study of photo oxidation on the surface of zinc oxide was carried out by Markhani and Laidler in the 1950's. By the 1970's researchers started to perform surface studies on photo catalysts (zinc oxide and titanium dioxide). In that period, while solar energy was being studied like an available renewable resource, Fujishima and Honda applied photochemistry in water treatment with a semiconductor electrode (which could be considered a solar powered cell).

In the 1980's and 1990's the increase concern for environmental preservation provoked that some scientist began to research about photochemistry for air, water and soil cleanup with TiO_2 as catalyst (Hagen, 1999).

Since that time, photocatalysis with TiO_2 has been reported as a promising way to destroy toxic and hazardous organic compounds in drinking water and industrial wastewater. A complete oxidative destruction of pollutants has been observed in most cases with a generation of CO_2 , H_2O and inorganic ions as final products. The possibility of use sunlight for photocatalysis has

increased the importance of this process coupled with the ease of large scale operation and process efficiency.

Advantages and disadvantages

In the table below, main advantages and disadvantages of photocatalytic processes are mentioned:

Advantages	Disadvantages
Possibility of using a clean energy source.	Reduced effectiveness if other reagents aren't used.
It can be combined with other oxidation processes.	Low yield of radiation.
Generally, byproducts aren't generated.	Limited availability of photocatalysts.
Normally, a complete mineralization can be achieved.	Limitations on mass transfer.

Table 2.6. Main advantages and disadvantages of photocatalytic processes (Rodríguez et al, 2006).

Principle of heterogeneous photocatalysis

A heterogeneous photocatalytic system for oxidative degradation of organic or inorganic oxidizable compounds includes the following components:

- A reactant
- A photon of the appropriate wavelength
- A catalyst surface (normally a semiconductor like TiO₂)
- A strong oxidizing agent

In processes in which a semiconductor solid is involved, the photoreaction mechanism begins when a chalcogenide semiconductor (oxides such as TiO₂, ZnO₂, ZrO₂, CeO₂, etc., or sulphides such as CdS, ZnS, etc.) is illuminated with photons which have an equal or greater energy than the energetic separation between the valence and conduction band (band gap).

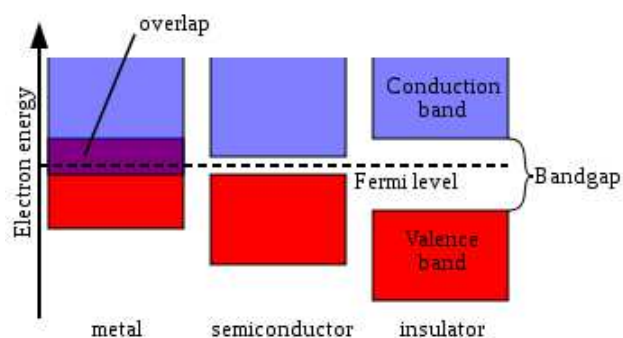


Figure 2.9. Bandgap for metals, semiconductors and insulators.

In this situation, the absorption of those photons takes place and electron-hole pairs (e^- and h^+) are created in the catalyst surface, which are dissociated in free photo-electrons in the conduction band and photo-holes in the valence band.

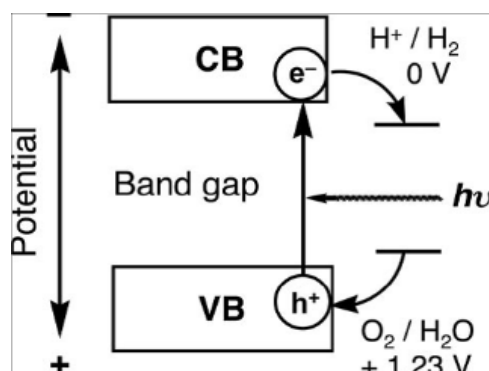


Figure 2.10. Energetic diagram of a semiconductor during photoexcitation process (Source: Lingsebigler, 1995).

Simultaneously an adsorption of reagents is produced and an electron is transferred to an acceptor molecule (Ox_2), producing a reduction reaction, while a photo-hole is transferred to a donor molecule (Red_1) which will be oxidized.

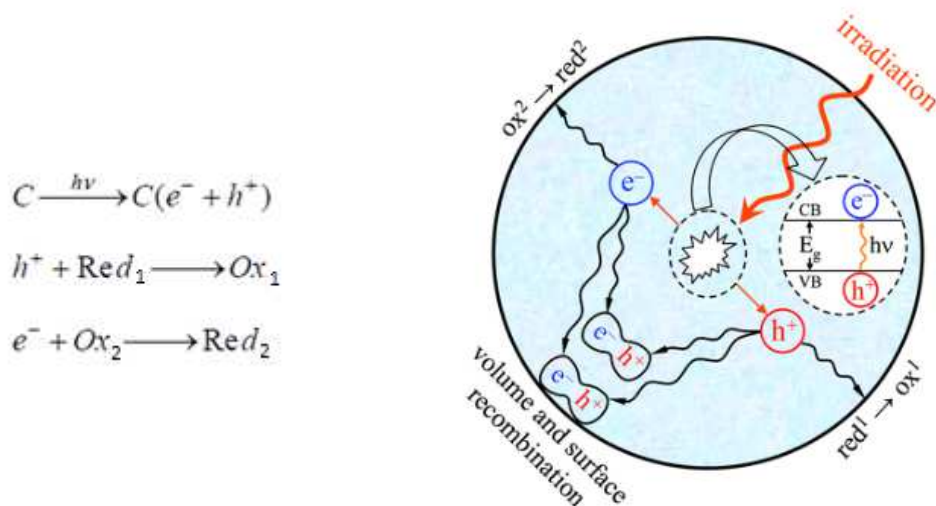


Figure 2.11. Global reaction in heterogeneous photocatalysis. (Source: Palmisano et al, 2007).

In the figure 2.12, we can observe how the reaction occurs when the radiation with an appropriate wavelength reaches the catalyst surface:

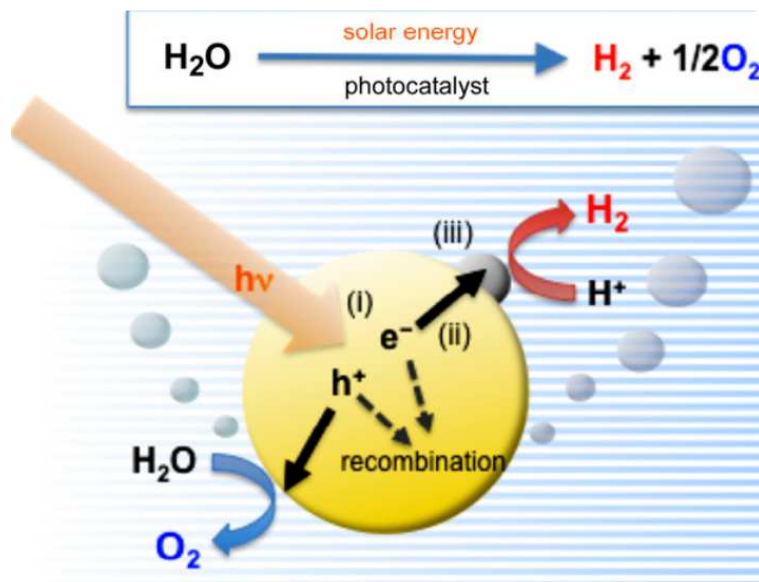


Figure 2.12 . Scheme of heterogeneous photocatalytic process (Source: Solar Energy Materials and Devices Group of Renewable Energy laboratory).

i : UV irradiation of the contaminant with a suitable catalyst (semiconductor) to promote a separation of charges.

ii: The migration of electrons that have been seen promoted to the conduction band, occurs and the holes that have been created in the valence band move towards the catalyst surface.

iii: The capture of holes and electrons by absorbed species generates highly reactive radicals capable of causing oxidation of polluting compounds.

Hydroxyl radicals produce the oxidation of organic compounds and their photocatalytic degradation, obtaining as final reaction products CO_2 and H_2O .

The photo-induced molecular transformations and reactions, involving electron transfer or energy transfer, will take place at the surface of the catalysts solely.

Choice of catalyst

A good catalyst is one semiconductor particle that meets the following characteristics:

- The catalyst is not altered during the process.
- The products formed are the desired.
- There is a great generation of electron - hole pairs.
- It is an exothermic reaction and the final products do not store energy of photons.

The table 2.7 shows some semiconductor compounds that can be used in photocatalytic reactions and the maximum wavelength required to activate the catalyst. The wavelength capable of producing the band gap, can be calculated by Planck equation which was explained above.

Compound	Band gap energy (eV)	Wavelength at band gap energy (eV)
BaTiO ₃	3.3	375
CdO	2.1	590
CdS	2.5	497
CdSe	1.7	730
Fe ₂ O ₃	2.2	565
GaAs	1.4	887
GaP	2.3	540
SnO ₂	3.9	318
SrTiO ₃	3.4	365
TiO ₂	3.2	387
WO ₃	2.8	443
ZnO	3.2	390
ZnS	3.7	336

Table 2.7. Semiconductors used as catalysts in photocatalytic processes (Source: Ullmann's Encyclopedia of Industrial Chemistry).

A lot of semiconductor substances have been tested for compound degradation. However, the best results have been obtained with TiO₂ catalyst (Andreozzi et al., 1999, Hermann, 1999). TiO₂ is selected as the most suitable substance due to it has a high stability against chemical action and photo-corrosion. It also has a low cost and is safe. In addition, TiO₂ has the advantage of using the solar UV radiation because the separation between valence and conduction band is suitable for these photons, with a less wavelength than 387 nm, that have sufficient energy to excite the catalyst (Hermann, 1999).

Photocatalysis with TiO₂

One of the most important properties of TiO₂ is based that upon ultraviolet radiation ($\lambda < 390$ nm), titanium dioxide exhibits photocatalytic activity through the action of conduction band electrons and valence band holes photoinduced from the crystal lattice of TiO₂. In presence of water and oxygen these species produce highly reactive radicals such as OH and O₂⁻, on the surface of TiO₂ (case A in the figure 2.13). That enables the oxidative destruction of a wide range of organic compounds on its surface.

On the other hand, these materials may also exhibit photocatalytically induced superhydrophilicity that converts the hydrophobic character of the surface to hydrophilic when exposed to UV light (case B in figure 2.13). This causes the formation of uniform

water films on the surface of these materials, which prevents the adhesion of inorganic or organic components, and thus retains a clean surface on the photocatalyst.

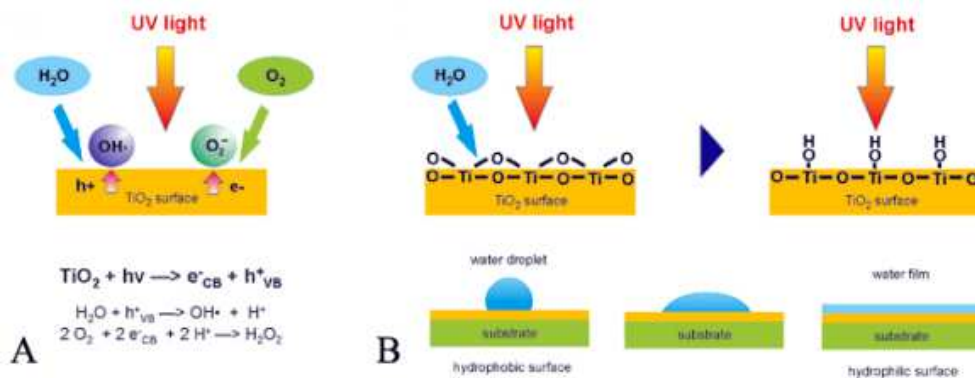


Figure 2.13 .Photocatalytic reaction on TiO_2 surface (Source: Research Centre for Nanosurface Engineering)

It can be argued that the mechanism of heterogeneous photocatalytic reaction takes place in the following stages:

- Transport of reagent in fluid phase to the catalyst surface.
- Adsorption of reagents on the catalyst surface.
- Photogeneration of electrons and electronic gaps in the catalyst by UV radiation.
- Migration of charges into catalyst surface.
- Reactions of electrons and electronic gaps with adsorbed species.
- Eventual reactions between products adsorbed on the catalyst surface and radical products generated.
- Desorption of products.
- Transport of products into fluid phase.

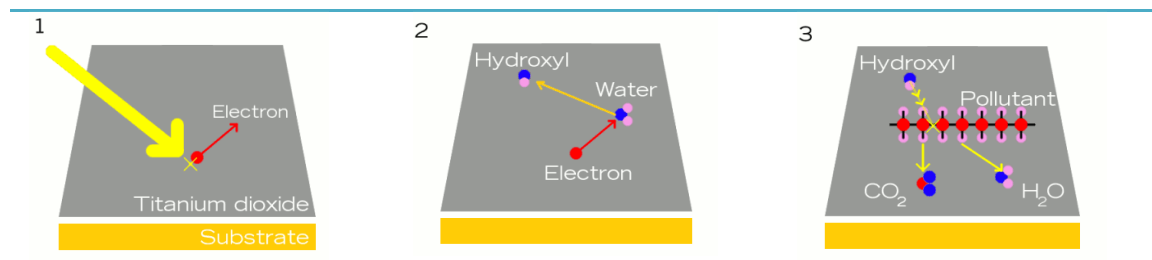


Figure 2.14. Sketch of a photocatalytic process (Source: ExplainThatStuff).

Reaction mechanism

The azo chromophore $-N=N-$ can undergo oxidation processes (photogenerated holes) and reduction (photogenerated electrons), besides the interaction with hydroxyl radicals, hence its ease of degradation. The reactions that occur during a photocatalytic process with TiO_2 are detailed below.

Following excitation of the TiO_2 molecule with light of appropriate wavelength, with photon energy in excess of the semiconductor band gap ($E_g > 3,23$ eV), an electron/hole pair is generated in the metal oxide particle [Reaction 1].



Dye solution + h_{VB^+} → Oxidation of products ($\text{R-COO}^- + \text{h}^+ \rightarrow \text{TiO}_2 + \text{R}^\circ + \text{CO}_2$) [Reaction 12]

Dye solution + e_{CB^-} → Reduction of products [Reaction 13]

The photogenerated electrons reduce the absorbed dye [Reaction 13] or react with electron acceptors (as H_2O_2 absorbed on the surface of TiO_2 or dissolved in water), reducing the hydroxyl radical [Reaction 7].

The photogenerated holes can oxidize the organic molecule to form R^+ [Reaction 12], or reacted with OH^- [Reaction 3] or water [Reaction 2] oxidizing into OH° radicals. These, together with other species, are responsible of heterogeneous photodecomposition of dye solutions.

For interactions with holes and electrons to be possible, the substrates should be absorbed into the catalyst surface. Dyes and H_2O_2 undergo a process of physical adsorption [Reactions 4 and 5] to start the reactions mentioned.

The process of recombination [Reaction 7] occurs when electrons and holes are not trapped efficiently by absorbed substrates. Then these two species return to their initial state, with a heat generation.

The resulting OH° radical is a strong oxidizing agent (standard redox potential 2.8 V) which can oxidize many azo dyes even until full mineralization.

Also, it can be observed the pH dependence [Reaction 3], given by the dissociation of water into ions.

Kinetics

It is assumed that the illuminated area of the reactor is uniform and it is supposed a quasi constant reaction rate which will require the following aspects:

- Uniform light scattering.
- Absence of mass transfer limitations.
- Effective mixing.
- Good fluid circulation.

It should be considered that the reaction volume (V) is not necessarily equal to the irradiated volume (V_{irr}). Therefore, the conversion for a organic reactant in a specific section of reactor (A_{irr}) depends on the mixture illuminated and the weight of catalyst (W_{irr}) that is irradiated.

Based on true rate constants (k), for a first order photoconversion, the rate constant can be expressed with apparent rate constants (k_{app}) by next equation:

$$k_{app} = k'_{app} \cdot \frac{V_{irr}}{V} = k''_{app} \cdot \frac{A_{irr}}{V} = k'''_{app} \cdot \frac{W_{irr}}{V}$$

Equation 2.2 .Apparent rate constant.

The degradation rate of an absorbed substance on catalyst, is identified with the true rate constant of the Langmuir - Hinshelwood kinetic model:

$$r = \frac{dC}{dt} = k\theta = -\frac{kKC}{1 + KC}$$

Equation 2.3.Degradation rate.

Where:

r: degradation rate

k: degradation rate constant

θ : occupation coverage of adsorption sites

K: adsorption equilibrium constant (defined by the ratio between adsorption and desorption rate constants $K = k_{ads}/k_{des}$.)

C: equilibrium concentration (after adsorption)

It is assumed that the term KC is negligible, because at low concentrations $kC \ll 1$ and the model follows a first order kinetics, so the integrated reaction rate can be determined by apparent rate constant:

$$\ln \frac{C}{C_0} = -k_{app} \cdot t$$

Equation 2.4 . Integrated rate equation.

Where:

C_0 : initial concentration of dye solution

t : time

Parameters involved in a photocatalytic process

Numerous research works about heterogeneous photocatalysis with TiO₂ have been developed in recent years in order to improve the technology of degradation of organic substances present in industrial wastewater. These works have been performed to study the influence of several parameters involved in photocatalytic processes. Parameters that have been studied in this work, are detailed.

Effect of pH

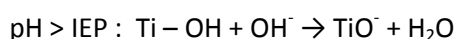
The pH affects the properties of catalyst surface and the chemical structure of the compound to degrade, and this is reflected in changes in the degradation rate and the flocculation tendency of the catalyst.

When photocatalysis with TiO₂ is applied for the degradation of organic matter, the pH must be optimized because this factor determines the semiconductor surface load and the system capacity to generate oxidant radicals which will allow the substrate to be transformed or mineralized (Zepp et al, 1992).

Heterogeneous photocatalysis is a process dependent of pH (Khataee et al, 2010, Alinsafi, 2005, Palmisano et al, 2007, Arslan, 2000, Zepp, 1992).

When the pH of solution varies, the properties of the solid-liquid interface are modified. Consequently, the adsorption/desorption efficiency and the separation of the electron/hole pair, are affected.

For a solution with a upper pH than the isoelectric point of TiO₂ the catalyst surface is negatively charged, while for a lower pH than the isoelectric point the opposite occurs (Guillard,2003). For TiO₂ Millenium – PC500, the isoelectric point (IEP) is situated in 6,2. (Gumy, 2005) . Next, the equilibrium can be seen:



The change of pH influences the adsorption process of dye molecules on the catalyst surface.

In alkaline medium, the number of hydroxyl radicals may be increased on the surface of TiO_2 particles, by entrapment of the hydroxyl ions by available photoinduced holes.

The holes are considered the most powerful oxidative specie at low pH, while at high or neutral pH hydroxyl radicals are the predominant species.

Clearly, when the polluting organic molecule and the catalyst surface have the same load, the adsorption is very low.

For these reasons, the photocatalytic activity of anionic azo dyes achieves a maximum under acid conditions followed by a decrease in the range of pH between 7 - 11. Furthermore, the higher degradation rate in acid pH is due to the efficiently process of electron transfer caused by the formation of a complex bond in the surface.

Effect of catalyst surface

Generally the advantageous features for a photocatalyst are a high surface area, a uniform size distribution of particle, the spherical form of particles and the absence of internal porosity. In photocatalytic processes, usually powders whose particles have micrometric diameters are employed.

The photocatalytic degradation with TiO_2 of dye solutions, is influenced by the important role of the photocatalyst surface. Several authors have reported that the photocatalytic process is based mainly on the generation of radicals that occur on the catalyst surface (Fox et al, 1993, Serpone and Pelizzeti, 1989).

Studies show that photocatalytic reaction takes place in the adsorption phase on TiO_2 surface, and not in solution (Guillard et al, 2003). The amine groups are mainly transformed into ammonium and nitrate. The azo groups ($-\text{N}=\text{N}-$) are mineralized in N_2 . The sulphur atoms in form of sulphite ($=\text{S}^+$) or sulphonates ($-\text{SO}_3^-$) are mineralized into sulphate.

In addition, the concentration of salts and reaction products, may affect the capacity of the catalyst in the photocatalytic process (Guillard et al, 2003).

Moreover, it must be considered that the presence of organic substrates, absorbed on photocatalyst surface, can compete with photogenerated holes and hydroxyl radicals (Younathan et al, 1986).

Inhibition of the activity of TiO₂

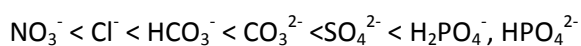
The slowing of oxidation in heterogeneous photocatalysis is caused by many compounds found in textile effluents (Guillard et al, 2003, Legrini et al, 1993).

The presence of impurities (such as CO₃²⁻, Na₂CO₃, NH₃, dissolved organic matter, detergents and chemical finishing) in dye solutions, consumes hydroxyl radicals and blocks the light penetration in solution. This situation provokes the inhibition of reactions in which hydroxyl radicals are involved.

Several hypotheses have been suggested to explain the inhibition of a photocatalytic process by the presence of ions:

- The trapping of OH radicals and oxidant species.
- The competition of adsorption between ions and the reactant at the catalyst surface.
- The reduction of light absorption by the photocatalyst due to the presence of ions.
- The increase of recombination of holes and electrons.

Inhibition of the photocatalytic process is affected by numerous ions, in the following order (Guillard et al, 2005, Chen et al, 1997):



Simulated effluents contain HPO₄²⁻ and SO₄²⁻ anions.

CHAPTER 3: OBJECTIVES AND JUSTIFICATION

The research work that is described in this report, was carried out at LRGP (Laboratoire Réactions et Génie des Procédés) of E.N.S.I.C. in Nancy (France) under the title "Heterogeneous photocatalysis of hydrolysed direct azo dyes and simulated dyehouse effluents on immobilised TiO₂ nanoparticles".

The main objective of this project was to study the treatment of wastewater from textile industries, which contain persistent organic substances, by an advanced oxidation process (AOP) called heterogeneous photocatalysis.

Processing operations currently implemented in wastewater treatment plants, are not effective for the treatment of water contaminated with toxic or non-biodegradable substances. Therefore, other processing steps to achieve this objective are needed. The high potential of AOP'S for water remediation with products non treatable by conventional techniques, is widely recognized. However, the high costs originated for the application of this technology to completely oxidize these organic pollutants, compared to conventional biological treatments, are also known. In any case, its use as a pre or post-treatment step to increase biodegradability of these wastewaters can be justified if, previously or subsequently, biological treatment is capable of degrading biodegradable intermediate products resulting from the implementation of the AOP.

From economic standpoint, the costs associated with the treatment of photocatalysis with UV lamps could be reduced through the use of solar radiation. This aspect allows to think that this technology could gain importance in a near future owing to the possibility of using a renewable energy source.

Then, the specific objectives that have been aimed at in the experimental work, are exposed:

- Feasibility study and comparison of heterogeneous photocatalysis by immobilized TiO₂, for degradation of neutral and hydrolyzed textile dye solutions and simulated dyehouse effluents.

- Evaluation of the toxicity of photocatalytic processes that have been studied.

- Toxicity study for the comparison of germination of six different plants with neutral dyes tested.

CHAPTER 4: MATERIALS AND METHODS

4.1. Materials

4.1.1. Titanium Dioxide

In all experiences TiO_2 was used. This photocatalyst was immobilized on cellulose paper, manufactured by Ahlstrom Research and Services (Pont-Evêque, France).

The nanopowder of TiO_2 used was MPC-500 which was bounded with SiO_2 on the paper. In the table 4.1 the nanoparticle properties are shown.

Type of TiO_2	Surface area (m^2/g)	Composition	Crystal size (nm)	Isoelectric Point (IEP)
Millenium-PC500 (MPC500)	> 250	> 97 % anatase	5 – 10	6,2

Table 4.1 . Properties of MPC500 TiO_2 nanopowder (Nasr-Esfahani, M. and Habibi, M.H., 2008).

4.1.2. Dyes

Four direct di-azo dyes were tested. These dyes were acquired from Sigma – Aldrich and their technical names are:

- Direct Yellow 50 (DY50)
- Direct Red 23 (DR23)
- Direct Red 81 (DR81)
- Direct Violet 51 (DV51)

In Annex I complete dye information can be found.

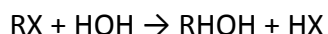
In order to study photocatalytic degradation with the different dyes in several conditions, solutions were made with ultrapure water at approximately 25 mg/l.

First, a study of neutral dyes was made. Later hydrolysed dyes and simulated dyehouse effluents were studied.

Hydrolysed dyes

Theoretical basis

The hydrolysis occurs when the reaction between a chemical compound RX and water takes place, producing an exchange between X and OH groups:



This process converts large molecules into smaller ones.

Factors influencing the hydrolysis are:

- pH influences the hydrolysis by the concentration of H_3O^+ or OH^- (when the pH rises, an increase of OH^- ions are produced).
- Temperature influences the hydrolysis according to the Arrhenius relation.

Dyeing process in a textile industry occurs in an alkaline pH range in order to increase the hydrophobicity and flexibility of the fibers to be dyed (Khouni et al, 2011).

On the other hand, three of the studied dyes have amide groups in their chemical structure:

- DY50: one amide group
- DR81: one amide group
- DV51: no amide groups
- DR23: two amide groups

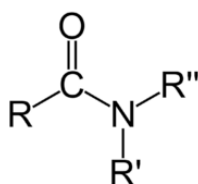


Figure 4.1 . Amide functional group

Hydrolysis of amides happens when a nucleophile such as water or hydroxide ion, attacks the carbon of a carbonyl group of amide. In aqueous base, hydroxyl ions are better nucleophilic polar molecules than water. As an amide results from the condensation of an amine and a carboxylic acid, the amide hydrolysis generates the amine and the acid mentioned.

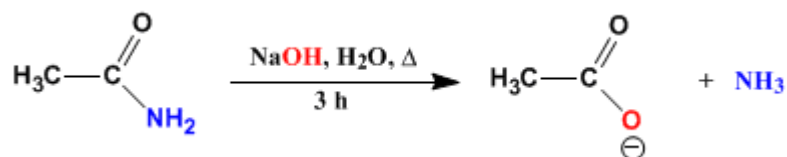


Figure 4.2. Basic hydrolysis of amides

Experimental procedure

The following hydrolysis procedure was carried out to look like an industrial textile process:

- Adjusting pH of solution at 12 with NaOH.
- Heating dye solution at 80°C during 1 hour 30 minutes.
- After hydrolysis, adjusting pH of solution pH at 6, 7 or 8 depending on the experience to test.

Simulated dyehouse effluents

In effluents generated in textile industries, there are a great number of pollutants due to the addition of determinate chemical substances during different stages of the production processes.

For this reason, simulated dyehouse effluents were created at laboratory.

The next amounts of chemical substances were added at dye solution to simulate synthetic textile water:

- Ammonium sulfate $[(\text{NH}_4)_2\text{SO}_4] \rightarrow 5,56 \text{ mg/l}$
- Sodium monohydrogen phosphate $[\text{Na}_2\text{HPO}_4] \rightarrow 5,56 \text{ mg/l}$

- Starch from potato → 2,78 mg/l

Then, hydrolysis was applied (Alinsafi, 2005).

Also, one experience with simulate synthetic textile water for DR23 at halved concentration of chemical substances were done to observe the influence of these substances in the photocatalytic reaction. This experience has been called "Simulated Light Dyehouse Effluent".

4.2. Methods

The following actions are needed to evaluate the efficiency of a photocatalytic process:

- Effectiveness of a degradation process must be controlled with the monitoring of the kinetics of dye degradation.
- The presence of reaction intermediates have to be determined.
- The safety of the final effluent should be ensured.

From analytical point of view, the task that involves a greater difficulty is the qualitative and quantitative evolution of intermediates or degradation products. As hydroxyl radicals are not selective in its attack, many products are formed in the intermediate stage to the complete mineralization of the dyes initially presents in the water to be treated.

Chemical analysis of these complex reaction mixtures is difficult, so the studies focus on monitoring the disappearance of the initial dye (Khataee et al, 2010, Alinsafi, 2005, Vulliet et al, 2003), as well as monitoring of TOC decrease and the appearance of inorganic ions. So, in this way, kinetics of dye degradation and mineralization rate are evaluated during the process.

However, it would be necessary to have a better knowledge of intermediate products that are generated, because in many cases these products may be more toxic and persistent than initial compounds (Bianco – Prevot et al, 1999). For this reason, a toxicological evaluation of these processes is also necessary.

Then, analytical techniques used in this study are described.

4.2.1. pH

The pH indicates if solution is acid or alkaline. This parameter was adjusted depending on the experience to test with sodium hydroxide (NaOH) or hydrochloric acid (HCl).

The pH – meter used in the laboratory was Radiometer PHM220 (Paris, France).

4.2.2. UV- Visible Spectrophotometry

UV-Visible spectrophotometry is an analytical technique used to determine the concentration of compounds, from the measure of its absorbance.

Textile effluents contain chromophores that absorb radiation in the visible or ultraviolet. The valence electrons of these groups are transported to the orbitals of higher energy level under the effect of radiation.

Physical principle

The principle of ultraviolet-visible spectrophotometry involves the absorption of ultraviolet-visible radiation by a molecule causing the promotion of an electron from a ground state to an excited state, releasing the excess energy as heat. For this method, the wavelength is comprised between 190 and 800 nm.

The molecules that have non-binding valence electrons in their molecular structure, when they are excited by light, emit color.

When a UV-Vis radiation passes through a solution containing an absorbent analyte, the beam intensity (I_0) is attenuated to I . This fraction of radiation that has failed to pass the sample is called transmittance (T) ($T = I / I_0$) but absorbance (A) is used because it is related linearly with concentration according to the Lambert – Beer equation:

$$A = \log (I/I_0) = \sum \epsilon_i \cdot l \cdot c_i \quad \text{Equation 4.1. Lambert - Beer Law.}$$

Where,

ϵ : molar absorption coefficient

l : optical path length

c_i : concentration of substance

The absorbance of a substance at a determined wavelength is the sum of the absorbances of each chromophore group i which absorbs at that wavelength.

Calibration Curve

The spectrum of a substance is a graphical representation of the absorbance (A) versus the wavelength (λ). This graph shows waves with peaks and minimum values.

For making quantitative determinations, the wavelength corresponding to a maximum value (peak) is chosen because, for that value, the error of measure is minimum and the sensitivity is maximum.

To verify the compliance of Beer's law, calibration curve must be performed. So, solutions of substance at known concentrations are prepared and their absorbance, at the chosen wavelength, is measured.

If Beer's law is valid for that substance at these concentrations, the relationship should be a straight line.

In the Annex II, calibration curves for the studied direct azo dyes are shown at concentrations between 1,5 and 25 mg/l.

Experimental procedure

In the experiences, the spectrophotometer used was SECOMAM Anthélie Light (Domont, France) which can be seen in figure 4.3



Figure 4.3. Spectrophotometer SECOMAM Anthélie Light.

Electromagnetic spectra of dye solutions were measured in a range of 200 to 700 nm.

Solutions were placed in a quartz cuvette, with an optical path of 10 mm, to measure the absorbance and a blank was previously done with distilled water.

Once the light has passed through the sample, the spectrophotometer shows a graph with measured absorbance versus wavelength.

4.2.3. Ammonium

Ammonium is one of the possible end-products of photocatalysis. For this reason, ammonium was analyzed in final dye solutions. This parameter will be necessary to indicate the efficiency of photocatalytic process. Nessler method was used to determine ammonium in samples.

Nessler method

To test this procedure samples were collected the end of the photocatalytic process.

10 ml of sample were introduced into a glass tube and then these substances were added:

- Two drops of mineral stabilizer (HACH)
- Two drops of polyvinyl alcohol dispersant (HACH)
- 400 μ l of Nessler reactive (HACH)

The blank was made with distilled water following the same procedure.

Before ammonium measurement, the tubes were shaken to homogenize the sample.

Nessler method is based in the generation of a yellow colour when Nessler reagent is decomposed in presence of ammonium ions.

To determine ammonium concentration in samples, the absorbance was measured with spectrophotometer HACH DR 2400 at 425 nm.



Figure 4.4. Spectrophotometer HACH DR 2400.

The concentration of samples was calculated using calibration curve.

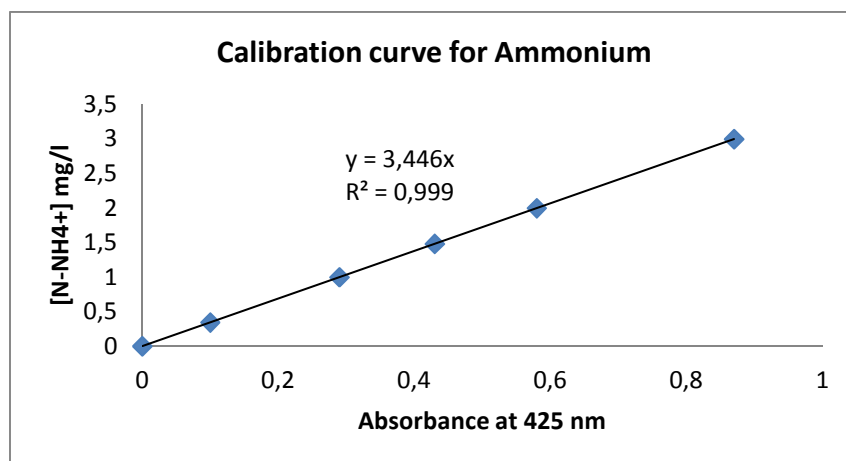


Figure 4.5. Calibration curve for ammonium

After analysis, chemical wastes were transferred to an appropriate container.

4.2.4. Total Organic Carbon (TOC)

Analysis and quantification of TOC in samples is important because this parameter is commonly used as indicator of water quality and treatment process efficiency. To do this, the amount of organic compounds in initial and treated effluents is studied.

The large number of intermediate compounds formed during dye degradation demonstrates the complexity of the photocatalytic process. Due to the high difficulty of tracking all possible intermediate products, it is possible to follow reliably the evolution of photocatalytic process, by TOC monitoring.

In short, to monitor the loss of colour is not sufficient. It is also necessary to reach the conversion of a significant percentage of organic carbon in inorganic carbon in the form of CO₂.

The contribution of total carbon (TC) in water samples is made by organic and inorganic substances. Therefore total organic carbon (TOC) and inorganic carbon (IC) must be distinguished. The IC is made up of carbonates and CO₂ dissolved in water, while TOC has two parts: the volatile or purgeable organic carbon (POC) and the non-volatile organic carbon or non-purgeable (NPOC). If the volatile organic portion is negligible, it is assumed that the NPOC is equal at TOC.

Non-Purgeable Organic Carbon (NPOC)

The method used for TOC analysis is called Non-Purgeable Organic Carbon (NPOC) (Chamorro et al, 2010).

In this method, IC is removed from a sample by purging the acidified sample with a purified gas, and then TOC may be determined by means of TC measuring method as TC equal TOC.

The method occurs in three stages:

- Acidification

Addition of acid to removes carbonate ions and converts them into carbon dioxide.

- Oxidation
Oxidation of carbon in the remaining sample to generates carbon dioxide and other gases. This oxidation step was performed by combustion.
- Detection and Quantification
The measurement of generated carbon dioxide is done by a non-dispersive infrared detector (NDIR).

The technique used is the total combustion of organic matter into CO₂ and detection of this product with non-dispersive infrared detector. The sample is prepared by acidification and aeration to remove the inorganic carbon. The treated sample is injected into a furnace where water is evaporated and organic carbon generates CO₂ by catalytic combustion. CO₂ is carried by an air stream until the UP detector, which provides a variation of voltage proportional at concentration of total organic carbon (TOC).

A TOC Analyzer Shimadzu was used.



Figure 4.6. TOC Analyzer Shimadzu.

4.2.5. Ion Chromatography for nitrates and sulphates

Technology

Ion Chromatography is a variant of High Pressure Liquid Chromatography (HPLC). It is an effective method for separation and determination of ions, based on the use of ion exchange resins. When an ionic sample passes through these columns, the ions experience a separation due to the different retentions they undergo when interacting with the stationary phase of the analytical columns. Once separated, the sample flows through a detector which registers the signal obtained with respect to the retention time. The result is a chromatogram where the peak position indicates the type of ion and its area indicates the amount of that ion.

Nitrates (NO_3) and nitrites (NO_2) are oxidation products of nitrogen. Nitrate is more stable and can be transformed into nitrite. Ion chromatography is suitable for measuring the amount of nitrates, nitrites as well as sulphates in solution.

Health dangers of nitrates

Nitrate is not generally hazardous to health unless it is reduced to nitrite.

Nitrate is one of the most common groundwater contaminants. It must be controlled in drinking water because excess levels can cause methemoglobinemia in babies. Furthermore, the emergence of nitrates in water might indicate the presence of other hazardous pollutants such as bacteria or pesticides.

Substance	Type of problem	Approximate level that would causes problems
Nitrate	Risk of infant methemoglobinemia if the water is consumed by young children	- Recommended: less than 50 mg/l.
		- Acceptable: 50 mg/l to 100 mg/l.
		- No recommended: more than 100 mg/l.

Table 4.2. Amount of nitrate that would causes health problems (Source: World Health Organization, 2007).

4.2.6. Toxicity Study

Although the purpose of a photocatalytic process is to reach complete mineralization of all organic carbon, in some cases partial degradation of the contaminant may be acceptable if the final product is harmless.

The determination of toxicity is essential in determining the efficiency of a photocatalytic process. In the case of treatment of effluents from textile industries, the desired product is an effluent that can be discharged without affecting any of the species of ecosystem.

Germination studies are considered short-term and primary assessment methods for acute toxicity effects.

For example, plant toxicity studies have been designed to evaluate the phytotoxic effects of dye wastewaters (Palácio et al, 2009), and alfisol soil (J. Celis et al, 2007) and bioremediated explosives (Frische, 2003).

In this research project, two toxicity studies were performed.

In order to study the toxicity of samples before and after photocatalytic process, a toxicity test with lettuce seeds was made.

Furthermore, toxicity studies were realized with six types of different plant seeds to compare the response about toxicity in neutral dyes.

Toxicity test with lettuce seeds

Toxicity tests with *Lactuca sativa L.* have been commonly made due to the high sensitivity of lettuce to toxic chemicals (Sobrero and Ronco, 2004, Banks and Schultz, 2005).

The acute toxicity test with lettuce seeds is performed to evaluate the adverse effects of a pure compound or a complex mixture in the germination process and in the development of the seedlings during the first days of growth.

The inhibition of germination and the elongation of radicle and hypocotyl are determined to study the response of a toxicity test.

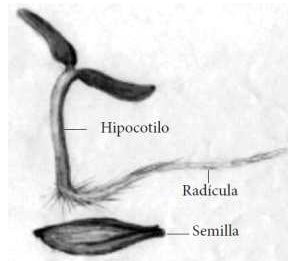


Figure 4.7. Morphology of seed and lettuce seedling

One of the major stages of plant germination is the germination of seed. This process takes place in four steps:

- Inhibition or physical inlet of water
- Generation of enzyme systems and initiation of protein and RNA synthesis
- Emergence of the radicle
- Initiation of growth

The activation of seeds is inhibited by presence of toxic compounds which affect the germination.

The bioassay with lettuce seeds allows evaluating the phytotoxicity of colored samples with high turbidity by direct way and without necessity of prior filtration.

This assay can be applied to study the toxicity of pure soluble compounds, surface and ground water, water for human consumption, domestic and industrial wastewater, besides soil leachates, sediments, sludges and other solid materials.

Procedure

The material used in the experience is detailed below:

- Lettuce seeds
- Measuring instrument
- Tweezers
- Absorbent paper
- Containers
- Foil

- Freezer bags
- 5 ml syringe
- Initial samples of dyes
- Final samples of dyes
- Pure water samples → Positive control
- Salt water samples → Negative control

These tests are performed using initial and final samples of each dye that was analyzed by photocatalysis. The initial sample was collected at the beginning of experience and the final sample was taken 24 hours after.

Samples were made as a control in the analysis of the experiences. Mineral waters (Vittel and Evian) were used as positive controls and salt waters (Vittel and Evian with a NaCl concentration of 5 g/l) were used as negative controls.

To carry out the procedure, two pieces of absorbent paper were placed in each glass vessel and 3 ml of sample to study was added. Then, twelve seeds were placed on the absorbent paper. The vessels were covered with aluminum foil, in which four small holes were made, and were stored in plastic bags. Afterwards, they were placed in a dark drawer at room temperature for five days to avoid that sunlight could affect in seeds germination.

Five days later, the vessels were opened and tested. The number of germinated seeds was counted and the length of the radicle and hypocotyl of each of those seeds was measured.

These assays follow the methodology proposed by Sobrero and Ronco (Sobrero and Ronco, 2004).

Calculations

Lettuce seeds were used as toxicity level bioindicators due to their response to concentrated and diluted by-product solutions.

In toxicity tests with lettuce seeds the following parameters were determined:

- Average radicle length
- Average hypocotyl length

- Relative toxicity
- Percentage of toxicity removal
- Germination index

Relative toxicity (RT)

$$RT = \frac{L_{Posit_Control} - L_{Sample}}{L_{Posit_Control} - L_{Negat_Control}}$$

Equation 4.2. Relative toxicity.

$L_{Posit_Control}$: Seed length of positive control solution

$L_{Negat_Control}$: Seed length of negative control solution

L_{Sample} : Seed length of dye solution sample

Toxicity removal (% $T_{REMOVAL}$)

$$\%T_{REMOVAL} = \left(\frac{RT_i - RT_f}{RT_i} \right) \times 100$$

Equation 4.3. Toxicity removal.

RT_i : Relative toxicity of initial dye solution

RT_f : Relative toxicity of final dye solution

Germination Index (GI)

$$AG = \frac{N_{Germ}}{N_{Seed}} \quad \text{Absolute germination}$$

$$GI = \frac{N_{Germ}}{N_{Posit_Control}} \times \frac{L_{Sample}}{L_{Posit_Control}}$$

Equation 4.4. Germination Index.

NGerm: Number of germinated seeds

NSeed: Total number of seeds

NPosit_Control: Number of germinated seeds in positive control

In positive control, AG = 1.

Comparison of plants for germination toxicity tests with neutral dyes

In order to know what type of plant is the most effective for germination testing in dye solutions, six types of plants have been studied.

Plants to be analyzed have been chosen on ease of seed handling and germination rate.

Common name	Scientific name	Source	Comments
Barley	<i>Hordeum L.</i>	Perez <i>et al.</i> (1986)	Insensitive to olive processing wastewater and organics; less affected by salinity than tomatoes
Cabbage	<i>Brassica oleracea L.</i>	US EPA (1994)	
Carrots	<i>Daucus carota L. spp. sativus</i>	Perez <i>et al.</i> (1986)	
Corn	<i>Zea mays</i>	Fletcher <i>et al.</i> (1985)	Relatively insensitive to target herbicides
Cucumber	<i>Cucumis sativus</i>	Wang (1986)	Sensitive to halogen-substituted phenols and anilines
Garden lettuce	<i>Lactuca sativa L.</i>	US EPA (1994) Wang (1986, 1991)	EPA's standard germination test plant; sensitive to metals, sensitive to inorganic compounds
Millet	<i>Panicum miliaceum</i>	Wang (1986)	Superior to cucumber and lettuce in phenol testing, sensitive to organic compounds
Oat	<i>Avena sativa</i>	US EPA (1994) Fletcher <i>et al.</i> (1985)	Sensitive to herbicides
Radish	<i>Raphanus L.</i>	Perez <i>et al.</i> (1986)	Less affected by salinity than tomatoes; insensitive to organics
Red clover	<i>Trifolium pratense L.</i>	Perez <i>et al.</i> (1986)	
Ryegrass	<i>Lolium perenne</i>	US EPA (1994)	Moderate sensitivity to salinity
Soybean	<i>Glycine max</i>	US EPA (1994) Fletcher <i>et al.</i> 1985	Relatively insensitive to target herbicides
Tomato	<i>Solanum lycopersicon L.</i>	US EPA (1994) Perez <i>et al.</i> (1986)	Sensitive to olive processing wastewater and organics; adversely affected by salinity
Wheat	<i>Triticum aestivum</i>	Fletcher <i>et al.</i> (1985)	Sensitive to target herbicides

Table 4.3. Plants used in germination tests (Banks and Schultz, 2005).

Six plants were analyzed to determine relative sensitivities to neutral dye solutions:

- Lettuce (*Lactuca sativa* L.)
- Millet (*Panicum miliaceum*)
- Radish (*Raphanus* L.)
- Cucumber (*Cucumis sativus*)
- Tomato (*Solanum lycopersicon* L.)
- Watercress (*Nasturtium officinale*)

Watercress is the only plant that does not appear in the previous table.

Assays followed the same method that toxicity tests with lettuce seeds.

In the next table, characteristics and observations of plant seeds in laboratory are described:

Plant	Seeds	Seedlings
Lettuce	Small and light	Easy to differentiate and enumerate
Millet	Medium-size	No germination
Radish	Small	Seedlings and roots emerged in absorbent paper, resulting in difficult enumeration
Cucumber	Big-size	Very easy to count and measure
Tomato	Small	Difficult to measure, low growth
Watercress	Medium-size	Seedlings and roots emerged in absorbent paper, resulting in difficult enumeration

Table 4.4. Characteristics and observations of plant seeds.

CHAPTER 5: INSTALLATION

At ENSIC in Nancy, a photocatalytic reactor has been previously manufactured by researchers (Khataee, Pons and Zahraa, 2010).

The experiences have been developed in a fixed bed reactor where the catalyst is immobilized into a fixed support.

Experimental setup

The pilot plant of photocatalysis is constituted by a fixed bed reactor (37° inclination angle), with dimensions of $30 \times 30 \text{ cm}^2$, which acts as support of non-woven paper made of cellulose fibres. The catalyst TiO_2 is fixed on the paper.

In the next picture, the setup can be seen.

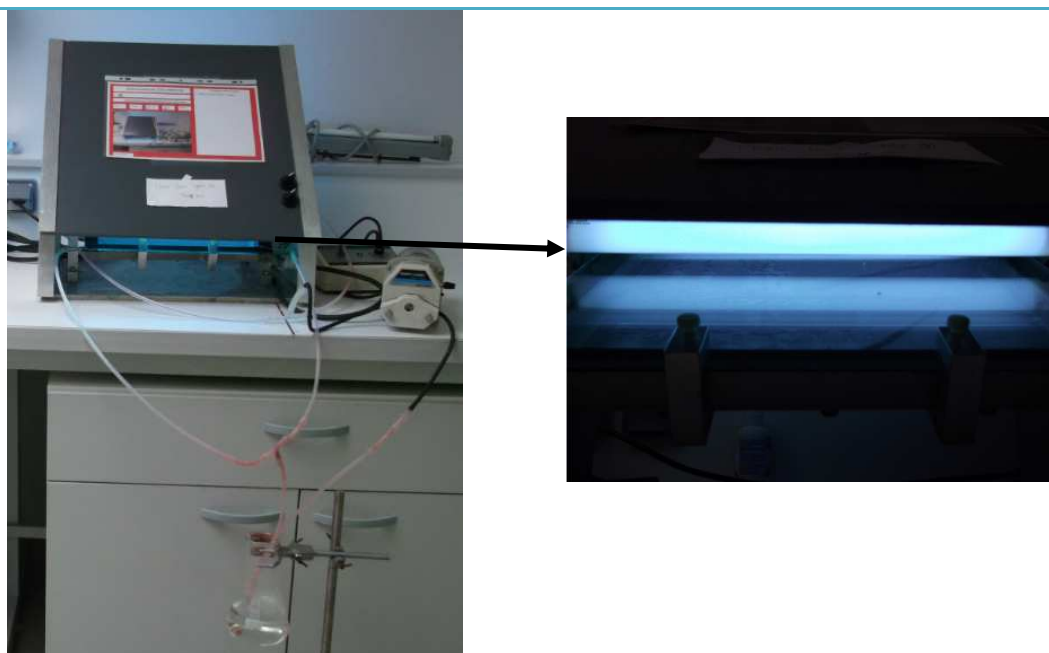


Figure 5.1. Experimental installation of photocatalysis

500 ml of dye solution are pumped from a reservoir to the reactor, with a flowrate of 200 ml/min, to ensure a good distribution of liquid. A glass window ($30 \times 30 \text{ cm}^2$) covers the reactor to prevent evaporation of the solution which could occur due to heating by UV / sun. UV radiation is produced by two lamps (Black light Blue, F15T8, BLB 15 W, DUKE (Essen, Germany)), with a power of 15 W which emit at a wavelength of 395 nm, located in parallel to

the reactor. The solution flows down on the paper and is collected at the bottom. Then, it returns to the reservoir containing the sample to be treated.

Flow Diagram

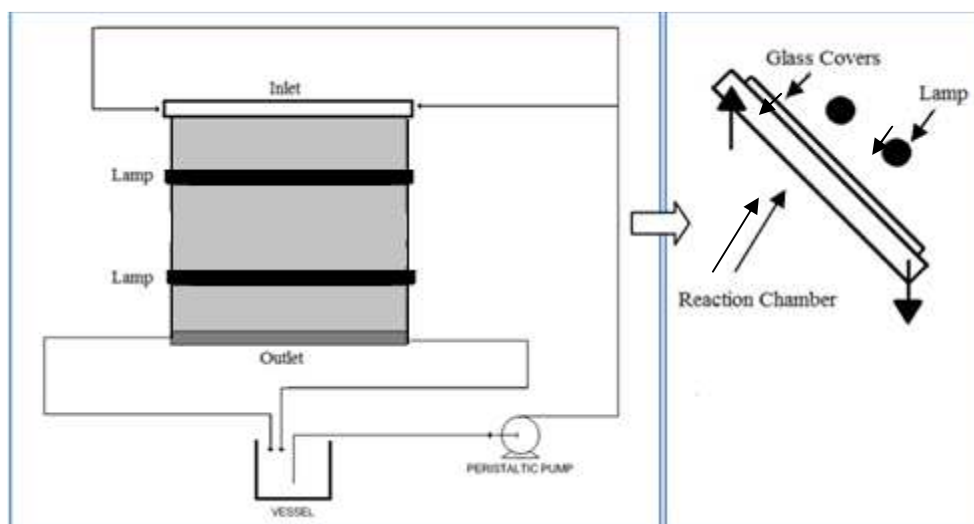


Figure 5.2. Flow diagram of photocatalytic reactor.

Procedure

Previously to the development of experience, the dye solution to be treated is circulated through the reactor during 30 minutes.

The first sample is collected at the beginning of the experiment. Next, the UV lamps are activated and samples are taken during the next 8 hours. The collection of final sample is done after 24 hours of process.

The reactor is rinsed with ultrapure water under UV radiation between experiences with different dyes.

CHAPTER 6: RESULTS AND DISCUSSION

Four types of direct azo dyes were tested in neutral and hydrolysed solutions. Simulated dyehouse effluents based on these dyes were also studied.

6.1. Applied Method

Experiences were made at LRGP in the ENSIC for each type of dye, collecting samples during eight hours. Besides, a last sample was taken 24 hours later of the beginning of the experiment.

First, calibration curves were established (Annex II). To do this, dye solutions at different known concentrations were prepared and their absorbance was measured by UV-spectrophotometry with a spectrum analysis from 200-700 nm. Following this procedure, maximum wavelength was obtained for each dye. In the figure 6.1, it can be seen the example of the azo dye “Direct Violet 51”:

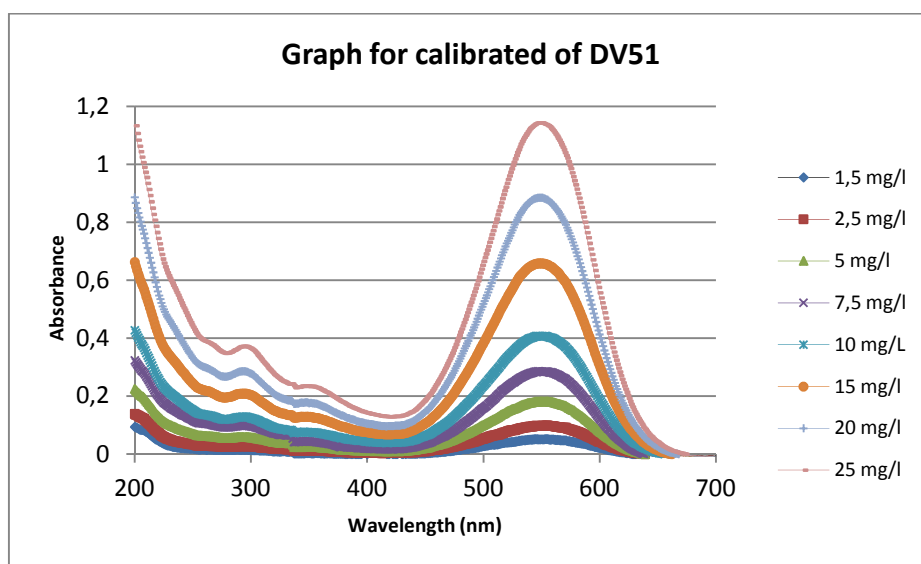


Figure 6.1 . Graph for calibrated of DV51.

Then, absorbances at λ_{\max} versus dye concentrations were represented, obtaining a linear relationship (Figure 6.2):

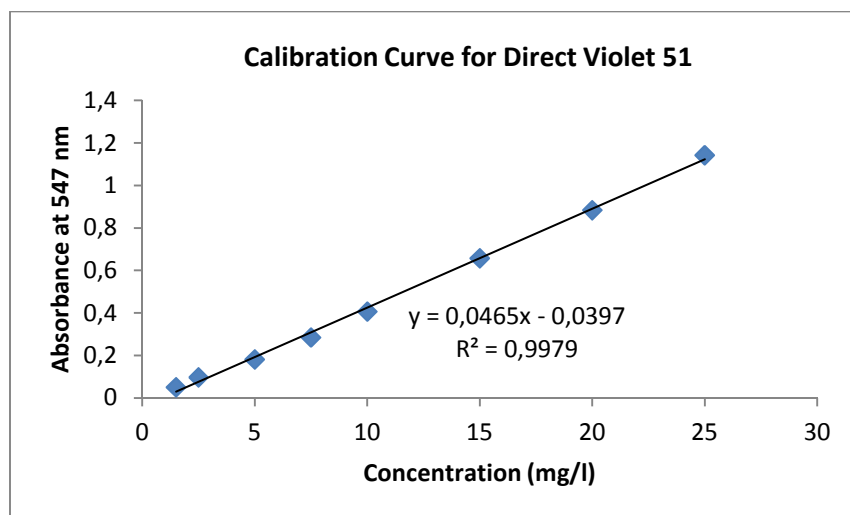


Figure 6.2 . Calibration curve for Direct Violet 51.

In all cases, calibration curves have shown a linear relationship, with a R^2 value higher than 0,99.

Using the mentioned relationships, concentrations were calculated for all experiences by the measure of absorbances by spectrophotometry.

Then $\ln C_0/C$ versus time was represented. The slope of the straight line obtained accounts the apparent constant rate of reaction.

In Annex III a table summarizes the experiments.

6.2. Spectrophotometry

Photocatalytic reaction follows a first-order kinetic model, as it has been explained. Although neutral dyes achieved complete decolorization, in most experiences with hydrolysed dyes and simulated dyehouse effluents total decolorization not happened. All spectra of dye solutions can be found in Annex IV.

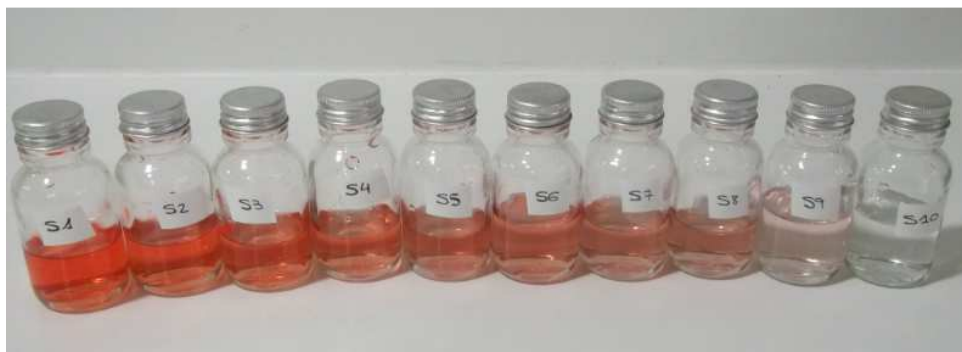


Figure 6.3. Samples for Direct Red 23.

In an azo dye, the interaction between an azo group (-N=N-) and two aromatic species originates the colour (Khataee et al, 2010). These mentioned aromatic nuclei are:

- An acceptor group frequently containing a chromophore (such as $-\text{SO}_3^-$ group).
- A donor group frequently containing an auxochrome (such as OH group).

The mechanism of dye degradation takes place when the fragile groups NH of these dyes loose an H atom by OH radicals (Zahraa et al, 1999).

The adsorption of dye solutions, produced by electrostatic attraction, is the first step and it occurs at the surface of TiO_2 . Adsorbed species are mineralized by hydroxyl radicals (Daneshvar, 2003). Therefore, this stage controls the photocatalytic degradation.

$$\%CR = \left(\frac{C_0 - C_E}{C_0} \right) \cdot 100$$

Equation 6.1. Percentage of colour removal.

In the Annex V kinetics results are summarized.

Photocatalytic decolorisation of the four dyes in neutral, hydrolysed and simulated dyehouse effluents is shown in the next figures (Figure 6.4, Figure 6.5, Figure 6.6, Figure 6.7) .

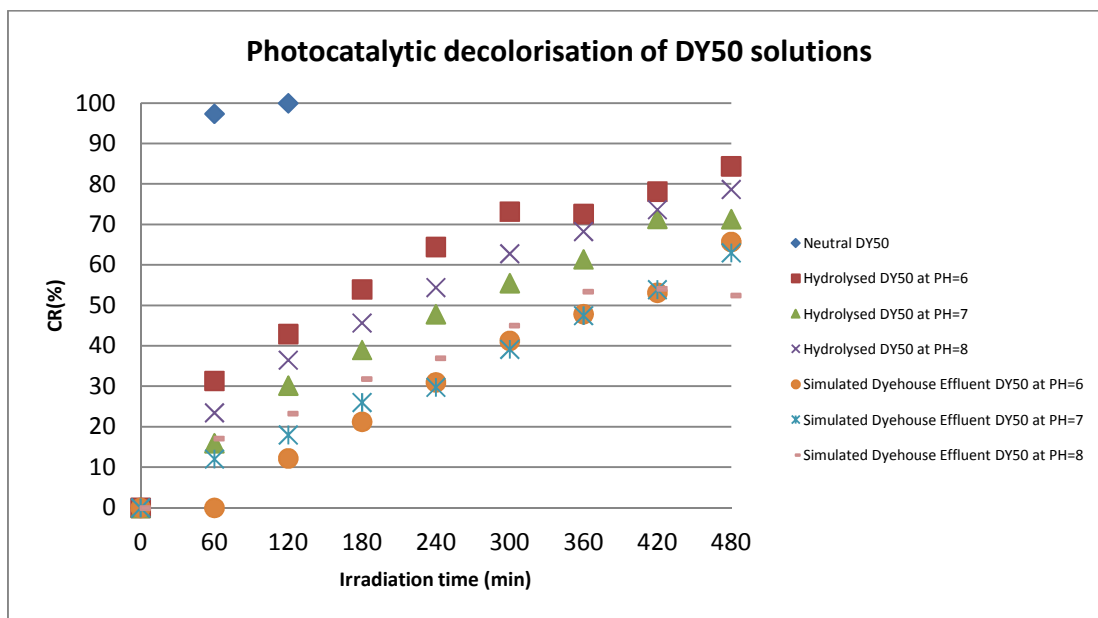


Figure 6.4. Photocatalytic decolorisation of DY50 solutions.

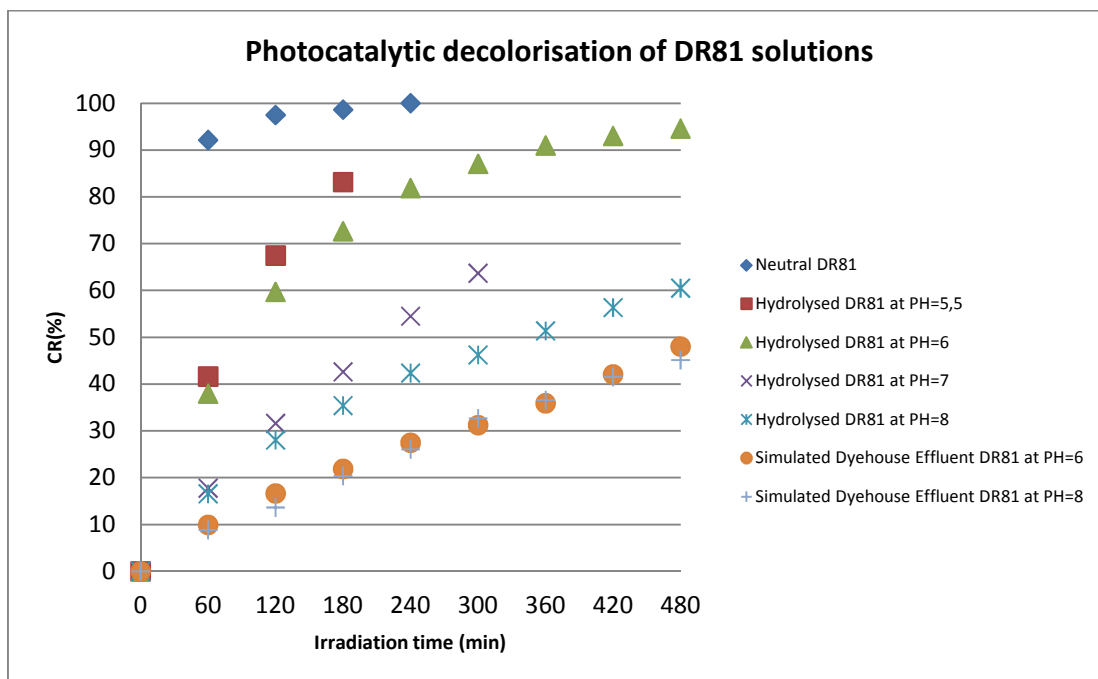


Figure 6.5. Photocatalytic decolorisation of DR81 solutions.

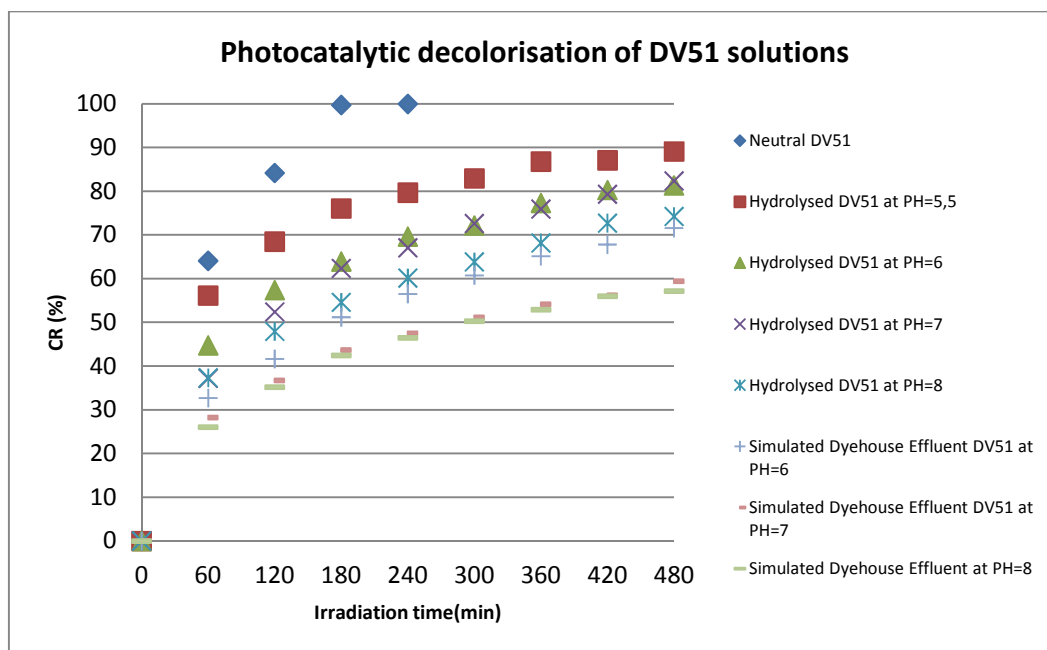


Figure 6.6. Photocatalytic decolorisation of DV51 solutions.

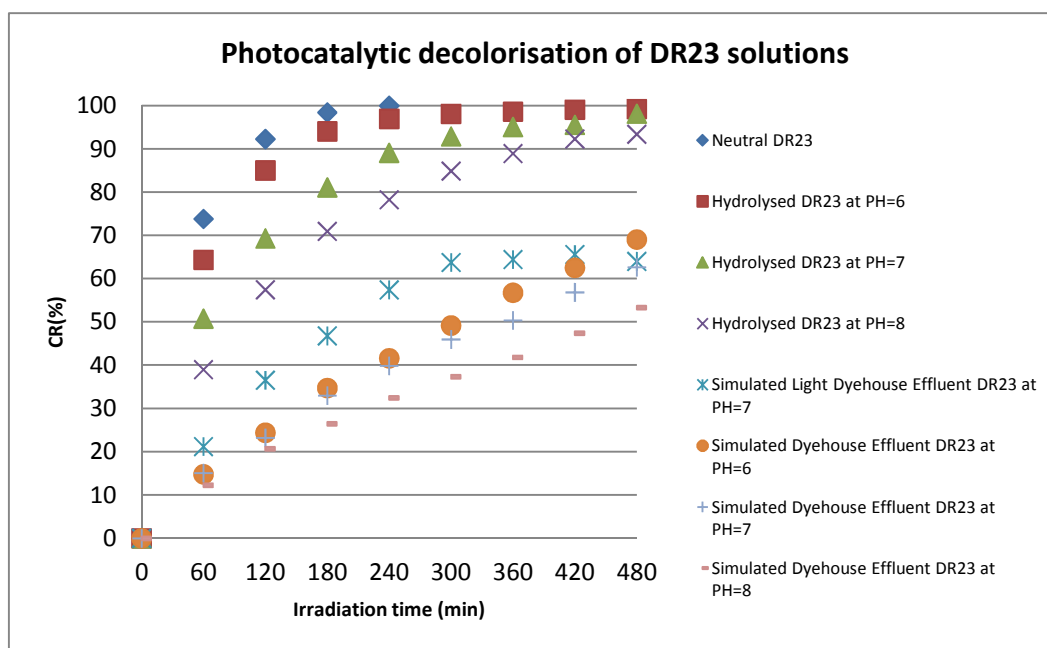


Figure 6.7. Photocatalytic decolorisation of DR23 solutions.

Viewing the previous graphs in which colour removal is represented versus irradiation time, it can be concluded that decolorization of neutral solutions occurred faster than the one of hydrolysed solutions and the latter, faster than the one simulated dyehouse effluents for all dyes that have been tested. Hydrolysis produces a breakdown in a dye molecule which retards the reaction. On the other hand, inorganic salts formed a double layer in catalyst surface which inhibits the adsorption of dyes.

Moreover, it has been observed that decolorization decreases with pH increases (for pH values between 6- 8). The reason for this observation may be attributed at the fact that the catalyst surface is positively charged in acidic solution and negatively charged in alkaline solution, according to the isoelectric point of charge of TiO₂ (Khataee et al 2010, Alinsafi, 2005).

Also, in figure 6.8 it can be seen how chemical substance concentration affects in the photocatalytic reaction because an increase of concentration delays decolorization due to the presence of impurities in dye solutions, consume hydroxyl radicals and blocks the light penetration in solution (Guillard et al, 2003).

A comparison between different studied neutral azo dyes shows that chemical structure of dyes influences the degradation rate:

Dye	Azo groups (-N=N-)	Chromophore (-SO ₃ ⁻)	Aromatic rings	H Bond Donor	H Bond Acceptor	k _{app}
DY50	2	4	6	2	17	0,0496
DR81	2	2	4	2	12	0,0421
DV51	2	2	5	2	13	0,0308
DR23	2	2	6	5	7	0,0220

Table 6.1. Apparent constant rates and structural characteristics of neutral dyes.

Analyzing the results, it can be concluded that generally a higher number of H bond acceptor groups (in which chromophore groups are included) in dye molecule implies that photocatalytic reaction happens faster. This fact is related with the negative charge of -SO₃⁻ groups that capture hydrogens of water, increasing solubility of dye molecule in water. Owing

the increase of solubility, the mass transfer between catalyst surface and dye solution, is improved.

In addition, in dyes with the same number of azo and $-\text{SO}_3^-$ groups when the number of aromatic rings grows, the photocatalytic reaction is slower because a greater number of bonds have to be degraded.

Decolorisation reactions of hydrolysed solutions of Direct Red 23 were the fastest of all hydrolysed solutions. This fact, can be originated because this dye presents the greatest amount of NH fragile groups, which are easier to degrade by hydrolysis.

Next, the decolorisation for dyes in different conditions is compared:

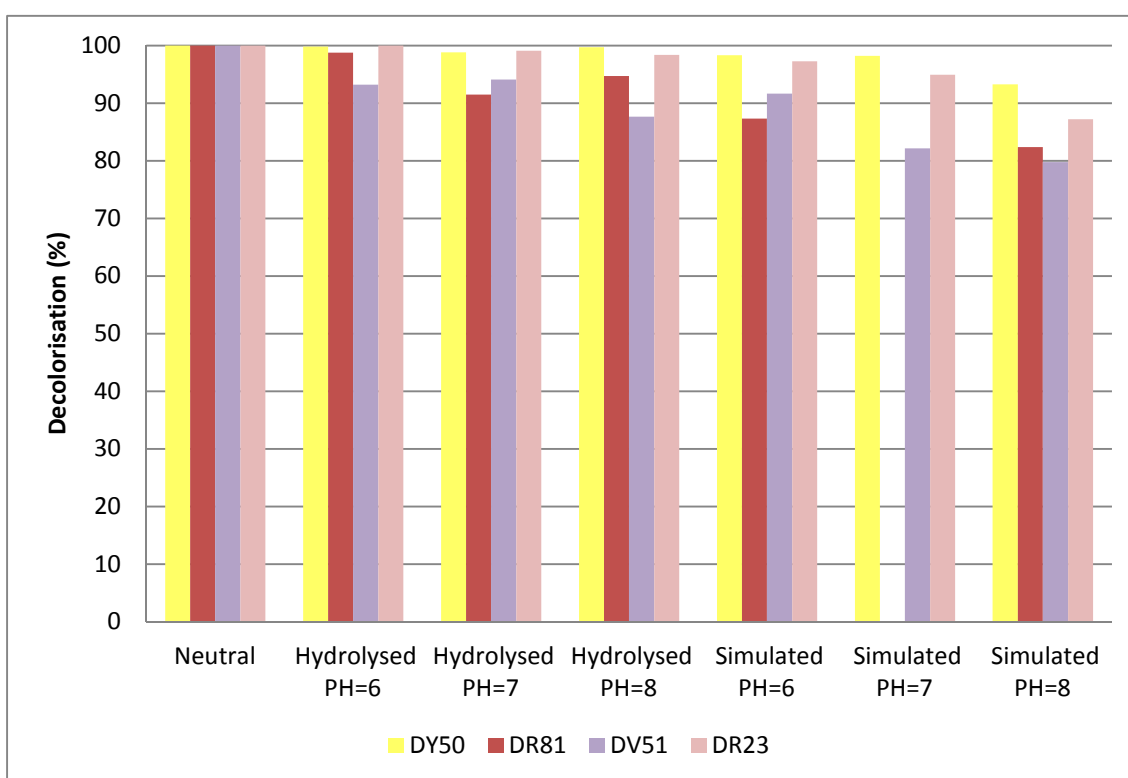


Figure 6.8. Decolorisation comparison for dye solutions.

The decolorisation is larger than 80% in all experiences, except for simulated dyehouse effluent of DV51 at pH =8.

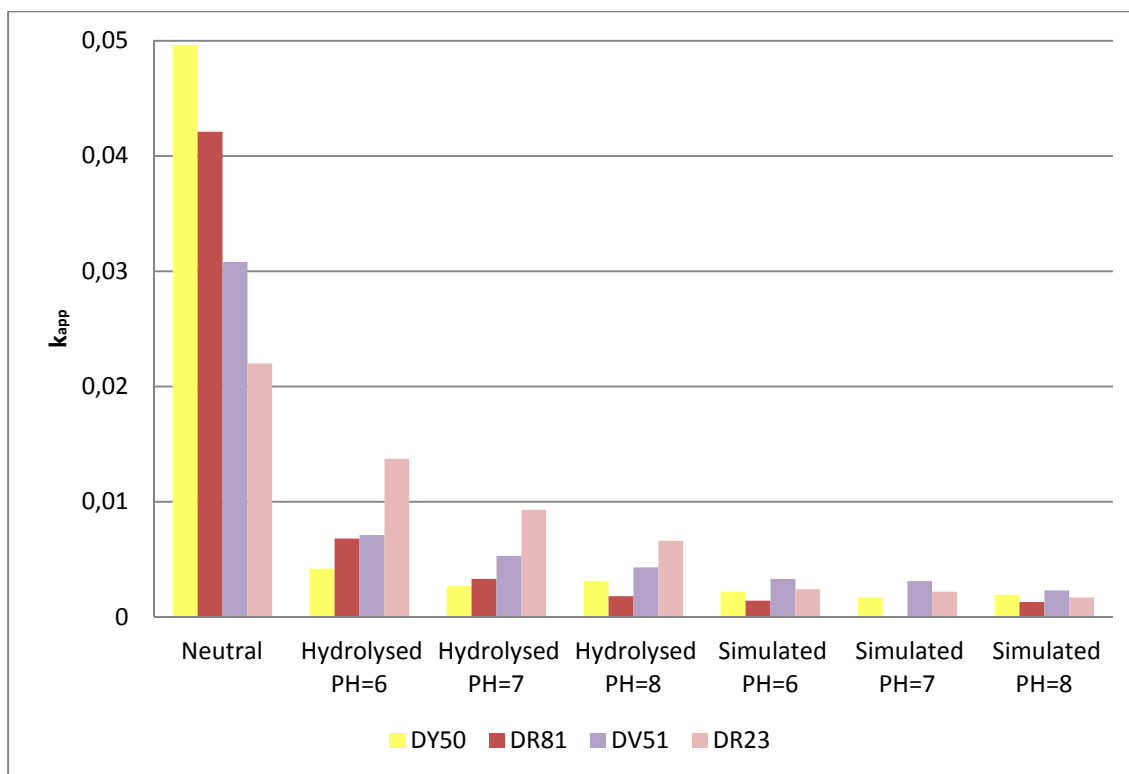


Figure 6.9. Apparent rate constants for dye solutions.

It is observed that apparent rate constants decrease largely in hydrolysed solutions and simulated dyehouse effluents with respect to neutral solutions, due to the effects discussed above involving changes on catalyst surface. This situation provokes an inhibition in the photocatalytic reaction more pronounced in the case of effluents due to the presence of chemical ions.

The adverse behavior occurred for the degradation of hydrolysed solutions (figure 6.9). The degradation rate constants for this solutions at pH=6 can be observed in the table 6.2.

Dye	Azo groups (-N=N-)	Chromophore (-SO ₃ ⁻)	Aromatic rings	Amide groups	k _{app}
DR23	2	2	6	2	0,0137
DV51	2	2	5	0	0,0071
DR81	2	2	4	1	0,0068
DY50	2	4	6	1	0,0042

Table 6.2. Apparent constant rates and structural characteristics of hydrolysed dyes at pH=6.

In hydrolysed dyes, degradation is favored in dyes with more amide groups and less sulfate groups. This fact can be attributed at the easy of degradation of amides by hydrolysis in carboxyl acids and the substitution between sulfate ions and hydroxyl radicals during this process.

6.3. Total Organic Carbon

The values of total organic carbon were determined for initial and final samples.

In the Annex VI results of TOC analysis are shown.

The amount of TOC in final samples reflects the quantity of organics in solution and the decrease of TOC between initial and final dye solutions shows the degree of degradation of the photocatalytic process.

The figure 6.10 represents the amount of TOC removed in the experiences.

While dye solutions are degraded quickly, with a total decolorization in neutral dye solutions, TOC is degraded much more slowly and a proportion of it remains in the final samples.

The largest removal of TOC is produced in acidic solutions at pH=6 due to the positively charged catalyst surface at these conditions, and therefore, the increase of OH radicals to oxidize organic carbon into CO₂. TOC removal decreases as pH increases. Moreover, when chemical ions appear in solution the TOC removal is lower due to the competitiveness to degrade organic carbon on catalyst surface.

In the specific case of the dye "Direct Violet 51", for hydrolysed solutions and simulated dyehouse effluents at pH=7 and pH=8 the photocatalytic process was inefficient because there was not any removal of TOC.

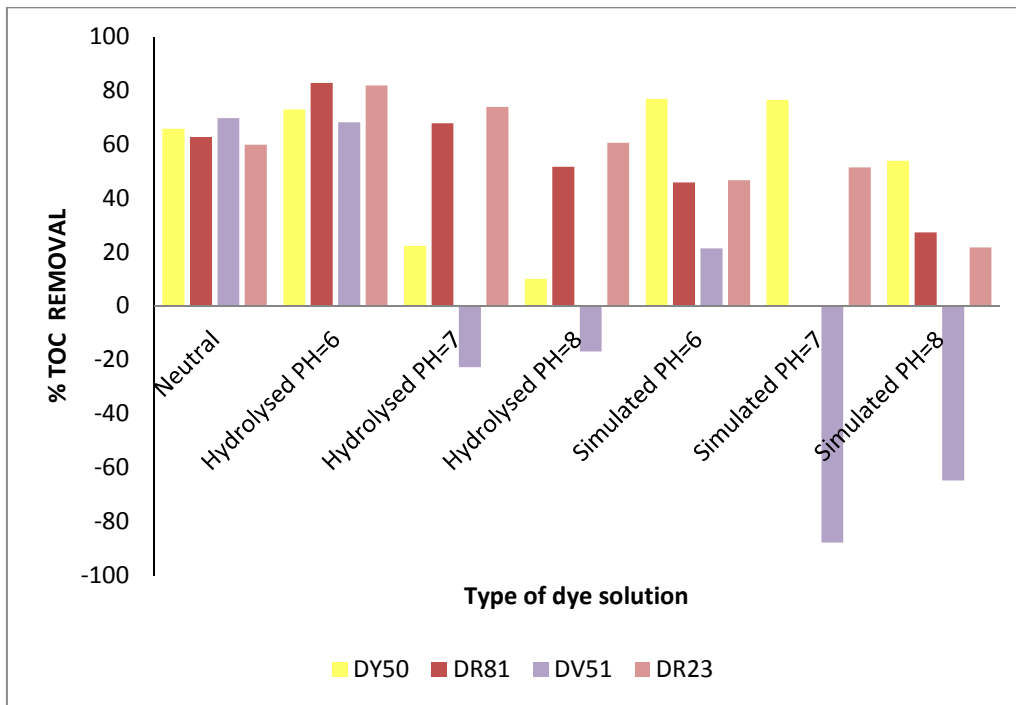


Figure 6.10. Percentage of TOC removal for studied experiences.

6.4. Ammonium and nitrates

All of dyes that have been tested contain a source of nitrogen including two azo groups (see Annex VII).

Research works have demonstrated that the azo group is transformed into ammonium and N_2 by photocatalytic reaction (Khataee et al, 2010). In photocatalysis, the azo group ($R-N=N-R$) is attacked by hydroxyl radical to transform into two amine groups ($R-NH_2$). H° radicals generated by photoreduction of photons attacks nitrogen atom of these amine groups generating ammonium. Then, ammonium can be oxidized to nitrates by hydroxyl radicals.

A calculation was made in order to compare the amount of ions that was measured at laboratory and the amount expected. Then, an example of this calculation for Direct Violet 51 is detailed.

First, the molar concentration of dye is expressed in units of $\mu\text{mol/l}$:

$$\text{Direct Violet 51} = \frac{C_0}{M} = \frac{25\text{mg/l}}{719,1\text{g/mol}} \cdot 10^3 = 34,7 \mu\text{mol/l}$$

The highest expected amount of ammonium and nitrates is determined assuming that nitrogen atoms in the dye molecule that are not in azo bonds, are converted into these ions. In the case of Direct Violet 51, there is one nitrogen atom not in azo bond.

$$\text{Expected Ions in DV51} = \frac{34,7\mu\text{mol}}{\text{l}} \cdot 1_{\text{NITROGEN ATOM}} = 34,7\mu\text{mol/l}$$

In the Annex VII, the amount of measured and expected ions appears.

In the figure above, it can be seen clearly how the amount of ions measured in experiences with Direct Violet 51 that were inefficient from photocatalytic point of view, was greater than the amount expected. Moreover, in the experience with Direct Red 81 at pH=8 this situation also happened.

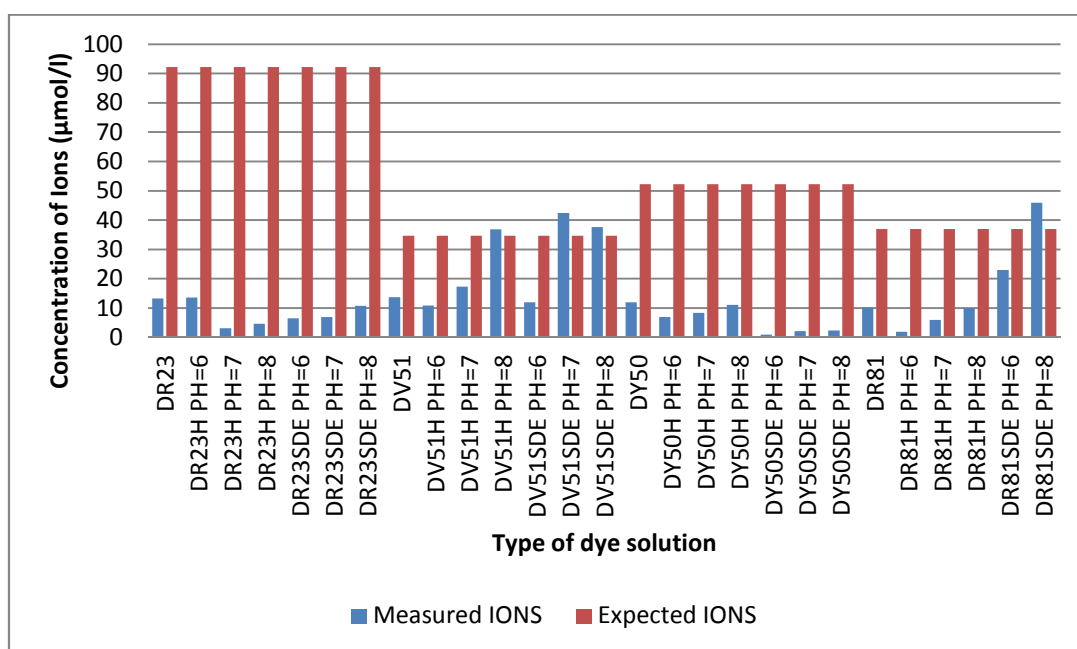


Figure 6.11. Comparison for ions of dye solutions.

The values for nitrates only were obtained in experiences with a total decolorization, but ammonium ions affected in a further way that nitrates.

However, in practically all experiences ions measured are less than ions expected. A reason for this behavior can be attributed at the formation of nitrogen gas over ammonium.

6.5. Toxicity

Toxicity tests with lettuce seeds

Some assumptions were made to calculate toxicity parameters:

- Calculations for toxicity test were made with controls of water EVIAN, because for this water the greater and the lower seed lengths were obtained.
- The seed length of positive control for water EVIAN was supposed to be 4,70 cm for calculations. The value measured was of 4,24 cm.

In the Annex IX, results for toxicity test with lettuce seeds are exposed.

In the laboratory, lettuce seed growth was measured in initial and final dye solutions and positive and negative controls with two types of water. In the next figure samples for toxicity test are shown. It can be seen that final samples scarcely have coloration.



Figure 6.12. Some samples for toxicity test.

In almost all experiences seed germination was around 100% (figure 6.13). The neutral dye with the lowest absolute germination was Direct Yellow 50. Other experiences with minor germination were initial hydrolysed solutions which can be the result of generation of toxic amines during the process of hydrolysis.

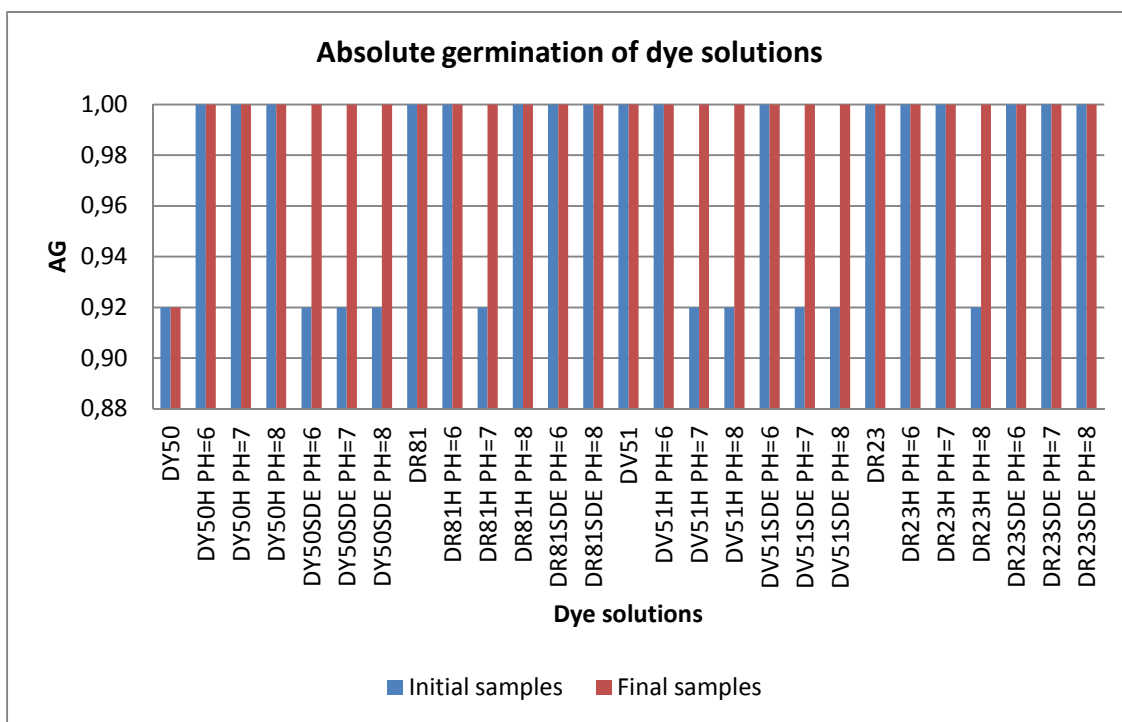


Figure 6.13. Absolute germination of dye solutions.

In the figure 6.14 it can be observed a comparison between initial and final samples for the average length of seeds of dye solutions. All experiences the average length of germinated seeds was upper than 3,0 cm. In addition, the growth generally was greater in final samples than in initial samples, this fact is directly related with the application of photocatalytic process.

In positive controls with pure water the average seed lengths were 4,24 cm for EVIAN water and 3,84 cm for VITTEL water. These values have reached in a high number of studied experiences, so it could be argued that samples allow practically a standard growth of seedlings.

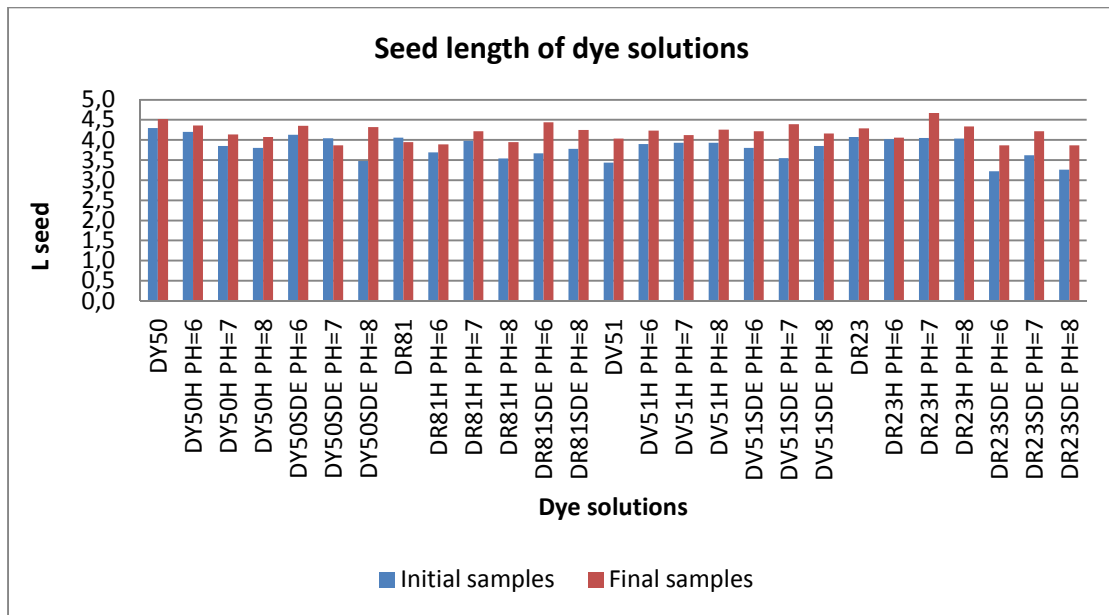


Figure 6.14. Average seed length of dye solutions.

Relative toxicity only reached a value of 50% in two experiences as it can be seen in figure 6.15. These are the experiences with simulated dyehouse effluents of Direct Red 23 at pH 6 and 8. As it could be expected, at pH=7 usually appeared a less toxicity than at acidic or basic pH due to the addition of chemical substances to adjust the pH.

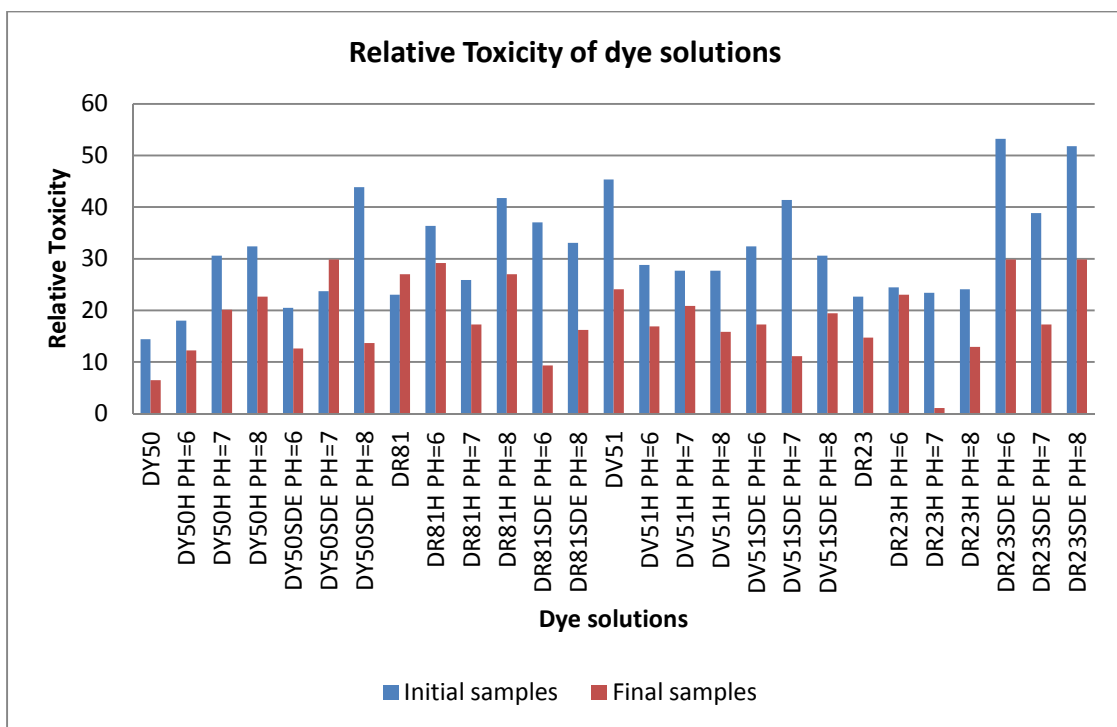


Figure 6.15 . Relative toxicity of dye solutions.

The decrease in relative toxicity was significant in most of dye solutions, although some exceptions appeared which could be due to the emergence of toxic amines during the degradation process of azo dyes.

As it would be expected, simulated dyehouse effluents were the most toxic samples in general by the presence of chemical substances on them.

In initial samples for neutral dyes, toxicity was attributed at azo dye; but in final samples and hydrolysed solutions toxicity was ascribed at toxic amines that are generated during hydrolysis and photocatalytic process. Although neutral dyes are completely degraded by photocatalytic process, the toxicity of final samples is attributed to the mentioned toxic amines.

The percentage of toxicity removal is included in figure 6.16. Direct Red 23 was the dye solution with the greatest toxicity removal. In addition, in photocatalytic process with hydrolysed dyes the highest toxicity removal has been obtained. This fact implies that toxic amines have been reduced in final samples of these solutions.

A remarkable point of this study, was that after photocatalytic process not all dyes decreased in toxicity how it can be seen in the figure 6.16.

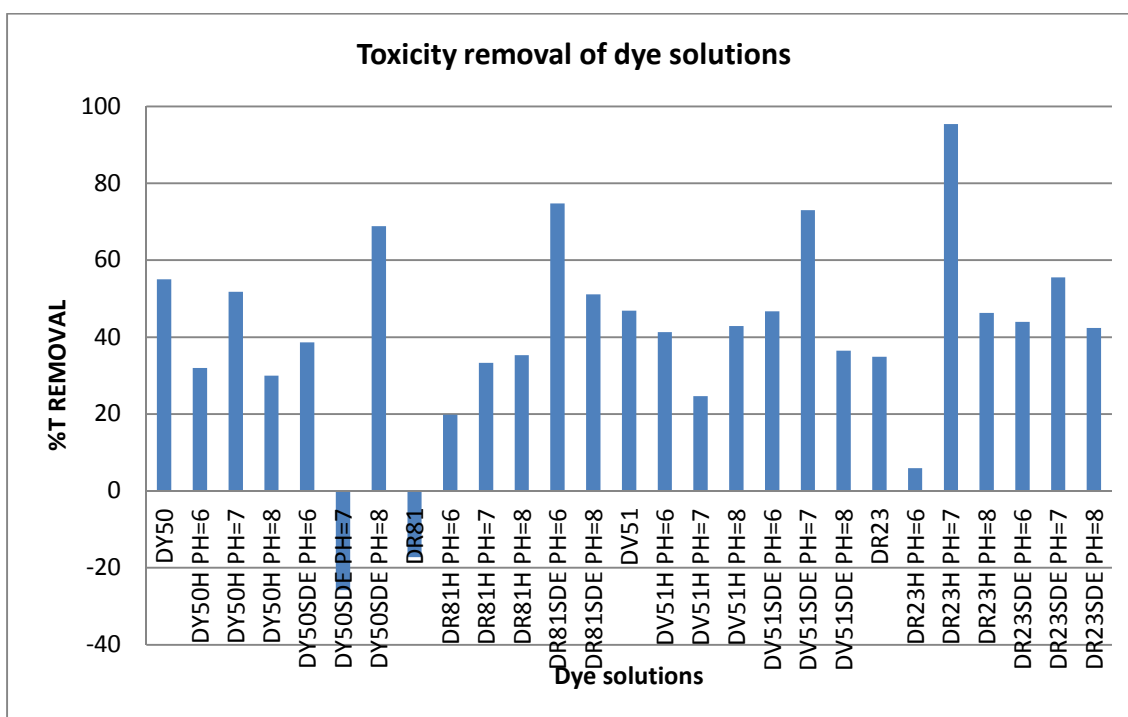


Figure 6.16. Toxicity removal of dye solutions.

From toxicity tests performed, it is not possible establish a relationship between the results obtained for the different dye solutions and the chemical structure dyes.

The germination index was higher than 0,8 in all final samples (figure 6.17).

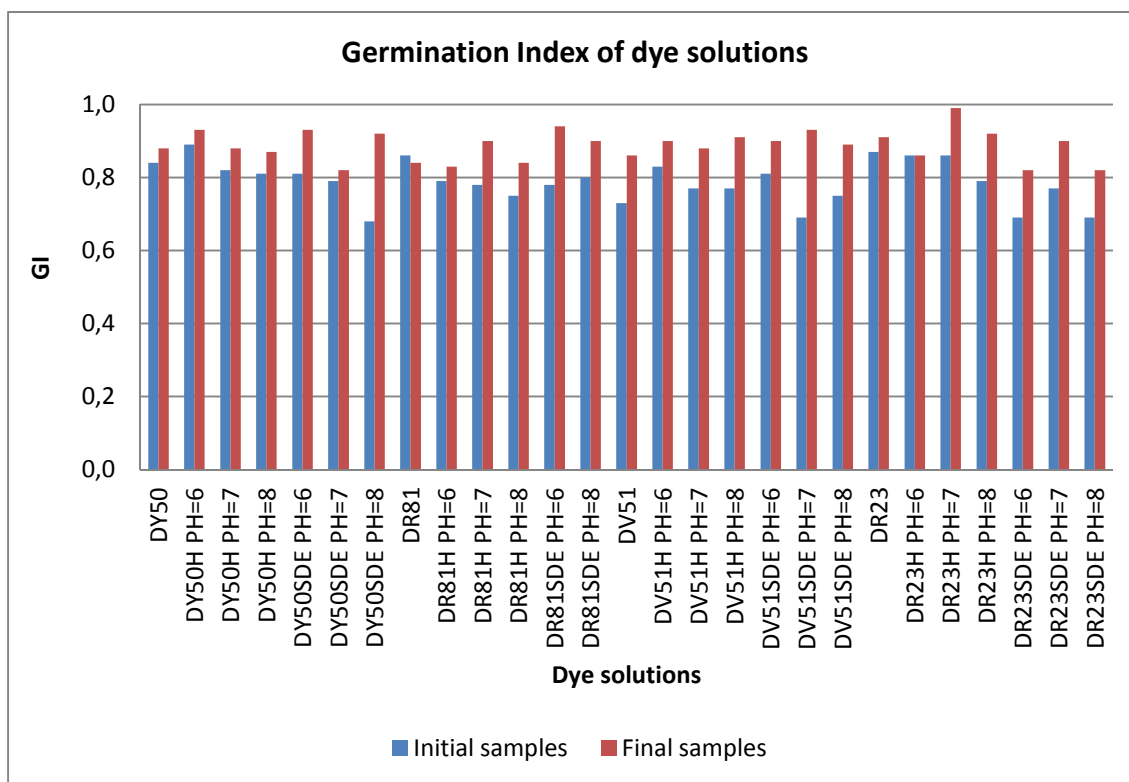


Figure 6.17. Germination Index of dye solutions.

Compared with the positive control seeds with 100% germination index, dye solutions contained some phytotoxicity inhibitions.

Dye solutions had a stronger inhibitory effect on root length and germination seed percentage. Generally, a value of germination index below 50% indicates that phytotoxic compounds might have not been metabolized, inhibiting germination (Epstein, 1997). However, in the case of dyehouse effluents, the salt concentrations might have inhibited seed development and thus reduced germination index.

On the other hand, in tested samples the inhibition of root growth appeared as more sensitive phytotoxicity indicator than the number of germinated seeds. The higher toxicity of these solutions can be attributed mainly at the combination of several characteristics such as their

high salinity and of any excess of organic compounds or ammonium ions (Hoekstra et al.,2002).

Analyzing the results obtained in toxicity test, although for the majority of tested dye solutions the decrease in toxicity is achieved, in some experiences a more toxic product was obtained. For this reason, a secondary treatment process should be applied.

Comparison of plants for germination toxicity tests

A comparison study of six types of plants for toxicity was performed with initial and final samples of neutral azo dyes. The samples for Direct Red 23 can be seen in the next figure:

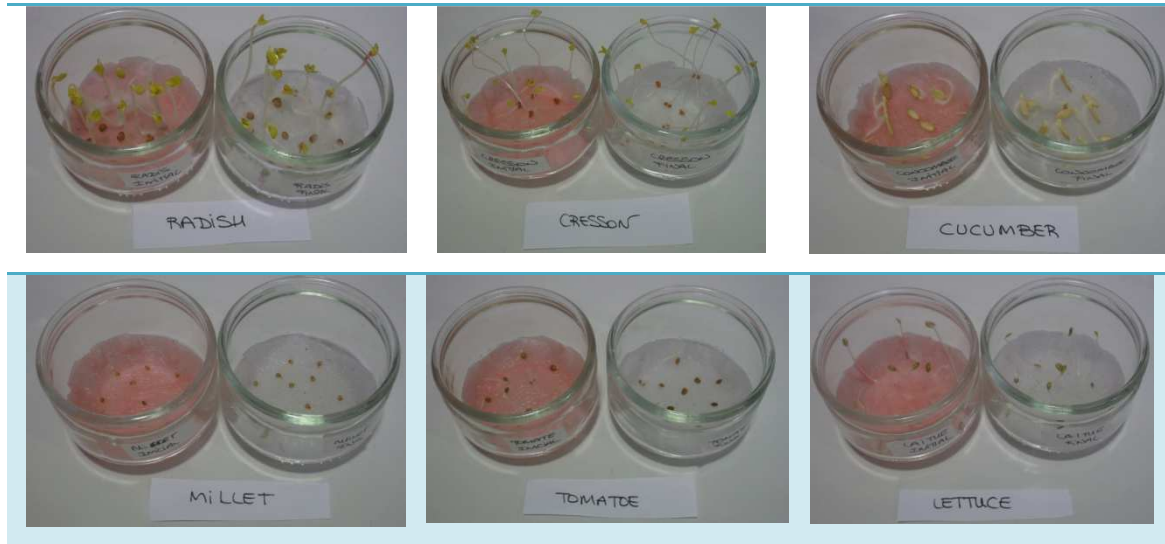


Figure 6.18 . Samples of DR23 for comparison toxicity test.

The experimental observations of germinating seedlings are shown in figure 6.19 .

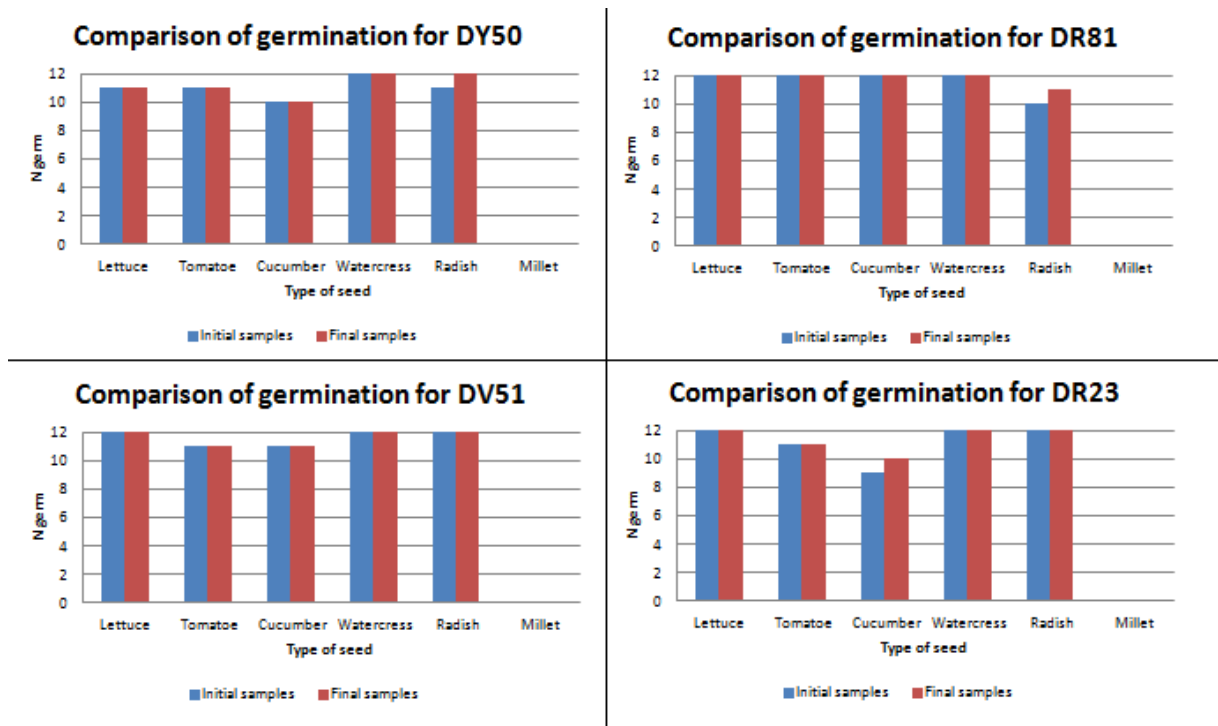


Figure 6.19. Comparison of germination for neutral dyes.

For germination test, the plants that have shown an increasing number of germinated seeds were radish, lettuce and cucumber. The seeds of millet have not germinated in any case.

The length of seeds was measured for experiences and results are shown in the figure 6.20. Radish, lettuce and watercress provided the best results for toxicity study although radish and watercress seeds were difficult to measure due to the emergence of long radicles into the absorbent paper.

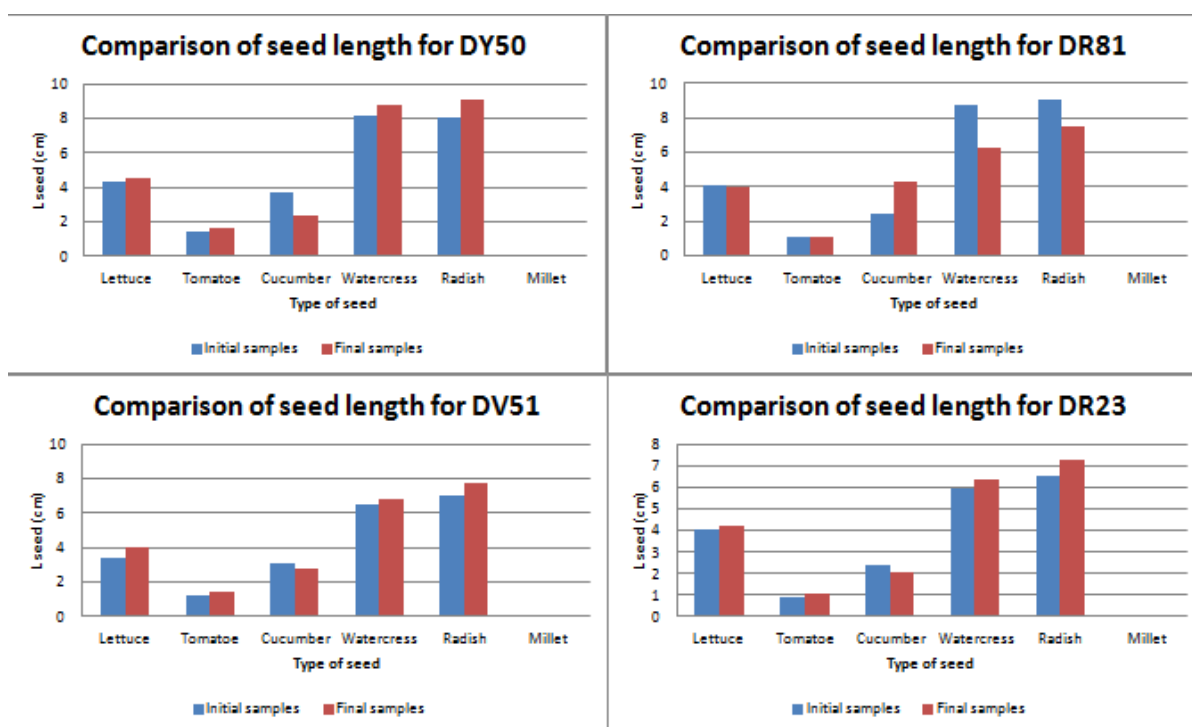


Figure 6.20. Comparison of seed length for neutral dyes.

Radish and lettuce were seeds that have showed significant sensitivity to azo dyes.

According to the ease of procedure, lettuce seeds are the best plant to use for germination toxicity studies. This type of seed is sensitive to the pollutant and is relatively easy to enumerate. Other comparison studies of plants for germination toxicity tests have indicated the same (Banks and Schultz).

CHAPTER 7: CONCLUSIONS AND PERSPECTIVES

Photocatalytic decolorisation and mineralization of four direct azo dyes, with two azo groups, in neutral, hydrolysed solutions and simulated textile effluents has been tested in presence of immobilized TiO₂ nanoparticles on non-woven paper under UV radiation. Results have shown that decolorisation was complete in neutral solutions, but not in the majority of hydrolysed solutions and simulated effluents. It has been mentioned that the adsorption takes place at catalyst surface.

With regard to the pH of solution, for pH between 6 and 8, it has been observed that dye degradation was favored at acidic pH, which can be attributed at the positively charge of catalyst surface under those conditions. So, the adsorption occurs faster due to the anionic charge of dye molecule.

On the other hand, the effect of inorganic salts in simulated dyehouse effluents could be attributed to the formation of a double layer of these salts at catalyst surface which produces the inhibition in the adsorption of solutions.

It can also be concluded that degradation rate at catalyst surface depends on the type of catalyst employed, the characteristics of degraded sample and the chemical structure of dye involved in solutions. For example, it has been seen that in neutral dyes with a great number of sulfates in their structure, degradation was faster. In the same way, neutral dyes with the same number of sulfate groups in their structure were degraded more slowly when this structure had more aromatic rings. The first aspect can be explained because a greater number of sulfates in dye molecule, implies an increase in anionic charge of dye. The second one can be due to the fact that the dye molecules with more aromatic rings have a higher value of molecular weight. However, in hydrolysed solutions and simulated effluents this behavior did not happened since dye molecules were broken into smaller ones by hydrolysis and also some inorganic substances were added. In hydrolysed dyes, degradation was favored in dyes with more amide groups and less sulfate groups. The previous aspect can be attributed to the ease of degradation of amides by hydrolysis in carboxylic acids and the substitution between sulfate ions and hydroxyl radicals. In addition, it would be necessary to know thoroughly the mechanisms that take place during hydrolysis in order to understand clearly

how degradation phenomenon is produced and how inorganic salts acts in the reactions. This is a difficult task by the complexity to study how light interfere to degrade dye solutions.

By photocatalytic procedures, the degradation of all dye solutions was not achieved within the 24 hours of the experiment because in some experiences TOC was not removed, and in others the removal was rather low. Under acidic conditions, a greater TOC removal occurred due to the positively charge of catalyst surface at these conditions, and therefore, the increase of OH radicals to oxidize organic carbon.

For ammonium and nitrates, in practically all experiences the measured amount was less than expected. It could be due to the formation of N_2 over ammonium.

Concerning to the toxicity, final samples of dye solutions had acceptable germination index but, in some cases, there was not any toxicity removal.

In conclusion, in most cases, heterogeneous photocatalysis is a good treatment for textile wastewaters allowing practically total adsorption of dyes. However, TOC results showed that organic compounds remained in the solution. For this reason, and to decrease the toxicity of final samples, a secondary treatment process, possibly a biological treatment, should be applied.

The fact that the textile wastewater can be treated with solar irradiation would eliminate major operational costs making this methodology an attractive alternative treatment process.

REFERENCES

Alinsafi, A.: 2005, "Traitabilité de Rejets Liquides de l'Industrie Textile". Doctoral Thesis. National Polytechnic Institute of Lorraine (ENSIC Group, Nancy, France) and University of Cadi Ayyad (Marraketch).

Anastas, P., Wagner, J.: 1998, "Green Chemistry: Theory and Practice" p. 30.

Andreozzi, R., Caprio, V., Insola, M., Marotta, R.: 1999, "Advanced oxidation processes (AOP) for water purification and recovery". Catalysis Today. Volume 53, Issue 1: 51 – 59.

Arslan I., Bahnemann D.W., Balcioglu A.I.: 2000, "Heterogeneous photocatalytic treatment of simulated dyehouse effluents using novel TiO₂ – photocatalysts". Applied catalysis B: Environmental (26) : 193-206.

Banks, M.K. and Schultz, K.E.: 2005, "Comparison of plants for germination toxicity tests in petroleum-contaminated soils". Water, Air and Soil Pollution (2005) 167: 211 – 219.

Bianco – Prevot, A., Fabbri, D., Promauero, E., Morales – Rubio, A., de la Guardia, M.: 2010. "Continuous monitoring of photocatalytic treatments by flow injection. Degradation of dicamba in aqueous TiO₂ dispersions". Chemosphere 44 (2001): 249 – 255.

Candal, R.J., Bilmes, S.A., Blesa, M.A.: 2001, "Semiconductores con actividad fotocatalítica". Eliminación de contaminantes por Fotocatálisis Heterogénea. Chapter 4: 79 – 102.

Celis, J., Sandoval, M. and Briones, M.: 2007, "Bioensayos de fitotoxicidad de residuos orgánicos en lechuga y ballica anual realizados en un suelo alfisol degradado". R.C. Suelo Nutr. Veg., Vol.7, n.3 : 51 – 60.

Chamorro, X., Rodríguez, G., Enríquez, A.L.: 2010, "Montaje y validación del método de análisis por combustión y detección por IND del COT en agua". LunAzul Scientific Journal 30/01/2010.

Chen, H.Y., Zahraa, O., Bouchy, M.: 1997, "Inhibition of the adsorption and photocatalytic degradation of an organic contaminant in an aqueous suspension of TiO₂ by inorganic ions". Journal of Photochemistry and Photobiology A: Chemistry: 37 – 44

Chung, A., Gilks, B., Dai, J.: 1999, "Introduction of fibrogenic mediators by fine and ultrafine titanium dioxide in rat tracheal explants". AJP – Lung Physiol November 1.1999 Vol 277 no. 5 L975 – L982.

Cooper, S.G.: 1978, "The textile industry. Environmental control and energy conservation" p. 385.

Daneshvar, N., Salari, D. et al.:2003, "Photocatalytic degradation of azo dye acid red 14 in water: investigation of the effect of operational parameters". Journal of Photochemistry and Photobiology A: Chemistry 157 (1): 111 - 116

Epling, G.A., Lin, C.: 2002, "Investigation of retardation effects on the titanium dioxide photodegradation system". *Chemosphere*, 2002a, (46): 937 – 944.

Environmental Protection Agency (EPA): 2009, "Nanomaterial Case Studies: Nanoscale Titanium Dioxide in Water Treatment and in topical Sunscreen". EPA/600/R – 09/057 July 2009.

Environmental Protection Agency (EPA): "Water Laws & Executive Orders" Retrieved: 06/04/2012.

Epstein, E.: 1997, "The Science of Composting". Technomic Publishing Company, Inc., Pennsylvania, USA: 1-487.

ExplainThatStuff, Online Science Book: "How does a photocatalytic air purifier work?". Retrieved: 03/05/2012 from <http://www.explainthatstuff.com/how-photocatalytic-air-purifiers-work.html>

Figueiredo, J.L., Pereira, M.M., Faria, J.: 2008, "Catalysis from Theory to Application. An integrated course".

Fox, M.A., Dulay, M.T.: 1993 "Heterogeneous Photocatalysis" *Chem. Rev*, 93: 41.

Forero, J.E., Ortiz, O.P., Rios, F.: 2005, "Advanced oxidation processes as phenol treatment in industrial sewage". *Ciencia y tecnología del futuro*, 3: 97 – 109.

Frische, T.: 2003, "Ecotoxicological evaluation of in situ bioremediation of soils contaminated by the explosive 2,4,6-trinitrotoluene (TNT)". *Environ Pollut* 121 (1) : 103 – 13.

Guillard, C., Lachheb, H., Ksibi, M., Herrmann, J.M., Houas, A. and Elaloui, E.: 2003 "Influence of chemical structure of dyes, of pH and inorganic salts on their photocatalytic degradation by TiO₂ comparison of the efficiency of powder and supported TiO₂" *Journal of Photochemistry and Photobiology A: Chemistry*: 27 – 36.

Guillard, C., Puzenat, E., Lachheb, H., Houas, A. and Herrmann, J – M.: 2005, "Why inorganic salts decrease the TiO₂ photocatalytic efficiency". *International Journal of Photoenergy*. Vol 07.

Gumy, D., Hajdu, R., Giraldo, S., Pulgarin, C. et al.: 2005, "Influence of TiO₂ Physico – Chemical Characteristics on Photocatalytic E. Coli Inactivation" *SolarSafe Water Simposio*: 3 - 6

Hagen, J.: 1999, "Industrial Catalysis. A practical approach".

Hager, D.G.: 1990, "UV – catalyzed hydrogen peroxide chemical oxidation of organic contaminants in water". *Innovat. Hazard. Waste Treat. Technol. Ser*, 1990 (2) : 143 – 153.

Haneko, M. and Okura, I.: 2002, "Photocatalysis. Science and Technology"

Hamadani, M., Reisi – Vanani, A. and Majedi, A.: 2008, "Sol – Gel Preparation and Characterization of CO/TiO₂ Nanoparticles: Application to the Degradation of Methyl Orange". *J. Iran. Chem. Soc.*, Vol. 7, Suppl., July 2010: 552 – 558.

- Hermann, J.M.:1999, "Heterogeneous photocatalysis fundamentals and applications to the removal of various types of aqueous pollutants". *Catalysis Today*. Vol. 53, Issue 1: 115 -129.
- Hoekstra, N.J., Bosker, T. and Lantinga, E.A.: 2002, "Effects of cattle dung from farms with different feeding strategies on germination and initial root growth of cress (*Lepidium sativum* L.)". *Agric. Ecosyst. Environ.*, 83: 189-196.
- Hunger, K., Mischke, P., et al.: 2011, "Ullmann's Enc. Of Industrial Chemistry: Azo Dyes" p. 2497 – 2589.
- Khataee, A.R., Pons, M.N. and Zahraa, O.: 2010. "Photocatalytic decolorization and mineralization of orange dyes on immobilized titanium dioxide nanoparticles". *Water Science and Technology* 62,5: 1112 – 1120.
- Khouni, I., Marrot, B., Moulin, P. and Amar, R.B.:2011, "Decolourization of the reconstituted textile effluent by different process treatments: Enzymatic catalysis, coagulation/flocculation and nanofiltration processes". *Desalination* 268 (2011): 27 – 37.
- Legrini, O., Oliveros, E. and Braun, A. M.:1993, "Photochemical Processes for Water Treatment".*Chem.Rev* (93): 671 – 698.
- Linsebigler, A.L., Lu, G., Yates, J.T.:1995, "Photocatalysis on TiO₂ surfaces: Principles, Mechanisms, and Selected Results".
- Mantzavinos, D., Psillakis, E.:2004, "Enhancement of biodegradability of industrial wastewaters by chemical oxidation pre-treatment". *Journal of Chemical Technology and Biotechnology* 79: 431 – 454.
- Nasr – Esfahani, M., Habibi, M.H.: 2008, "Silver doped TiO₂ Nanostructure Composite Photocatalyst Film Synthesized by Sol – Gel Spin and Dip Coating Technique on Glass".*International Journal of Photoenergy*. Volume 2008, Article ID 628713, 11 pages.
- Neppolian, B., Choi, H.C., Sakthivel, S., Arabindoo and B., Murugesan, V.:2001, "Solar/UV – induced photocatalytic degradation of three commercial textile dyes". *Journal of Hazardous Materials* B89 (2002): 303 – 317.
- Pagga, U., Brown, D.: 1986. "The degradation of dyestuffs: part II. Behavior of dyestuffs in aerobic biodegradation tests". *Chemosphere* 15: 479 – 491.
- Palácio, S.M., Espinoza, F.R., Módenes, A.N., Oliveira, C.C., Borba, F.H. and Silva, F.G.:2009, "Toxicity assesment from electro-coagulation treated-textile dye wastewaters by bioassays". *Journal of Hazardous Materials* 172 (2009): 330 – 337.
- Palmisano, G., Augliaro, V., Pagliaro, M. and Palmisano, L.: 2007, "Photocatalysis: a promising route for 21st century organic chemistry". *ChemComm* 33: 3425 - 3437.
- Pekakis, P.A., Xekoukoulotakis, N.P., Mantzavinos, D.:2006, "Treatment of textile dyehouse wastewater by TiO₂ photocatalysis". *Water Research* 40: 1276 – 1286

Pfoertner, K. H.: 2011, "Ullmann's Enc. Of Industrial Chemistry: Photochemistry", p. 18675 – 18703.

Research Centre for Nanosurface Engineering: " Properties of TiO₂ photocatalyst". Retrieved: 03/05/2012 from http://www.nanopin.cz/en/en_page01.html

Ruza, J., Bordas, M.A., Espinosa, G., Puig, A.: 2007, "Manual para la gestión de vertidos" p. 161 – 171.

Rashed, I.G., Hanna, M.A., El-Gamal, H.F., Al – Sarawy, A.A., Wali, F.K.M.: 2005. "Overview on chemical oxidation technology in wastewater treatment". Ninth International Water Technology Conference, IWTC9 2005.

Rodríguez, A., Letón, P., Rosal, R., Dorado, M., Villar, S.: 2006, "Tratamientos avanzados de aguas residuales industriales. Informe de vigilancia tecnológica". CITME.

Solar Energy Materials and Devices Group of Renewable Energy Laboratory: "Photocatalytic Water Splitting". Retrieved: 01/05/2012 from: http://solar.iphy.ac.cn/index.php?page_id=1775&lang=en

Serpone, N, Pelizzetti, E.: 1989 "Photocatalysis: Fundamental and Applications" Interscience Publications.

Sobrero, M.C., Ronco, A.: 2004 " Ensayo de toxicidad aguda con semillas de lechuga (Lactuca sativa L.". p: 71-79. From: Ensayos Toxicológicos y Métodos de Evaluación de Calidad de Aguas.

Vulliet, E., Emmelin, C., Chovelon, J.M., Guillard, C., Hermann, J.M.:2003, "Photocatalytic degradation of the herbicide cinosulfuron in aqueous TiO₂ suspension". Environ Chem Lett (2003) 1: 62 – 67.

World Health Organization: 2007, "Nitrate and nitrite in drinking water". WHO/SDE/07.01/16. Retrieved: 20/04/2012 from: http://search.who.int/search?q=nitrate+and+nitrite+in+drinking+water&ie=utf8&site=default_collection&client=_en&proxystylesheet=_en&output=xml_no_dtd&oe=utf8

Younathan, J.N., Fox M.A .: 1986 "Radical Cation Intermediates in the formation of Schiff Bases on Irradiated Semiconductor Powders" Tetrahedron Lett., 45: 6285.

Zahraa, O., Dorion, C., Ould – Mame, S.M. and Bouchy, M.:1999, "Titanium dioxide deposit films for photocatalytic studies of water pollutants", J. Adv. Oxidation Technol, 4, 40 – 46.

Zepp, R., Faust, B. and Holgné, J.: 1992, "Hydroxyl Radical Formation in Aqueous Reactions (pH 3 – 8) of Iron (II) with Hydrogen Peroxide: The Photo – Fenton Reaction" Environ. Sci. Technol., 26 (2): 313 – 319

Zollinger, H.: 1991, "Color chemistry: Synthesis, properties and Applications of Organic Dyes and Pigments"

ANNEXES

ANNEX I: Chemical Information about studied Direct Azo Dyes

Technical name of dye: **Direct Yellow 50**

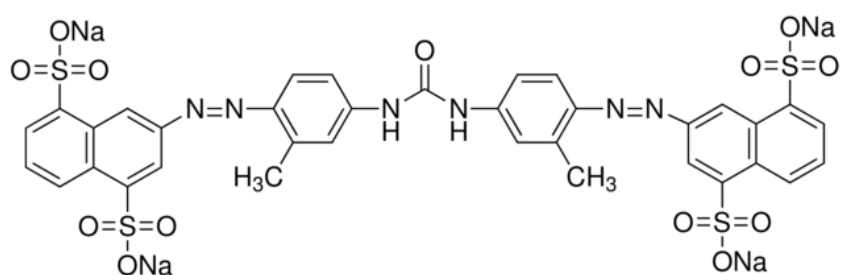
Formula: **C₃₅H₂₄N₆Na₄O₁₃S₄**

Molecular Weight: **956,82 g/mol**

UV absorption: λ_{\max} **395 nm**

H – Bond Donor: **2**

H – Bond Acceptor: **17**



Technical name of dye: **Direct Violet 51**

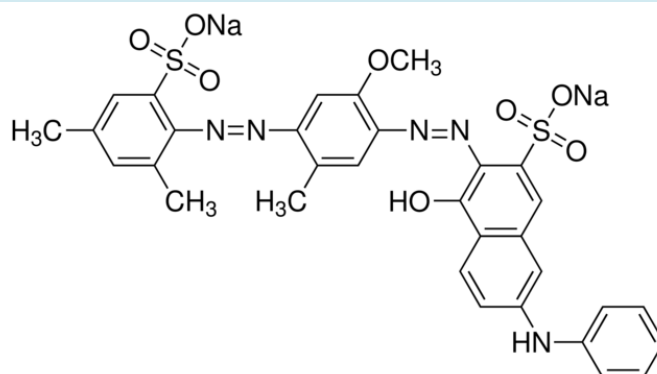
Formula: **C₃₂H₂₇N₅Na₂O₈S₂**

Molecular Weight: **719, 69 g/mol**

UV absorption: λ_{\max} **547 nm**

H – Bond Donor: **2**

H – Bond Acceptor: **13**



Technical name of dye: **Direct Red 81**

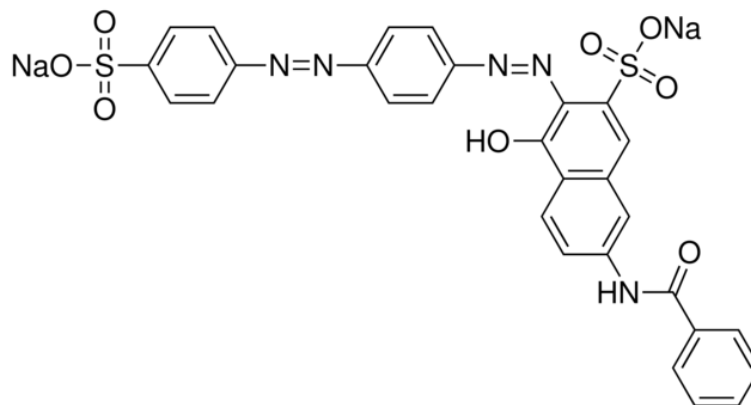
Formula: **C₂₉H₁₉N₅Na₂O₈S₂**

Molecular Weight: **675, 60 g/mol**

UV absorption: **λ_{\max} 510 nm**

H – Bond Donor: **2**

H – Bond Acceptor: **12**



Technical name of dye: **Direct Red 23**

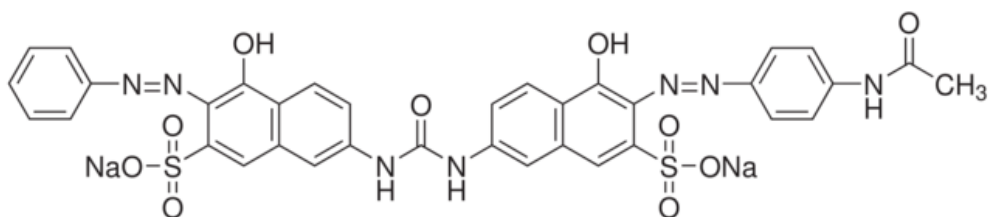
Formula: **C₃₅H₂₅N₇Na₂O₁₀S₂**

Molecular Weight: **813, 72 g/mol**

UV absorption: **λ_{\max} 503 nm**

H – Bond Donor: **5**

H – Bond Acceptor: **14**

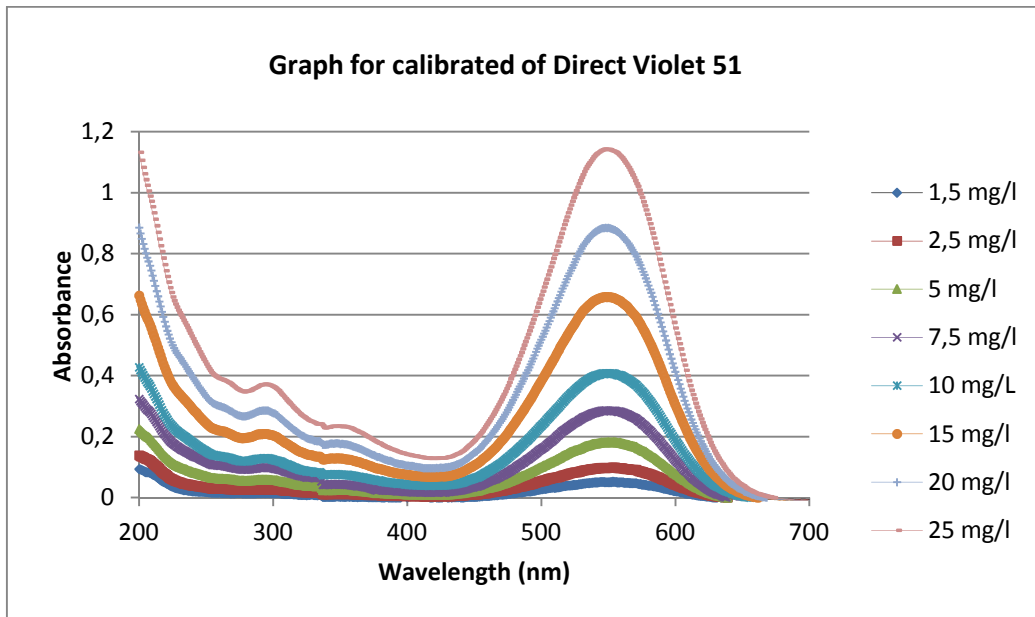


Source: Sigma Aldrich (France)

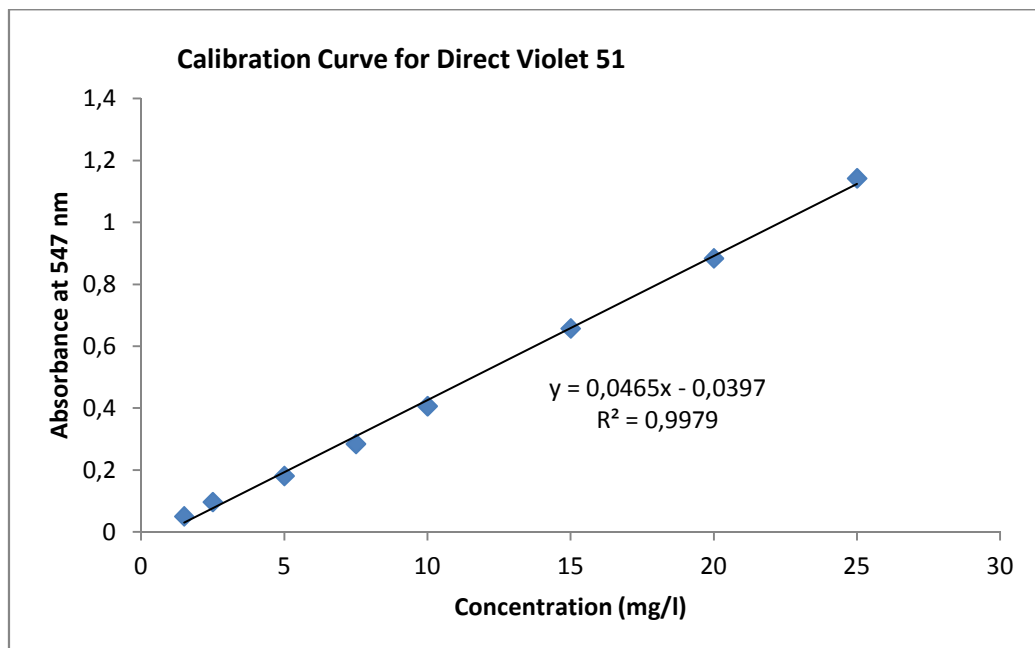
ANNEX II: Calibration Curves

CALIBRATION CURVE FOR DIRECT VIOLET 51

For Direct Violet 51 dye, the absorbance peak appears at a maximum wavelength of **547 nm**.

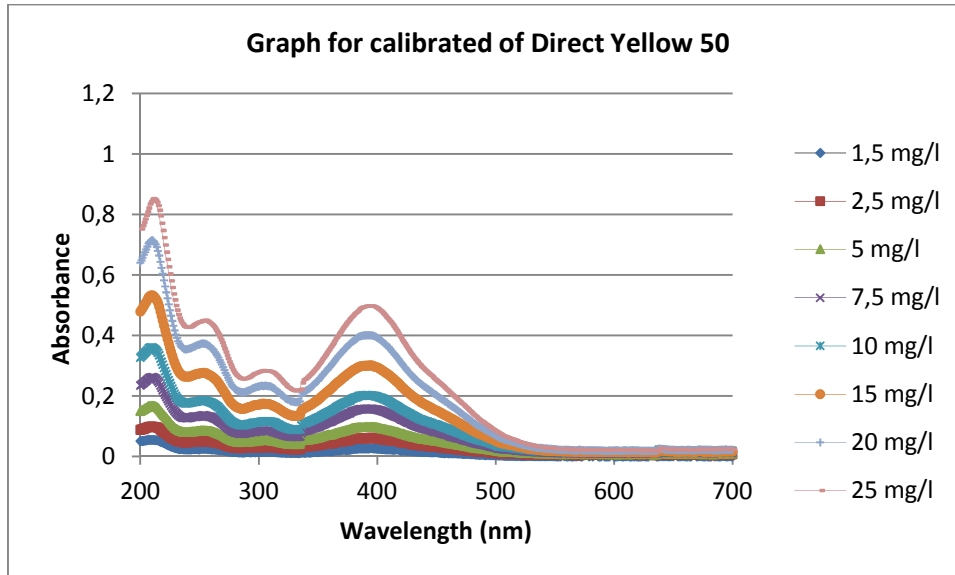


Concentration (mg/l)	1,5	2,5	5	7,5	10	15	20	25
Absorbance at λ_{max}	0,0511	0,0975	0,1816	0,2853	0,4073	0,6581	0,8846	1,1431

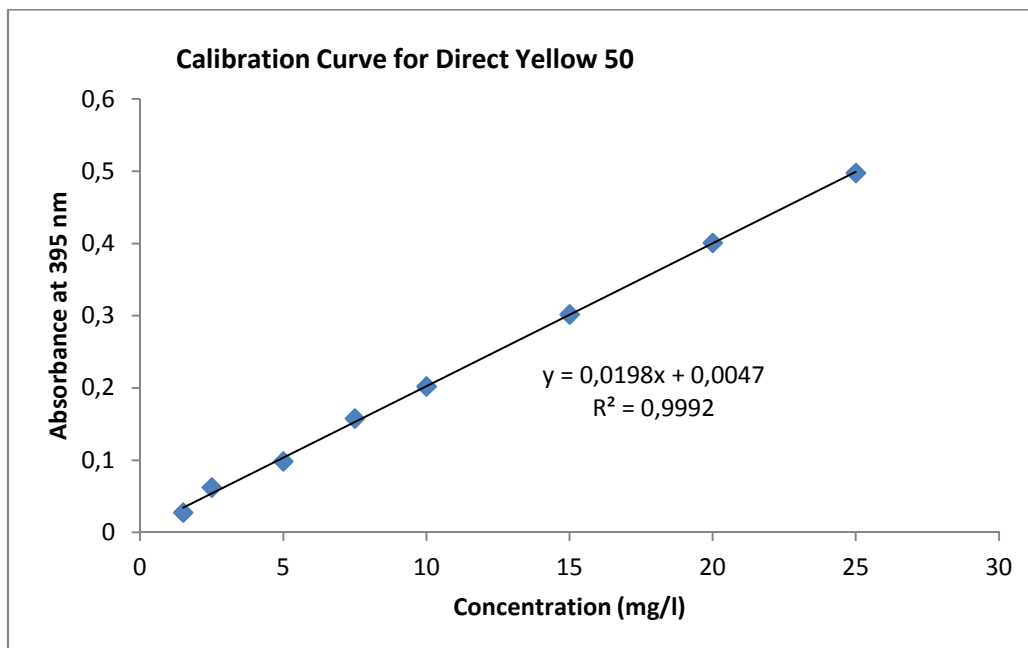


CALIBRATION CURVE FOR DIRECT YELLOW 50

For Direct Yellow 50 dye, the absorbance peak appears at a maximum wavelength of **395 nm**.

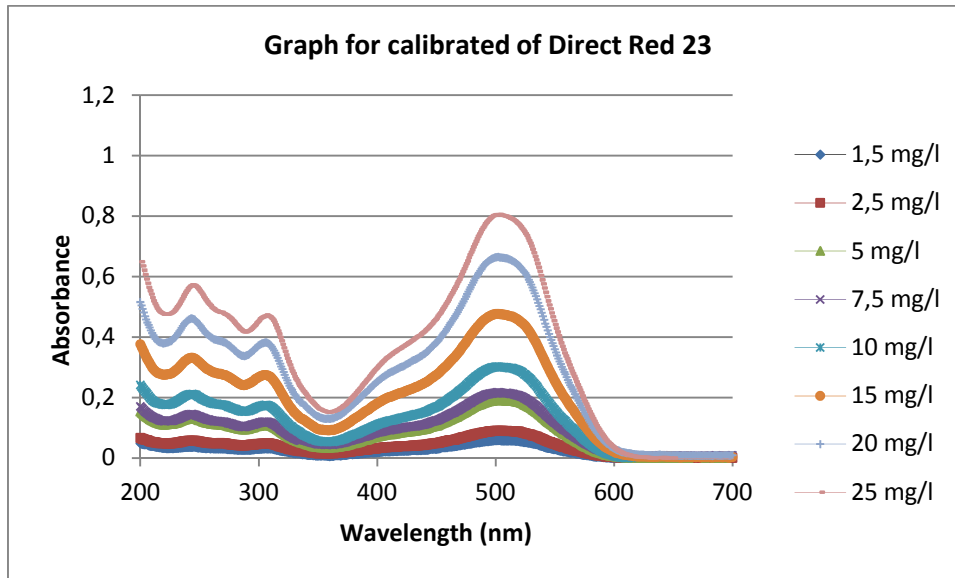


Concentration (mg/l)	1,5	2,5	5	7,5	10	15	20	25
Absorbance at λ_{max}	0,0275	0,0622	0,0983	0,1576	0,2021	0,3018	0,4008	0,4977

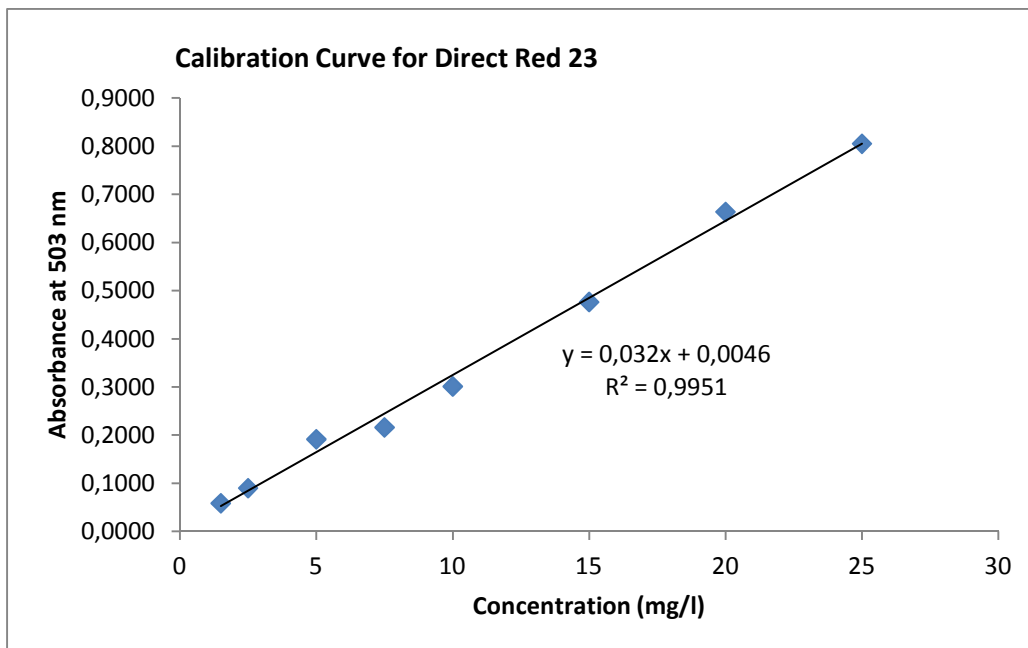


CALIBRATION CURVE FOR DIRECT RED 23

For Direct Red 23 dye, the absorbance peak appears at a maximum wavelength of **503 nm**.

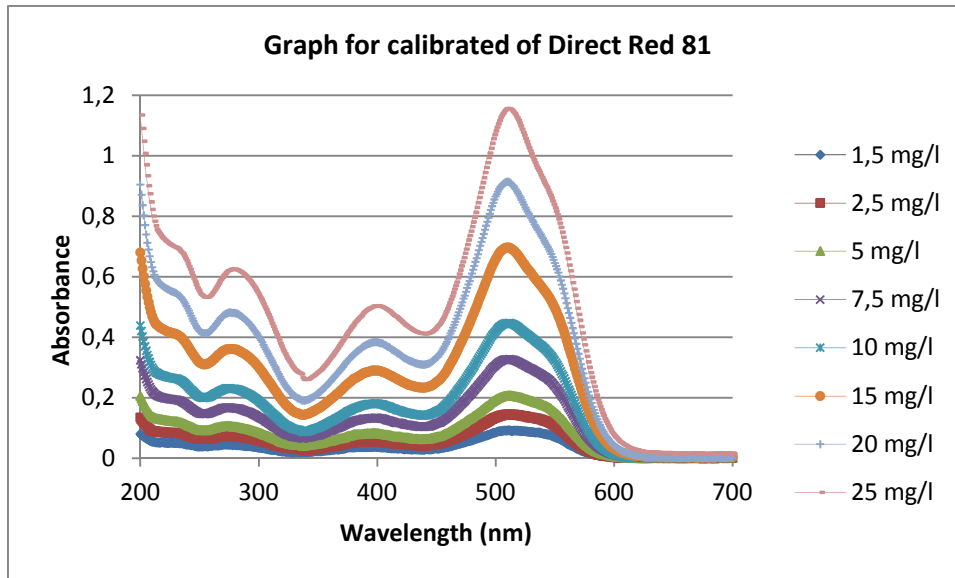


Concentration (mg/l)	1,5	2,5	5	7,5	10	15	20	25
Absorbance at λ_{max}	0,0589	0,0904	0,1919	0,2166	0,3016	0,4769	0,6641	0,8056

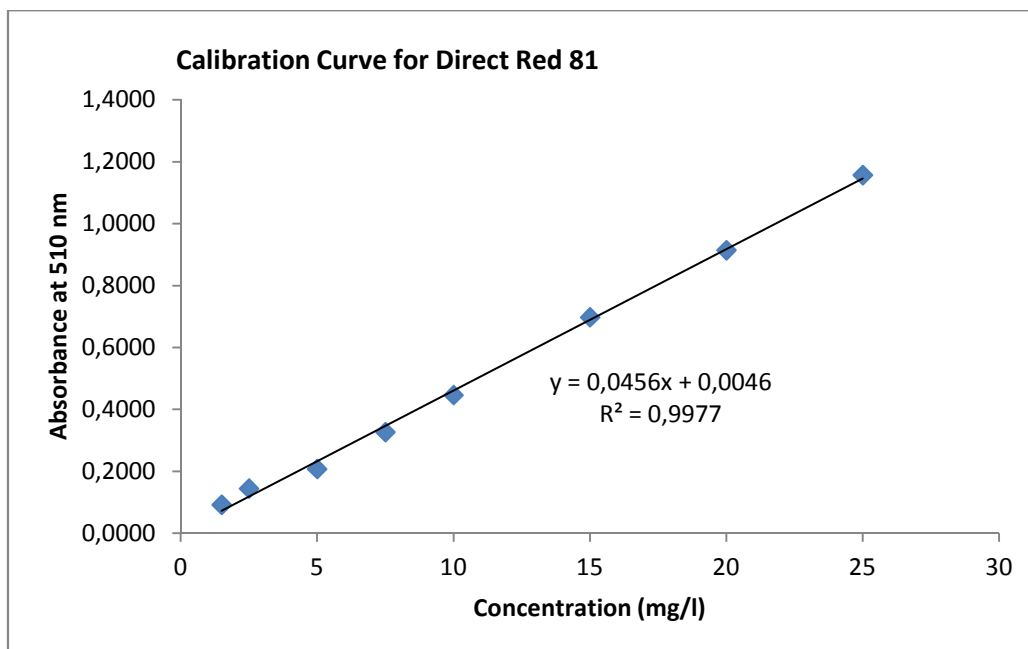


CALIBRATION CURVE FOR DIRECT RED 81

For Direct Red 81 dye, the absorbance peak appears at a maximum wavelength of **510 nm**.



Concentration (mg/l)	1,5	2,5	5	7,5	10	15	20	25
Absorbance at λ_{max}	0,0918	0,1443	0,2074	0,3268	0,4463	0,6975	0,9143	1,1568



ANNEX III: Summary table about studied experiences

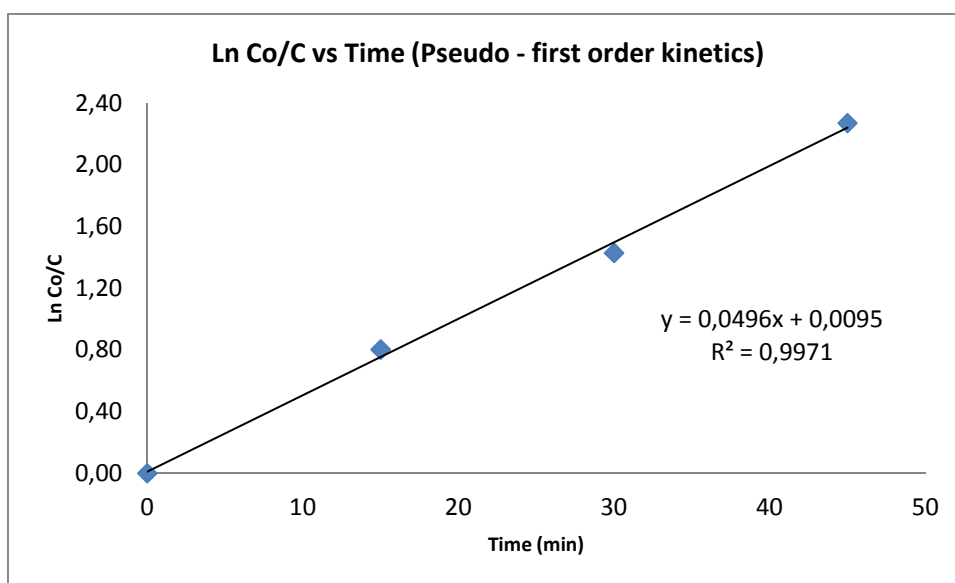
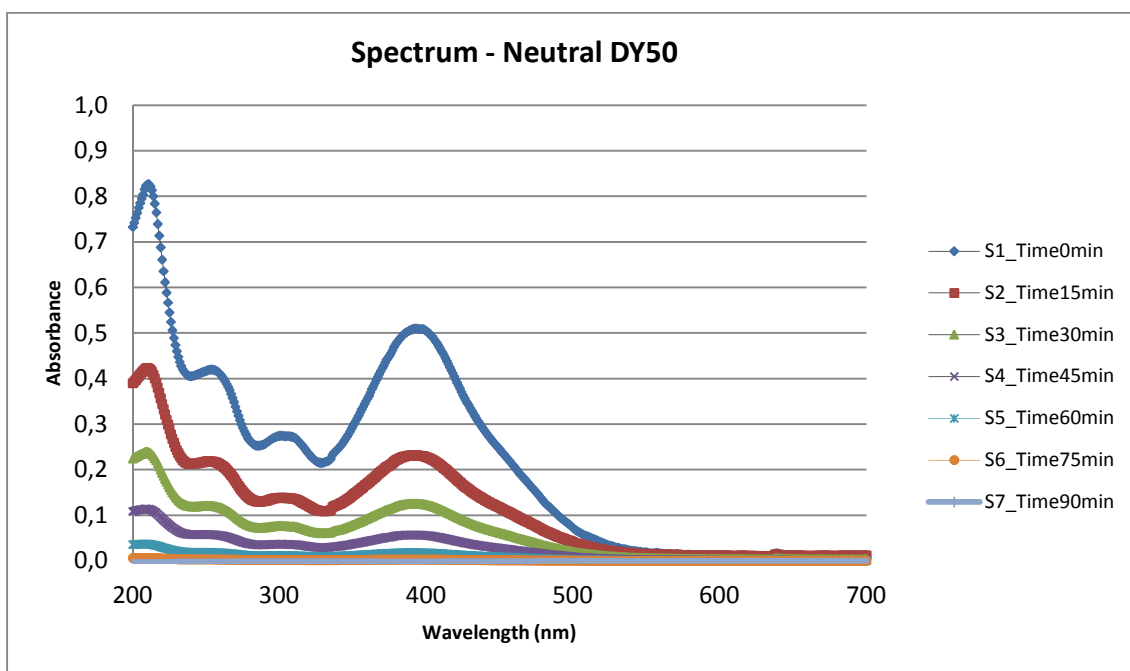
DYE	TYPE OF SOLUTION	PH	NAME
DY50	NEUTRAL		DY50
	HYDROLYSED	6	DY50H at pH = 6
	HYDROLYSED	7	DY50H at pH = 7
	HYDROLYSED	8	DY50H at pH = 8
	SIMULATED DYEHOUSE EFFLUENT	6	DY50SDE at pH = 6
	SIMULATED DYEHOUSE EFFLUENT (Test 1)	7	DY50SDE at pH = 7
	SIMULATED DYEHOUSE EFFLUENT (Test 2)	7	DY50SDE at pH = 7
	SIMULATED DYEHOUSE EFFLUENT	8	DY50SDE at pH = 8
DR81	NEUTRAL		DR81
	HYDROLYSED	5,5	DR81H at pH = 5,5
	HYDROLYSED	6	DR81H at pH = 6
	HYDROLYSED	7	DR81H at pH = 7
	HYDROLYSED	8	DR81H at pH = 8
	TEXTIL SYNTHETIC WATER	6	DR81SDE at pH = 6
	TEXTIL SYNTHETIC WATER	8	DR81SDE at pH = 8
DV51	NEUTRAL		DV51
	HYDROLYSED	5,5	DV51H at pH = 5
	HYDROLYSED	6	DV51H at pH = 6
	HYDROLYSED	7	DV51H at pH = 7
	HYDROLYSED	8	DV51H at pH = 8
	SIMULATED DYEHOUSE EFFLUENT	6	DV51SDE at pH = 6
	SIMULATED DYEHOUSE EFFLUENT	7	DV51SDE at pH = 7
	SIMULATED DYEHOUSE EFFLUENT (Test 1)	8	DV51SDE at pH = 8
SIMULATED DYEHOUSE EFFLUENT (Test 2)	8	DV51SLDE at pH = 8	
DR23	NEUTRAL		DR23
	HYDROLYSED	6	DR23H at pH = 6
	HYDROLYSED	7	DR23H at pH = 7
	HYDROLYSED	8	DR23H at pH = 8
	TEXTIL SYNTHETIC WATER	6	DR23SDE at pH = 6
	TEXTIL SYNTHETIC WATER	7	DR23SDE at pH = 7
	TEXTIL SYNTHETIC WATER	8	DR23SDE at pH = 8
	SIMULATED LIGHT DYEHOUSE EFFLUENT	7	DR23SLDE at pH = 7

ANNEX IV: Dye spectra

DIRECT YELLOW 50

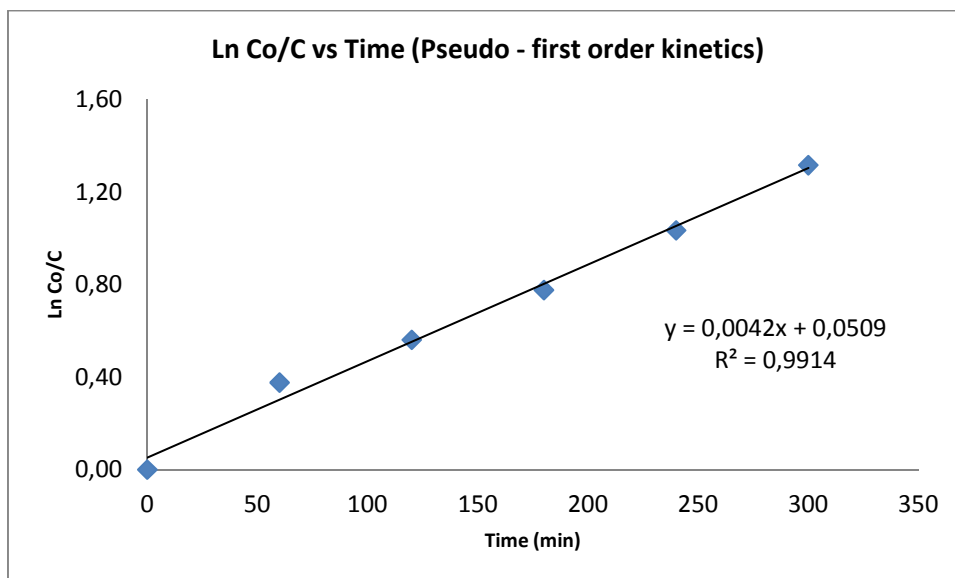
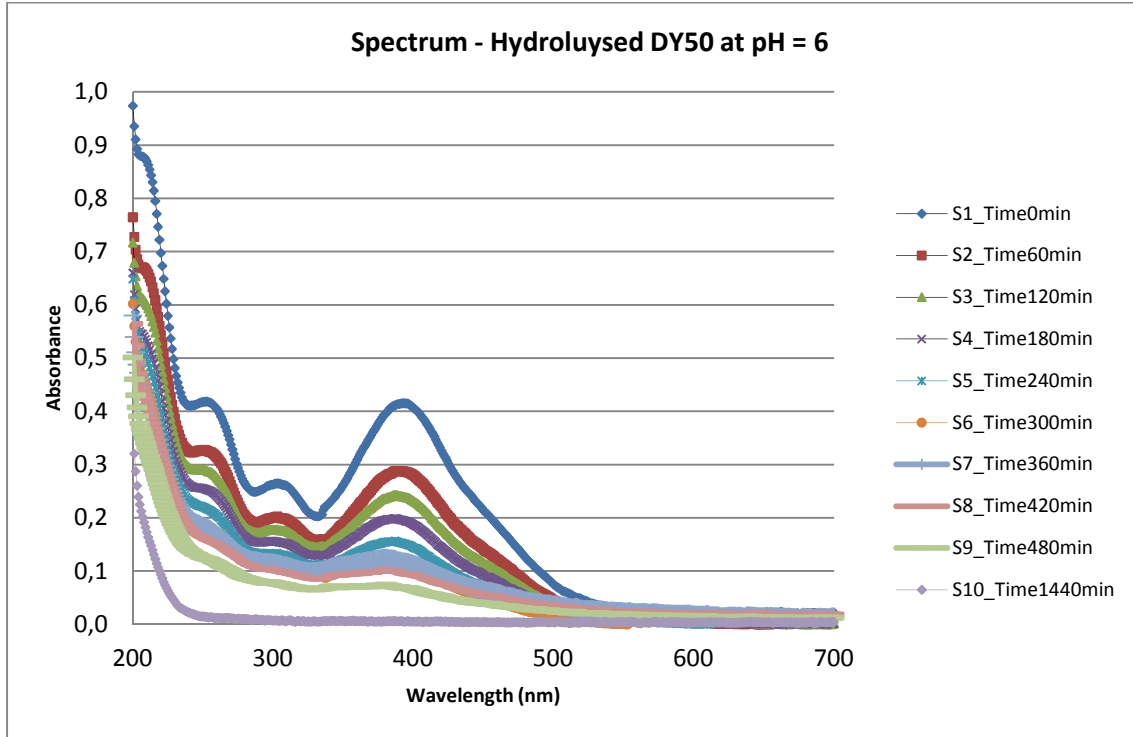
NEUTRAL DY50

SAMPLE	S1	S2	S3	S4	S5	S6	S7
Time (min)	0	15	30	45	60	75	90
Absorbance at $\lambda_{m\acute{a}x}$	0,5092	0,2308	0,1255	0,0567	0,0179	0,0031	-0,0013
Concentration (mg/l)	25,48	11,42	6,10	2,63	0,67	-0,08	-0,30
Ln (C ₀ /C)	0,0000	0,8025	1,4294	2,2723	3,6434	-	-



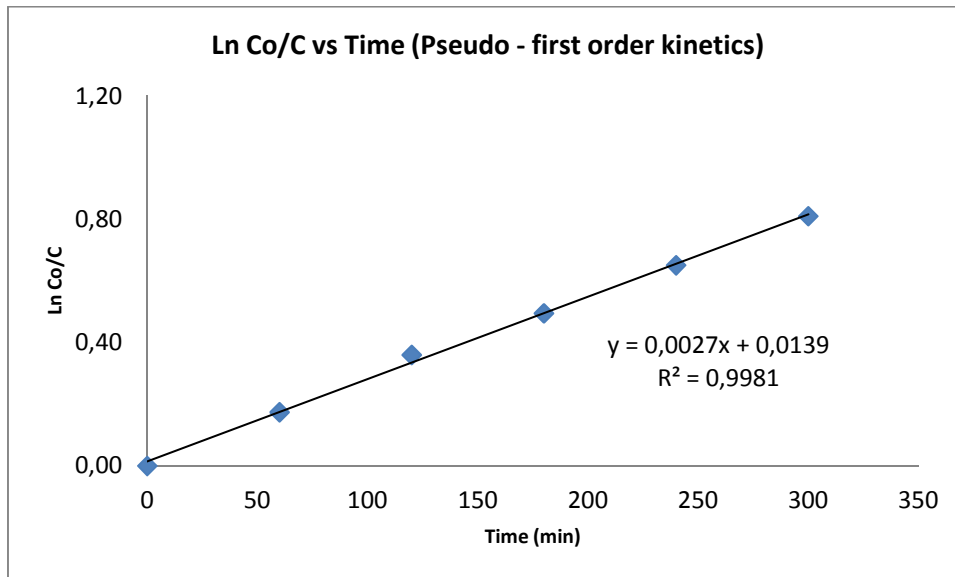
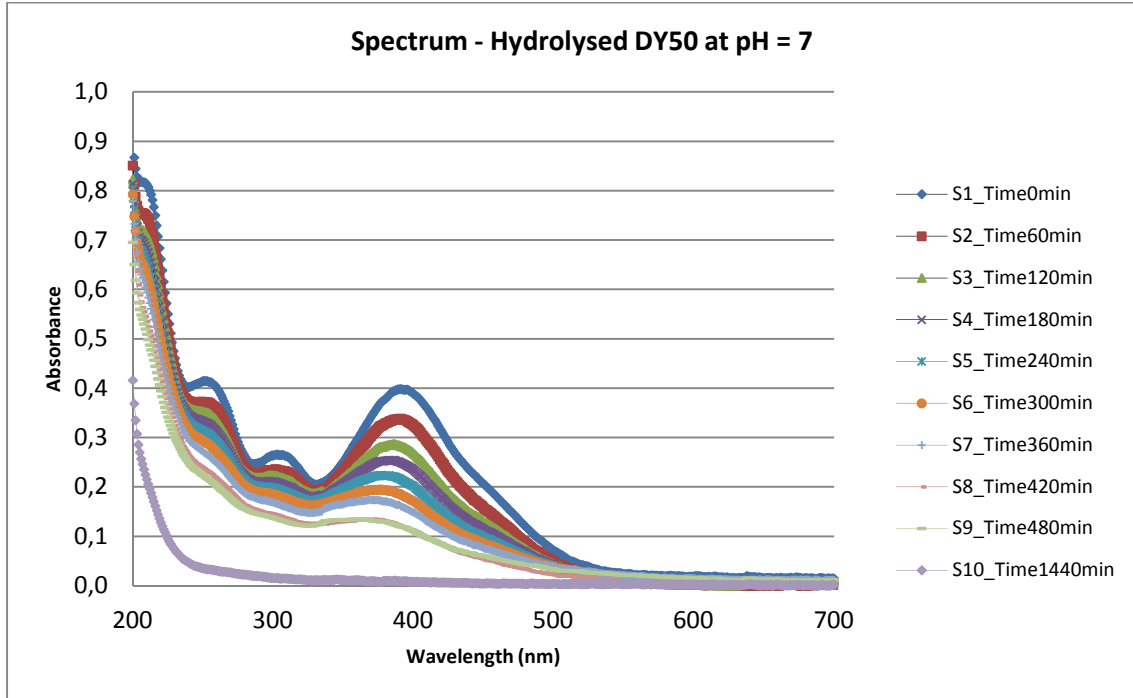
HYDROLYSED DY50 AT PH = 6

SAMPLE	S1	S2	S3	S4	S5	S6	S7	S8	S9	S10
Time (min)	0	60	120	180	240	300	360	420	480	1440
Absorbance at λ_{max}	0,415	0,286	0,239	0,193	0,150	0,115	0,117	0,094	0,069	0,005
Concentration (mg/l)	20,72	14,22	11,82	9,53	7,36	5,55	5,67	4,52	3,23	0,04
Ln (C ₀ /C)	0,000	0,377	0,561	0,777	1,035	1,317	1,296	1,522	1,859	6,373



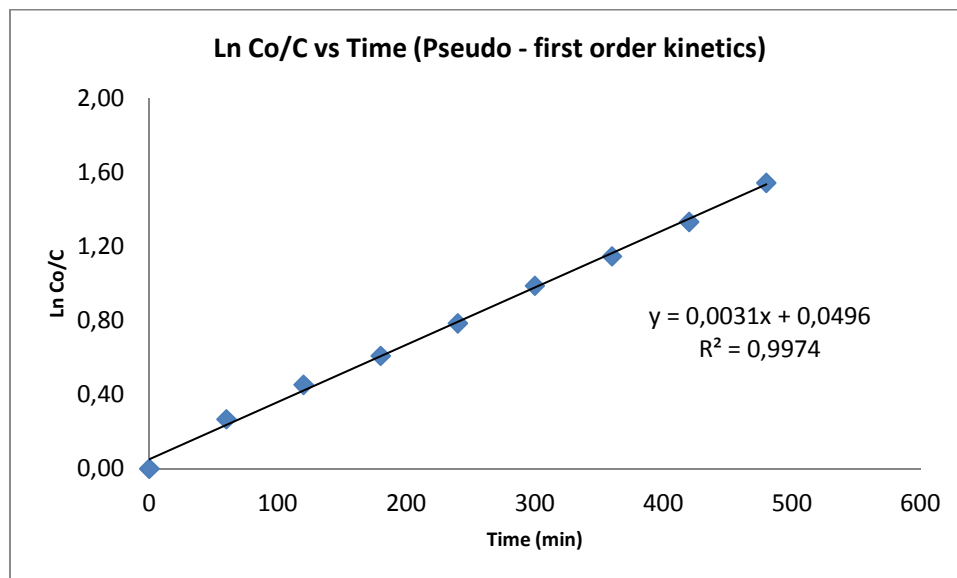
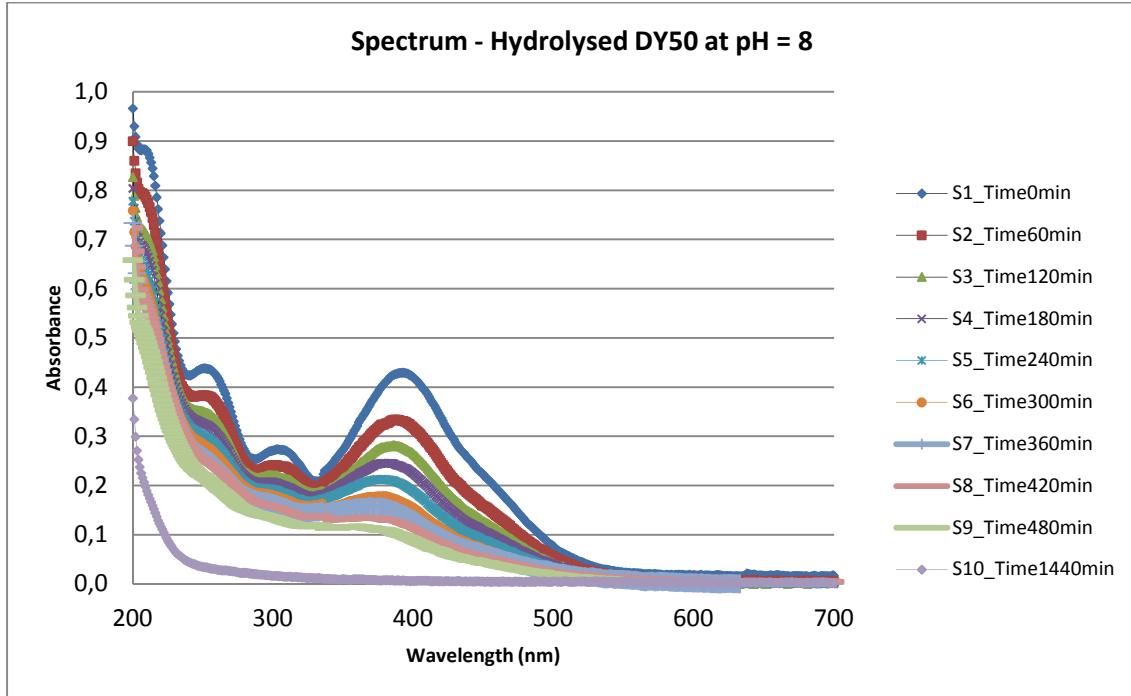
HYDROLYSED DY50 AT PH = 7

SAMPLE	S1	S2	S3	S4	S5	S6	S7	S8	S9	S10
Time (min)	0	60	120	180	240	300	360	420	480	1440
Absorbance at λ_{max}	0,397	0,334	0,279	0,244	0,209	0,179	0,156	0,116	0,117	0,009
Concentration (mg/l)	19,82	16,65	13,83	12,08	10,33	8,81	7,64	5,66	5,67	0,23
$\ln(C_0/C)$	0,000	0,174	0,359	0,495	0,651	0,810	0,953	1,253	1,251	4,446



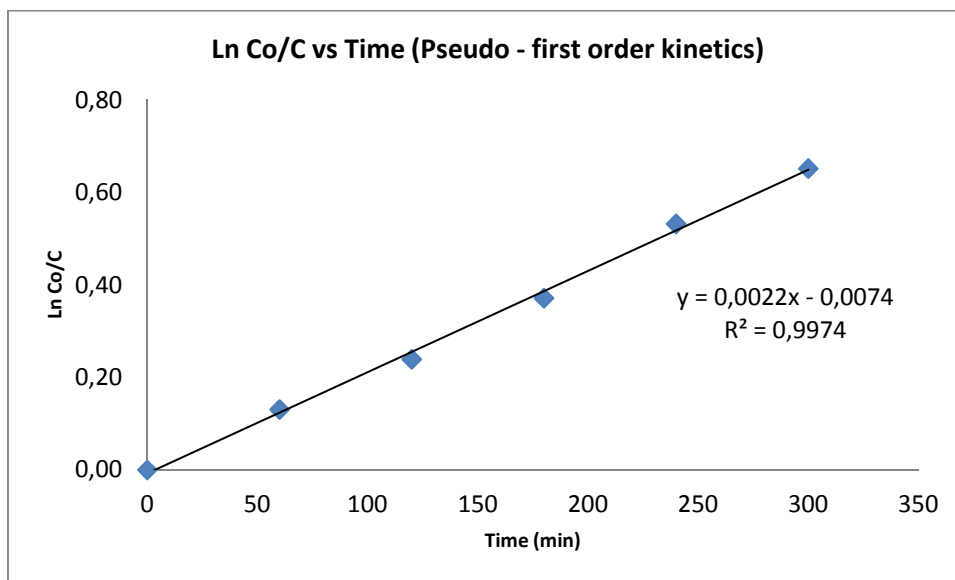
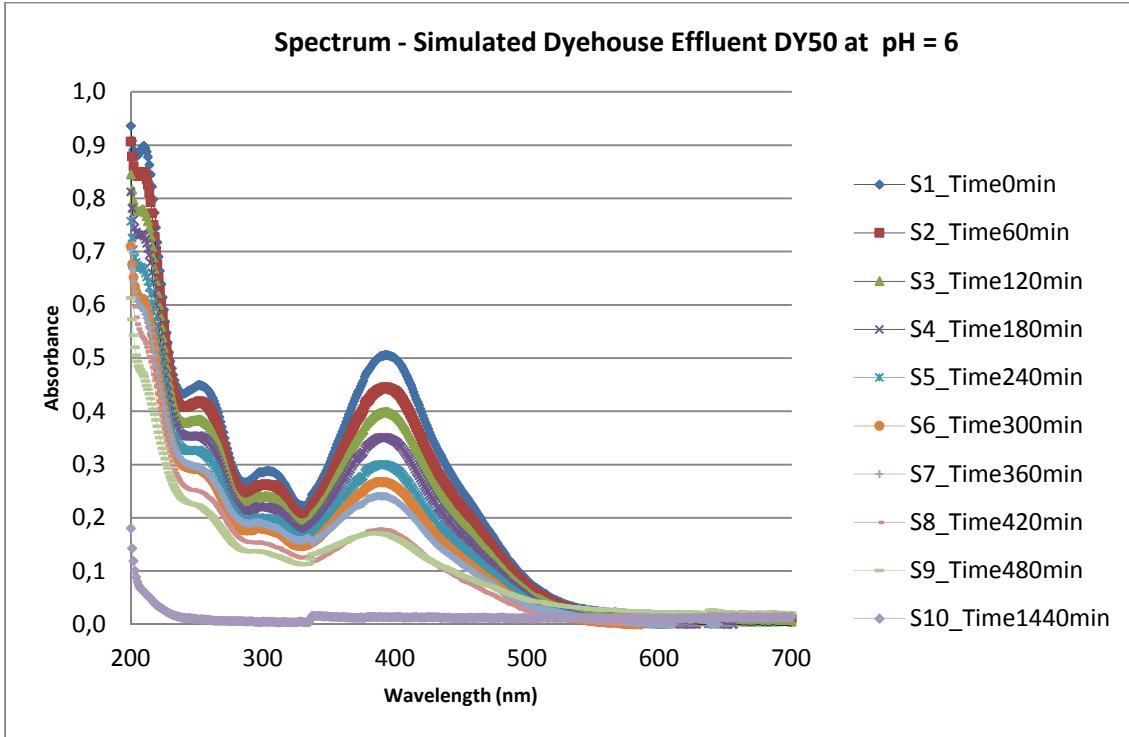
HYDROLYSED DY50 AT PH = 8

SAMPLE	S1	S2	S3	S4	S5	S6	S7	S8	S9	S10
Time (min)	0	60	120	180	240	300	360	420	480	1440
Absorbance at λ_{max}	0,428	0,329	0,274	0,235	0,198	0,162	0,139	0,116	0,095	0,006
Concentration (mg/l)	21,38	16,36	13,58	11,61	9,74	7,95	6,78	5,63	4,56	0,07
$\ln(C_0/C)$	0,000	0,268	0,454	0,611	0,787	0,989	1,149	1,335	1,546	5,712



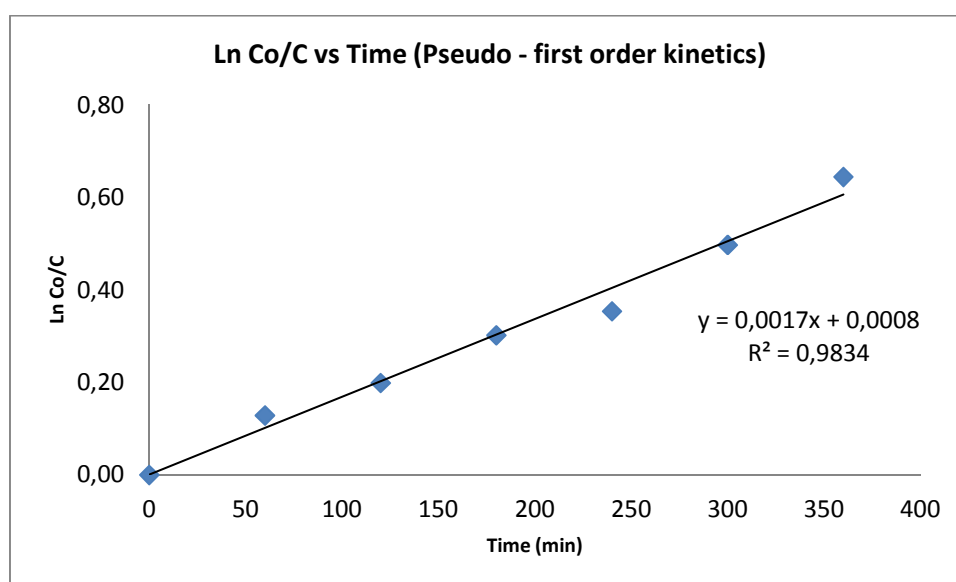
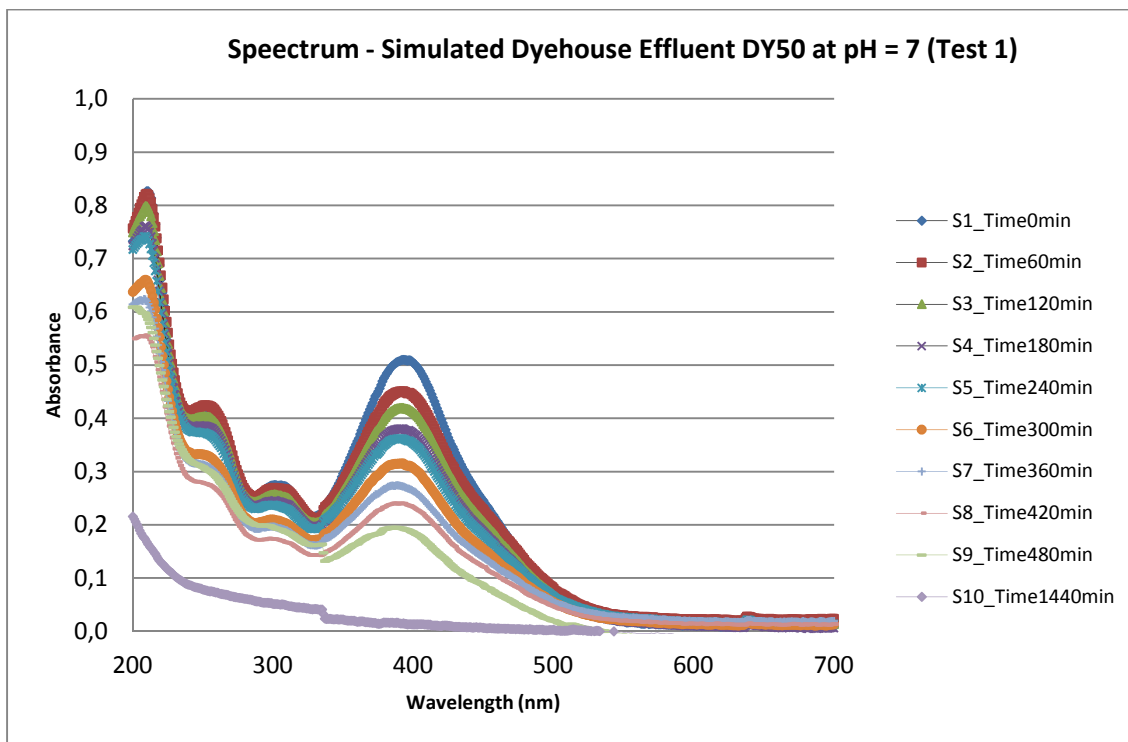
SIMULATED DYEHOUSE EFFLUENT DY50 AT PH = 6

SAMPLE	S1	S2	S3	S4	S5	S6	S7	S8	S9	S10
Time (min)	0	60	120	180	240	300	360	420	480	1440
Absorbance at λ_{max}	0,505	0,444	0,399	0,349	0,299	0,265	0,239	0,176	0,168	0,013
Concentration (mg/l)	25,28	22,18	19,90	17,43	14,84	13,17	11,83	8,66	8,23	0,43
Ln (C ₀ /C)	0,000	0,131	0,239	0,372	0,532	0,652	0,759	1,071	1,123	4,064



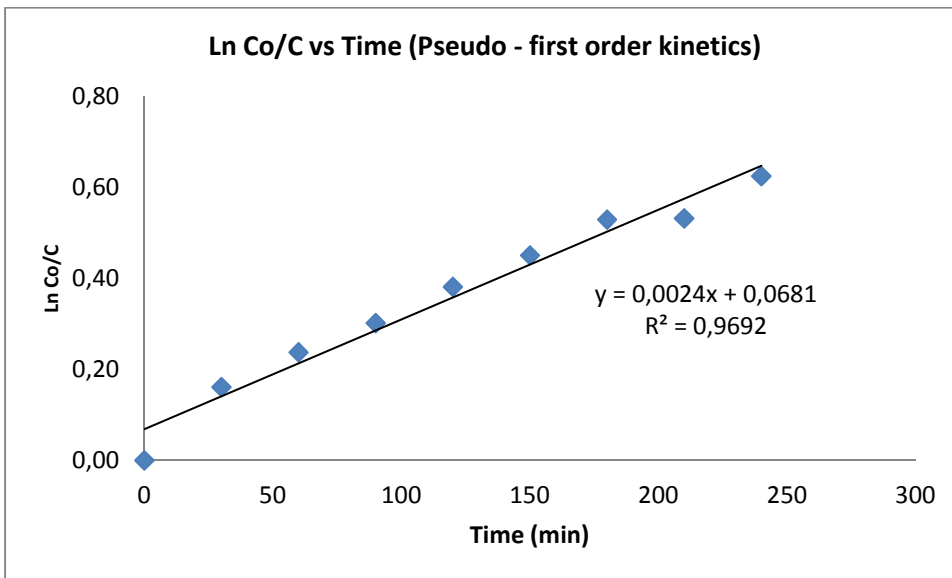
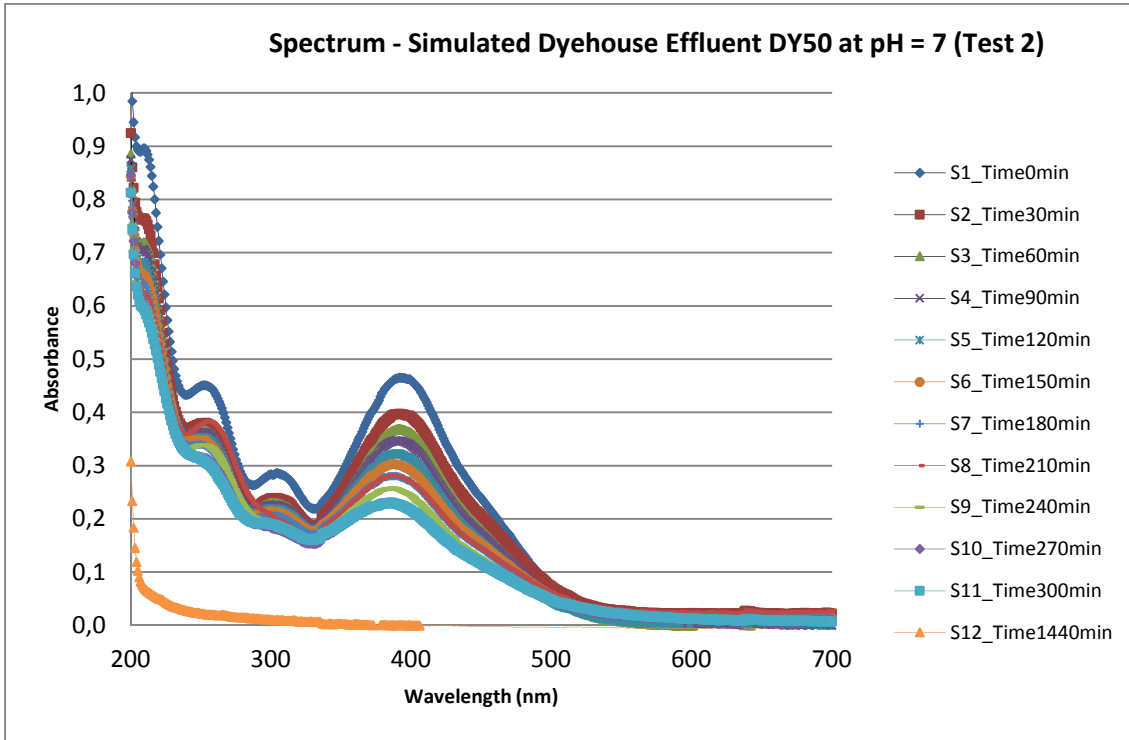
SIMULATED DYEHOUSE EFFLUENT DY50 AT PH = 7 (Test 1)

SAMPLE	S1	S2	S3	S4	S5	S6	S7	S8	S9	S10
Time (min)	0	60	120	180	240	300	360	420	480	1440
Absorbance at λ_{max}	0,509	0,448	0,418	0,378	0,359	0,312	0,269	0,237	0,191	0,014
Concentration (mg/l)	25,48	22,40	20,88	18,84	17,88	15,49	13,37	11,73	9,42	0,46
Ln (C ₀ /C)	0,000	0,129	0,199	0,302	0,354	0,497	0,645	0,776	0,995	4,015



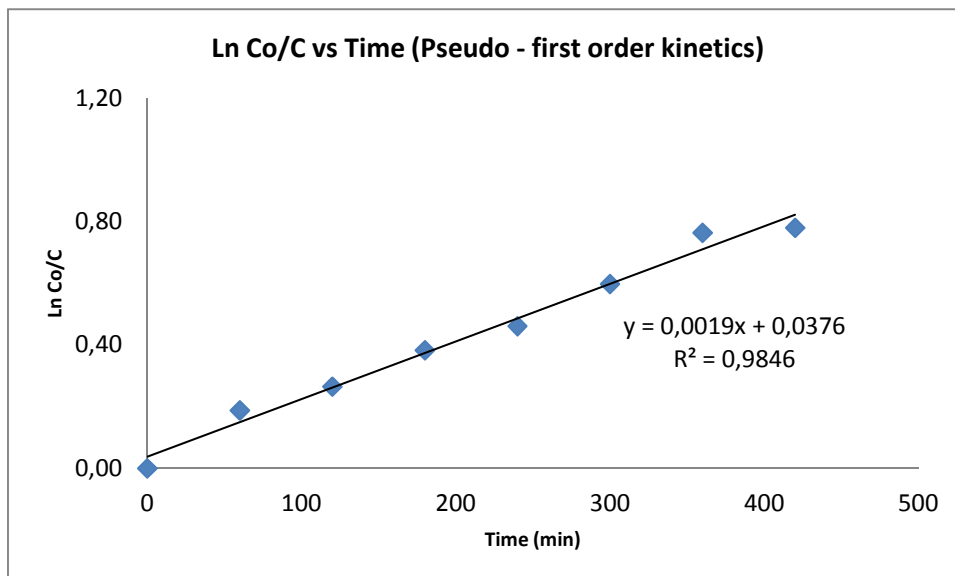
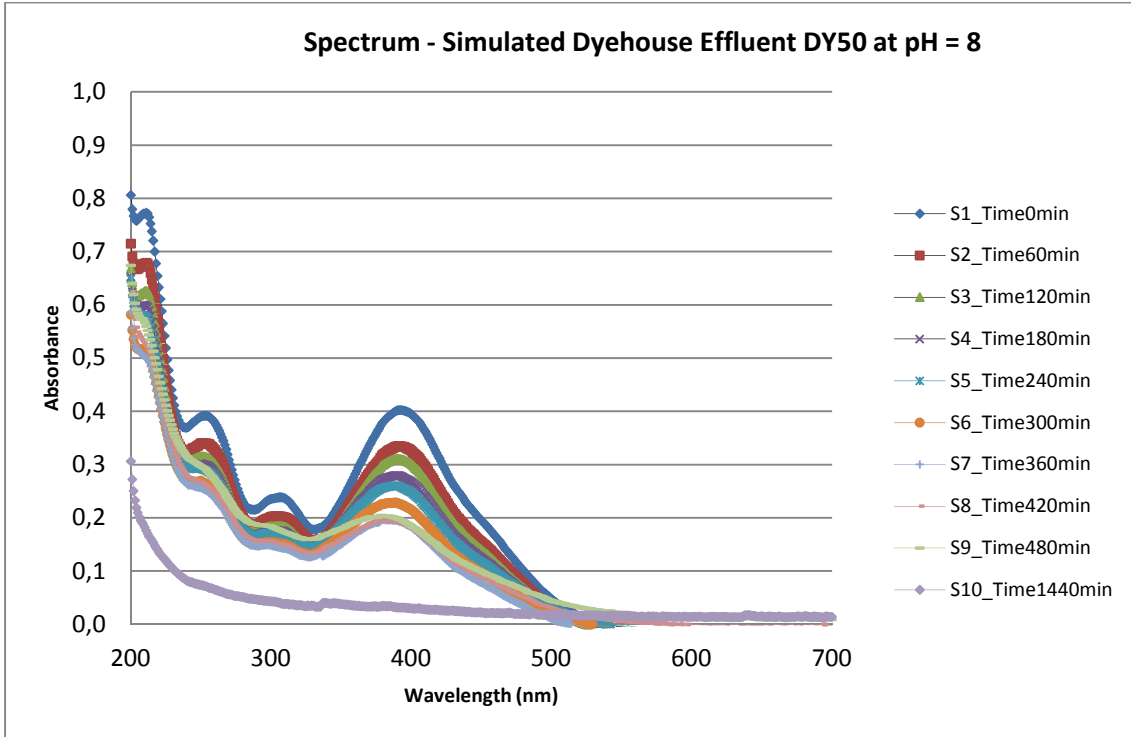
SIMULATED DYEHOUSE EFFLUENT DY50 AT PH = 7 (Test 2)

SAMPLE	S1	S2	S3	S4	S5	S6	S7	S8	S9	S10	S11	S12
Time (min)	0	30	60	90	120	150	180	210	240	270	300	1440
Absorbance at λ_{max}	0,467	0,396	0,367	0,345	0,319	0,298	0,275	0,275	0,251	0,223	0,2232	0,0004
Concentration (mg/l)	23,23	19,77	18,31	17,17	15,86	14,79	13,67	13,64	12,42	11,03	11,04	-0,22
Ln (C ₀ /C)	0,000	0,162	0,238	0,302	0,382	0,451	0,530	0,533	0,626	0,745	0,7444	-



SIMULATED DYEHOUSE EFFLUENT DY50 AT PH = 8

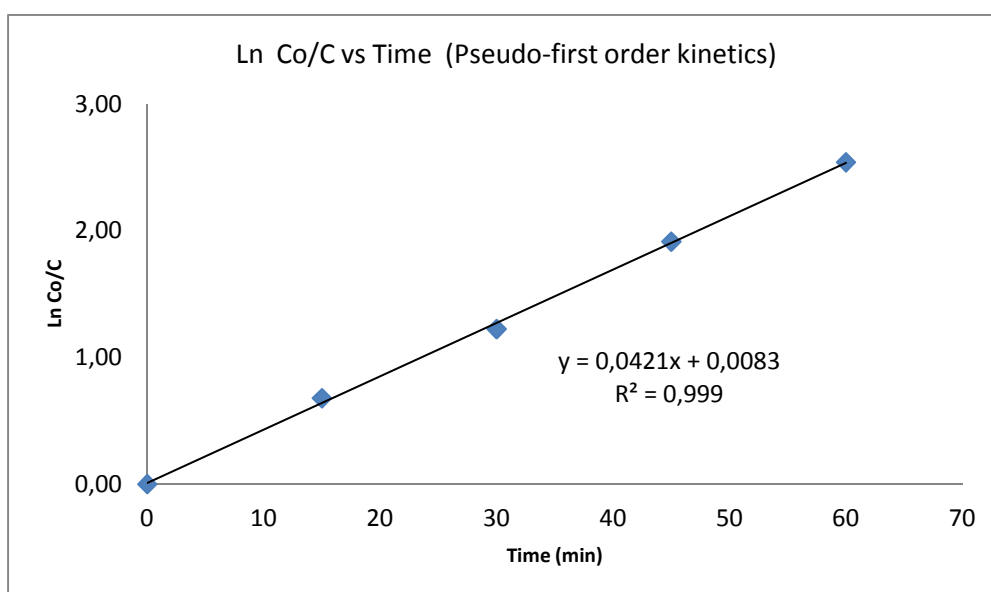
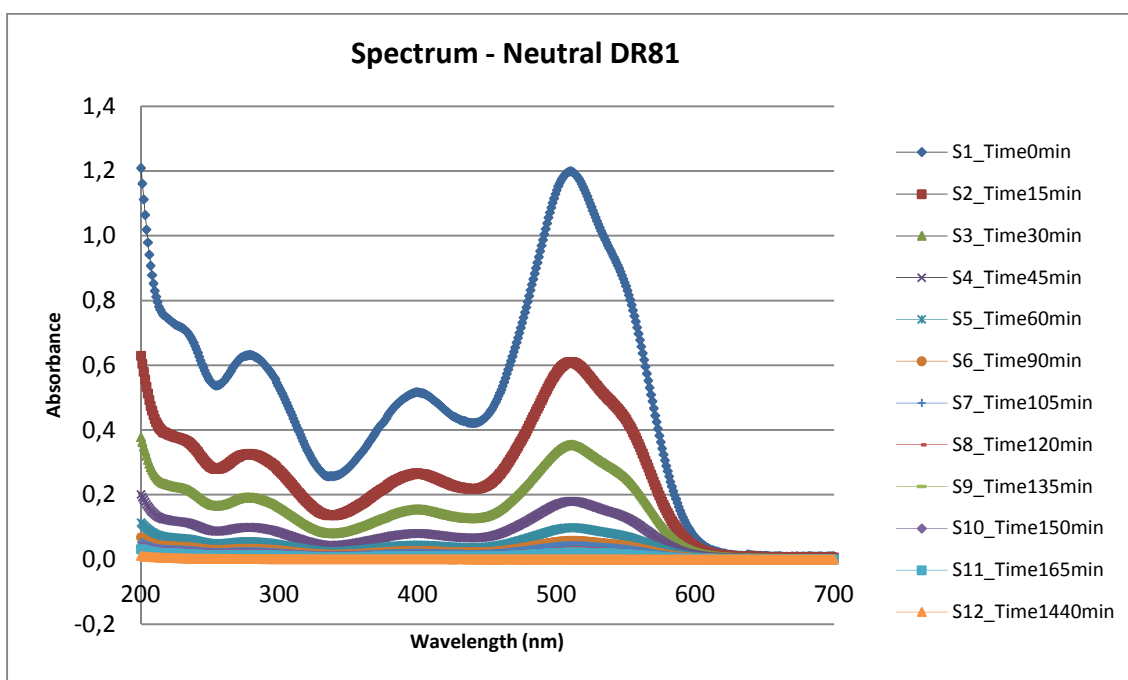
SAMPLE	S1	S2	S3	S4	S5	S6	S7	S8	S9	S10
Time (min)	0	60	120	180	240	300	360	420	480	1440
Absorbance at λ_{max}	0,401	0,333	0,309	0,275	0,255	0,223	0,189	0,186	0,193	0,031
Concentration (mg/l)	20,03	16,60	15,36	13,65	12,63	11,01	9,33	9,18	9,52	1,35
Ln (C_0/C)	0,000	0,188	0,265	0,383	0,462	0,598	0,764	0,781	0,741	2,698



DIRECT RED 81

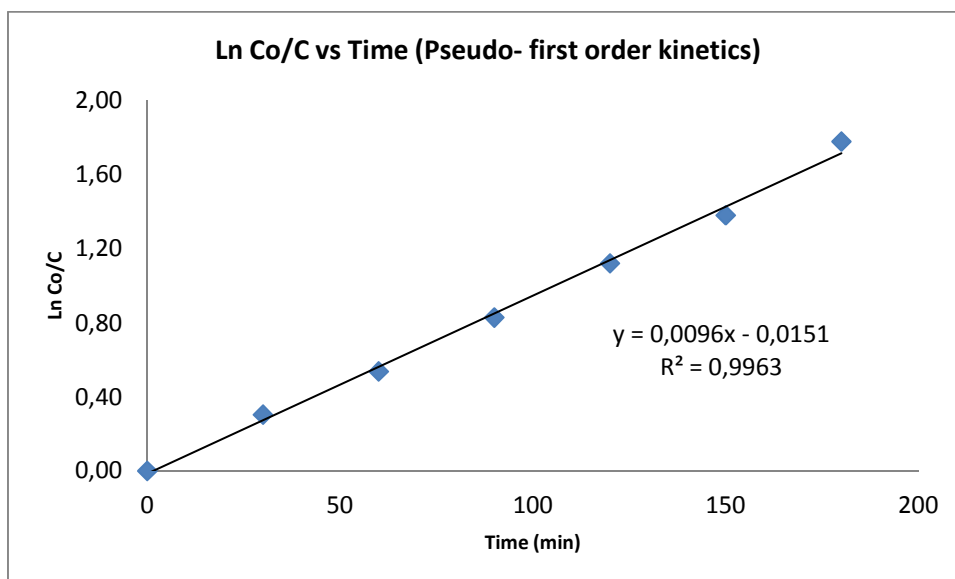
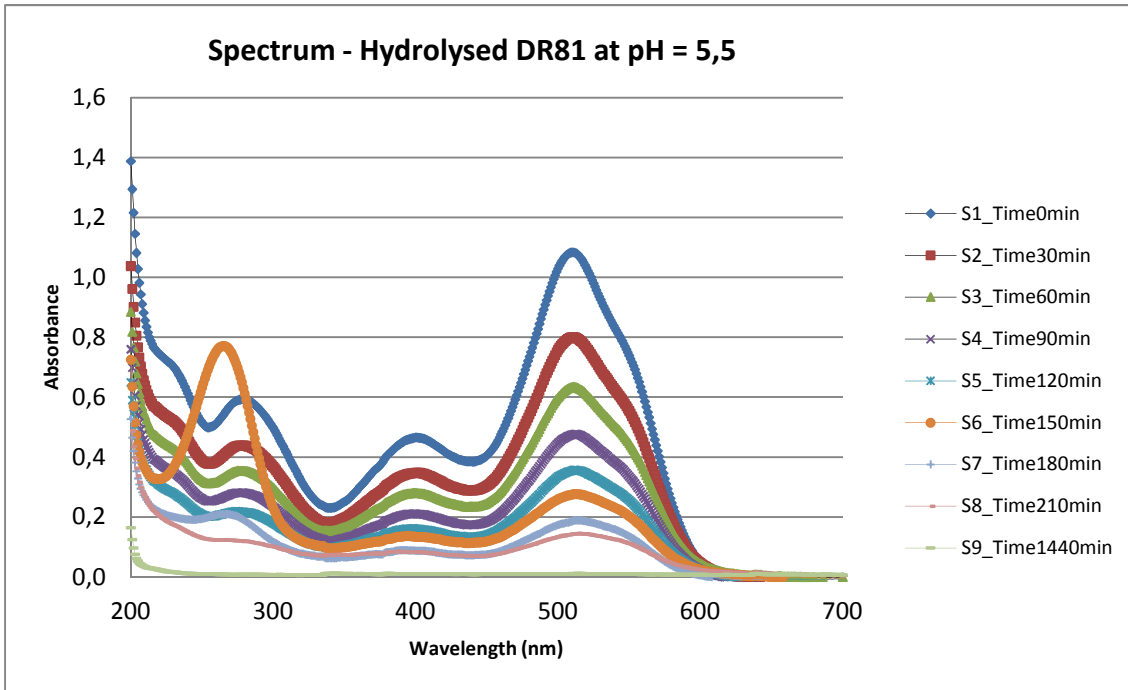
NEUTRAL DR81

SAMPLE	S1	S2	S3	S4	S5	S6	S7	S8	S9	S10	S11	S12
Time (min)	0	15	30	45	60	90	105	120	135	150	165	1440
Absorbance at λ_{max}	1,199	0,610	0,355	0,181	0,099	0,058	0,044	0,035	0,029	0,024	0,021	0,001
Concentration (mg/l)	26,20	13,29	7,69	3,86	2,06	1,17	0,87	0,66	0,52	0,42	0,36	-0,08
Ln (C ₀ /C)	0,000	0,679	1,226	1,916	2,542	3,106	3,408	3,678	3,912	4,133	4,286	-



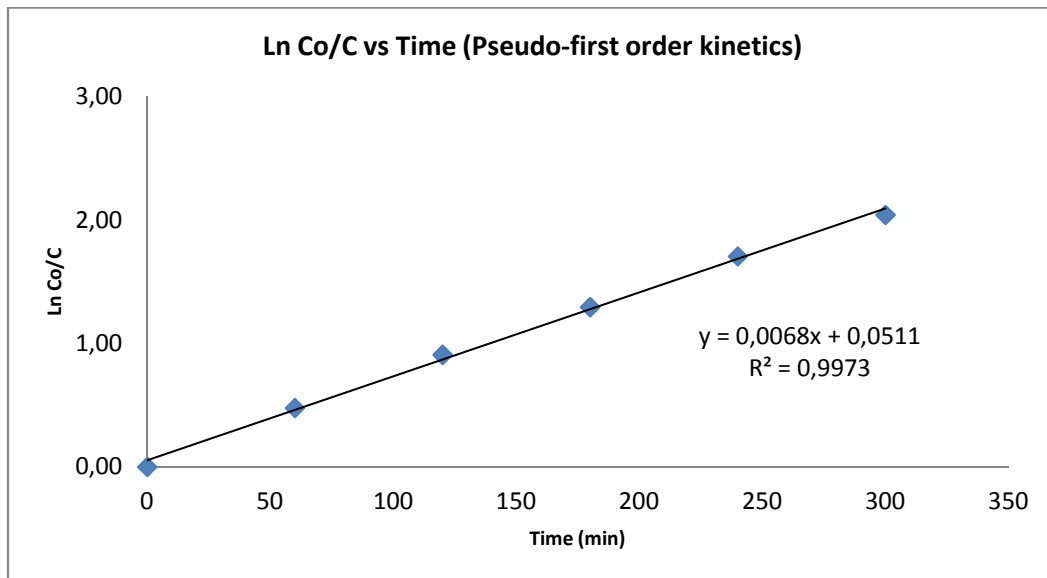
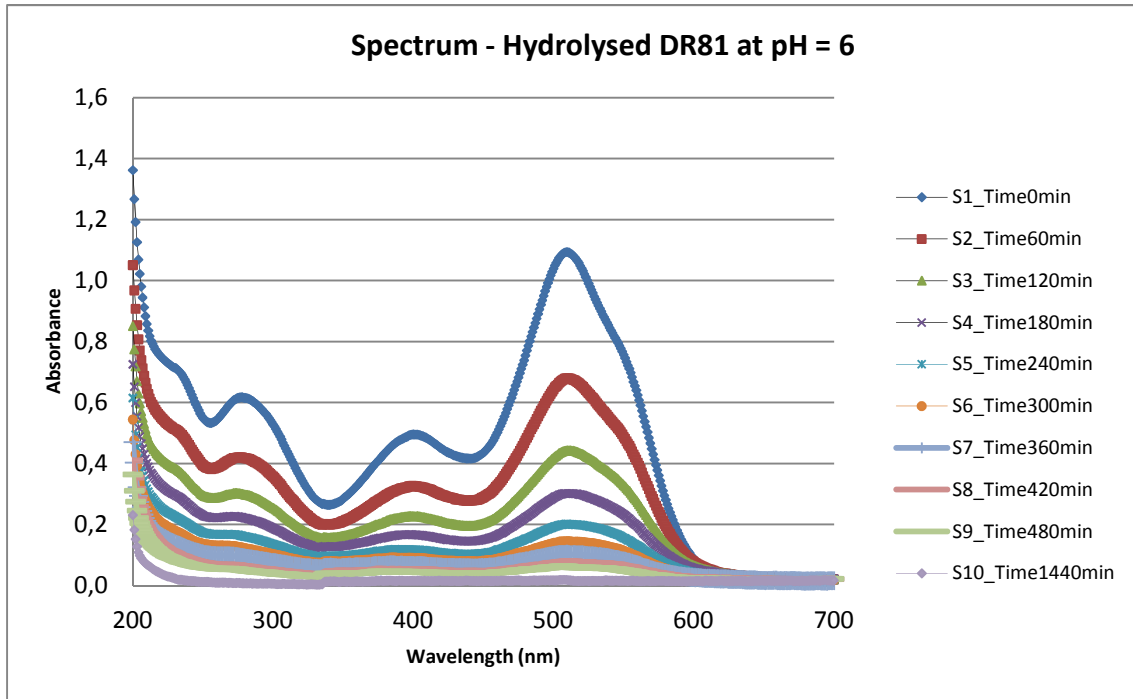
HYDROLYSED DR81 AT PH = 5,5

SAMPLE	S1	S2	S3	S4	S5	S6	S7	S8	S9
Time (min)	0	30	60	90	120	150	180	210	1440
Absorbance at λ_{max}	1,084	0,801	0,635	0,475	0,356	0,275	0,186	0,144	0,011
Concentration (mg/l)	23,66	17,46	13,82	10,32	7,70	5,94	3,98	3,06	0,14
$\ln(C_0/C)$	0,000	0,304	0,538	0,829	1,123	1,383	1,782	2,045	5,097



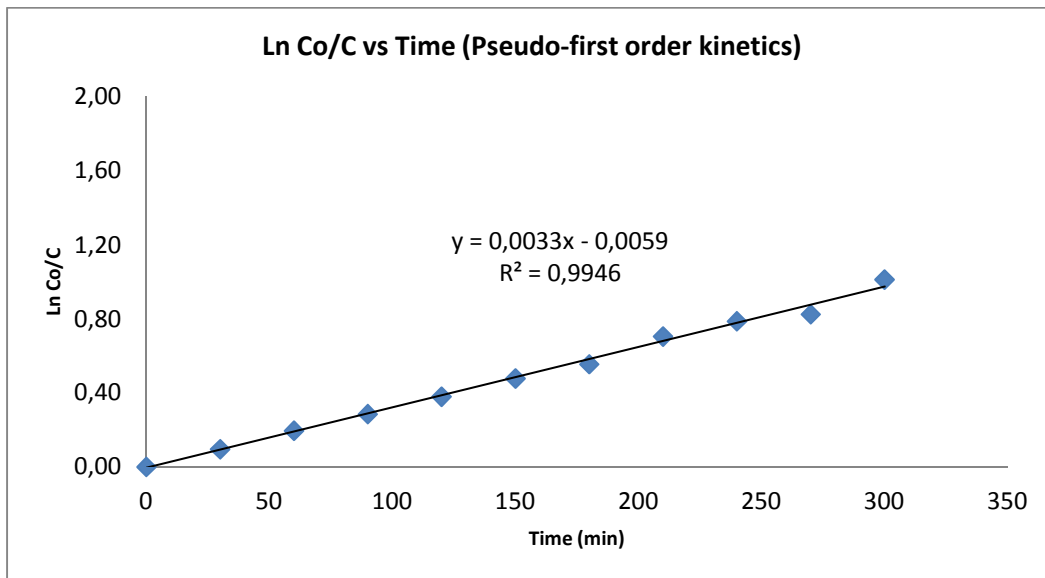
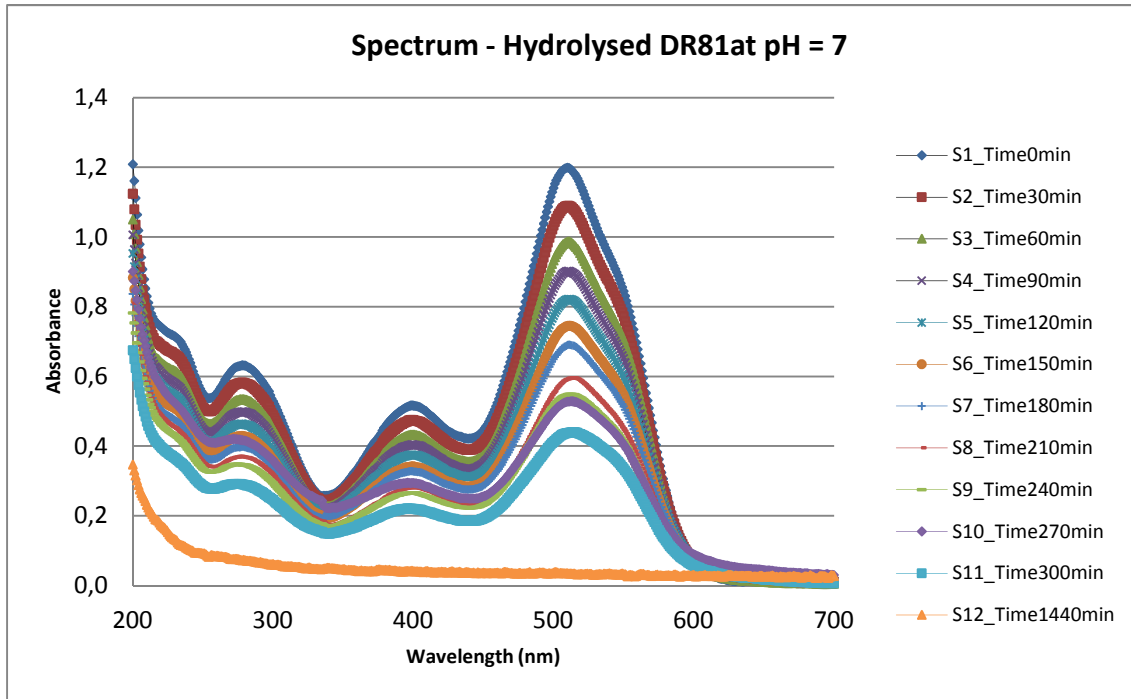
HYDROLYSED DR81 AT PH = 6

SAMPLE	S1	S2	S3	S4	S5	S6	S7	S8	S9	S10
Time (min)	0	60	120	180	240	300	360	420	480	1440
Absorbance at λ_{max}	1,0936	0,6801	0,4434	0,3024	0,2020	0,1456	0,1026	0,0805	0,0632	0,0183
Concentration (mg/l)	23,88	14,81	9,62	6,53	4,33	3,09	2,15	1,66	1,29	0,30
$\ln(C_0/C)$	0,0000	0,4776	0,9090	1,2966	1,7078	2,0443	2,4080	2,6636	2,9223	4,3756



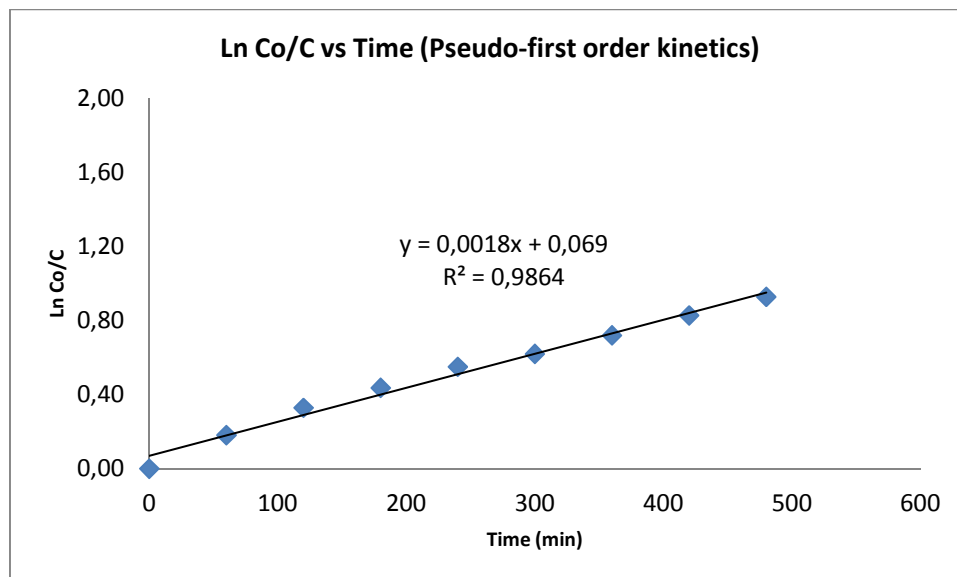
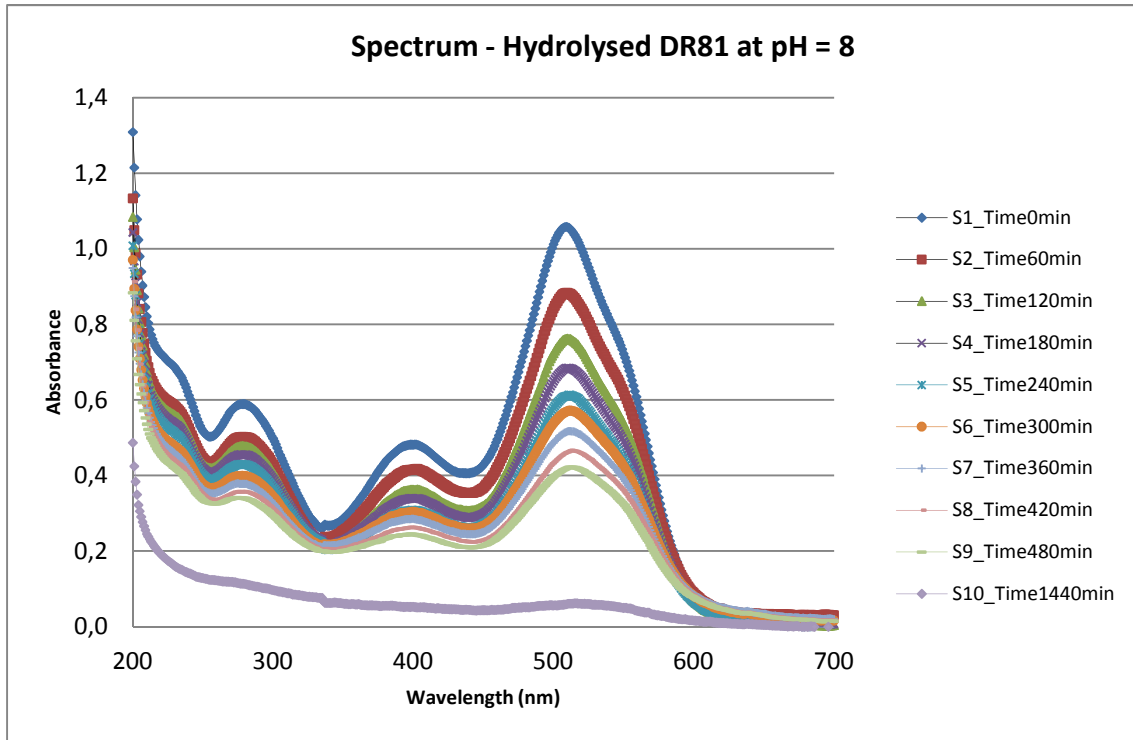
HYDROLYSED DR81 AT PH = 7

SAMPLE	S1	S2	S3	S4	S5	S6	S7	S8	S9	S10
Time (min)	0	30	60	90	120	150	180	210	240	270
Absorbance at λ_{max}	1,199	1,090	0,987	0,903	0,822	0,745	0,690	0,595	0,548	0,528
Concentration (mg/l)	26,20	23,80	21,55	19,69	17,92	16,24	15,04	12,94	11,92	11,48
$\ln(C_0/C)$	0,000	0,096	0,196	0,286	0,380	0,478	0,555	0,705	0,787	0,825



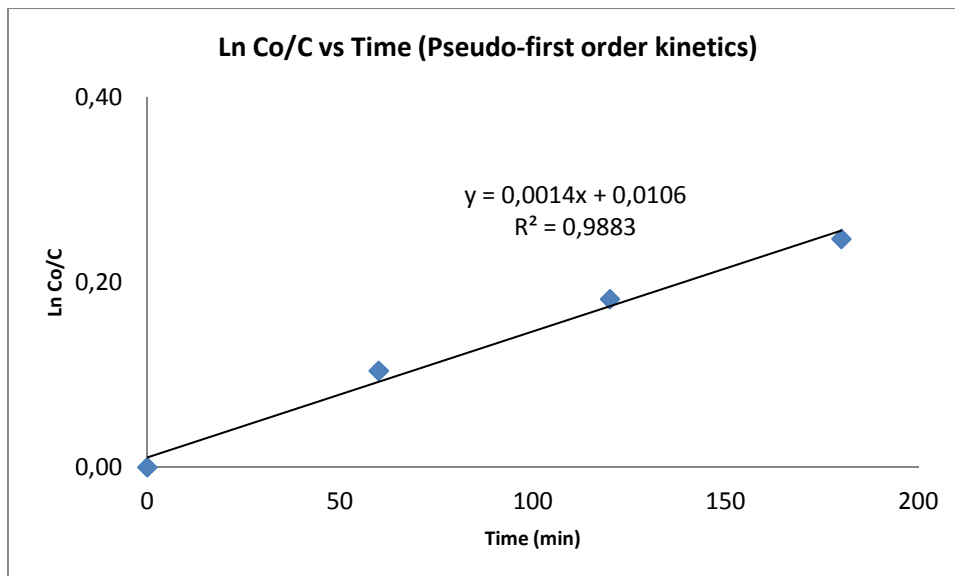
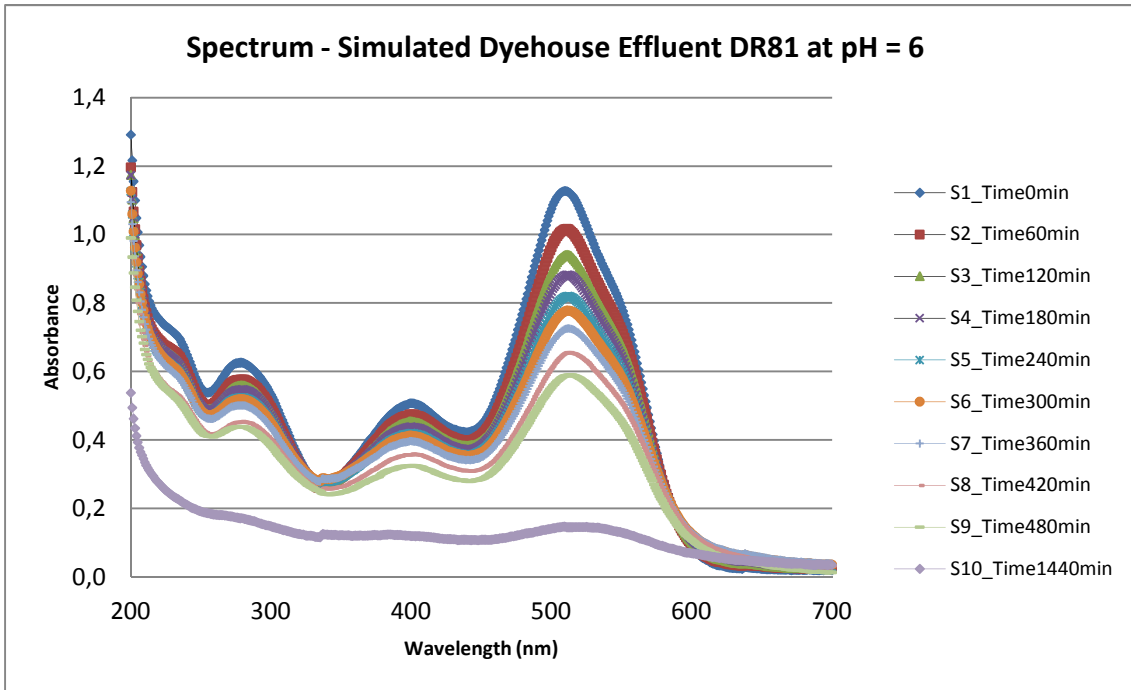
HYDROLYSED DR81 AT PH = 8

SAMPLE	S1	S2	S3	S4	S5	S6	S7	S8	S9	S10
Time (min)	0	60	120	180	240	300	360	420	480	1440
Absorbance at λ_{max}	1,058	0,883	0,762	0,685	0,612	0,571	0,517	0,464	0,421	0,061
Concentration (mg/l)	23,09	19,27	16,62	14,92	13,31	12,42	11,23	10,08	9,12	1,23
Ln (C ₀ /C)	0,000	0,181	0,329	0,437	0,551	0,620	0,721	0,829	0,929	2,936



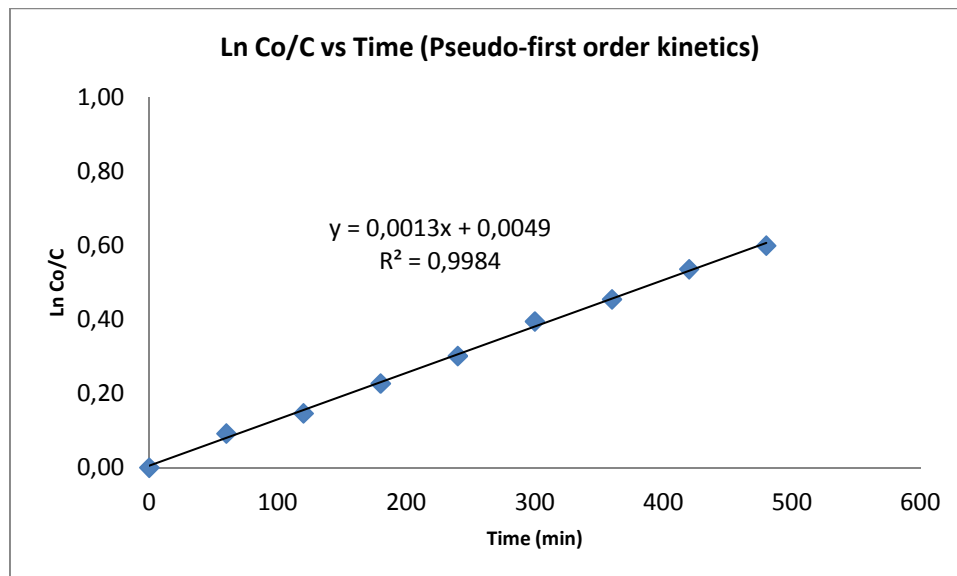
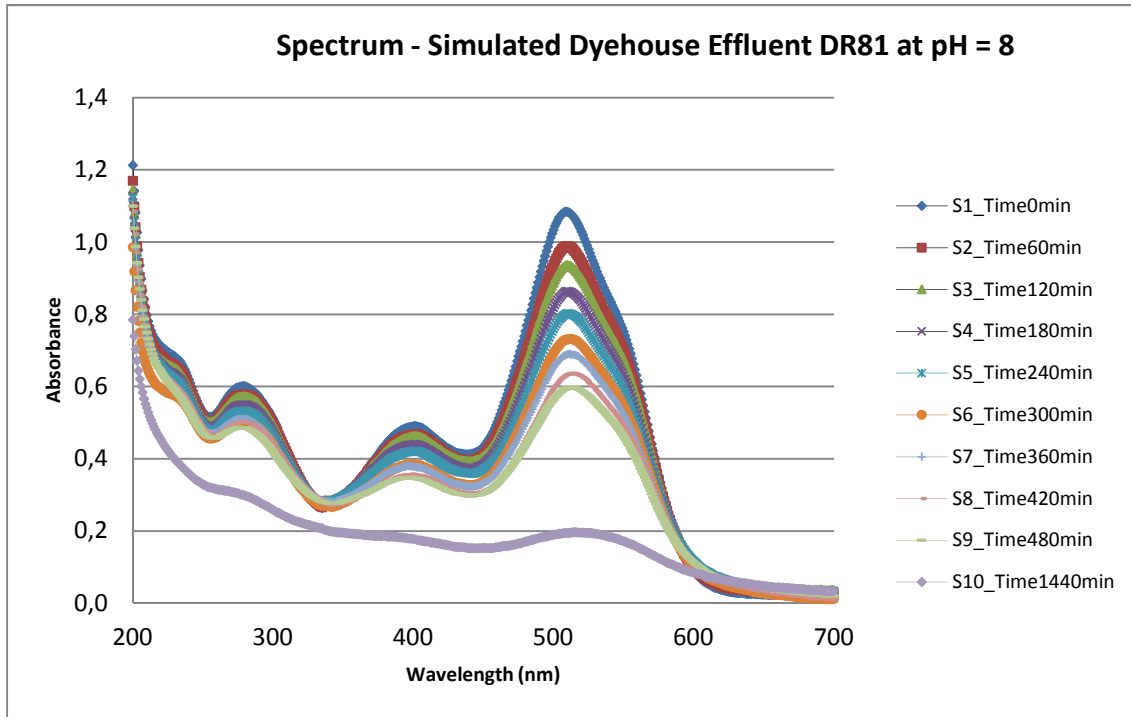
SIMULATED DYEHOUSE EFFLUENT DR81 AT PH = 6

SAMPLE	S1	S2	S3	S4	S5	S6	S7	S8	S9	S10
Time (min)	0	60	120	180	240	300	360	420	480	1420
Absorbance at λ_{max}	1,128	1,016	0,941	0,882	0,819	0,777	0,724	0,655	0,588	0,147
Concentration (mg/l)	24,63	22,19	20,53	19,24	17,86	16,94	15,79	14,27	12,80	3,12
Ln (C_0/C)	0,000	0,104	0,182	0,247	0,321	0,374	0,445	0,546	0,654	2,066



SIMULATED DYEHOUSE EFFLUENT DR81 AT PH = 8

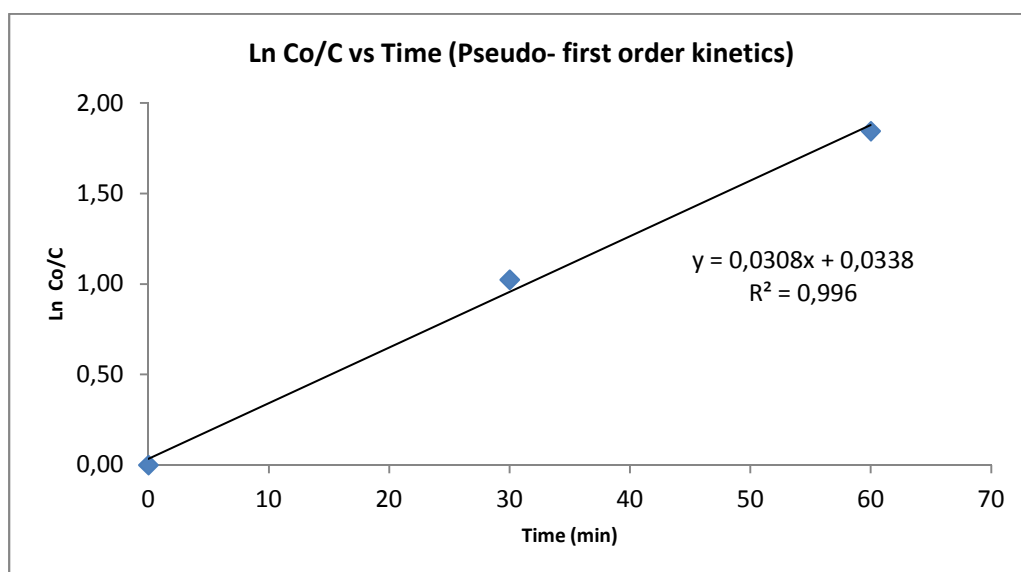
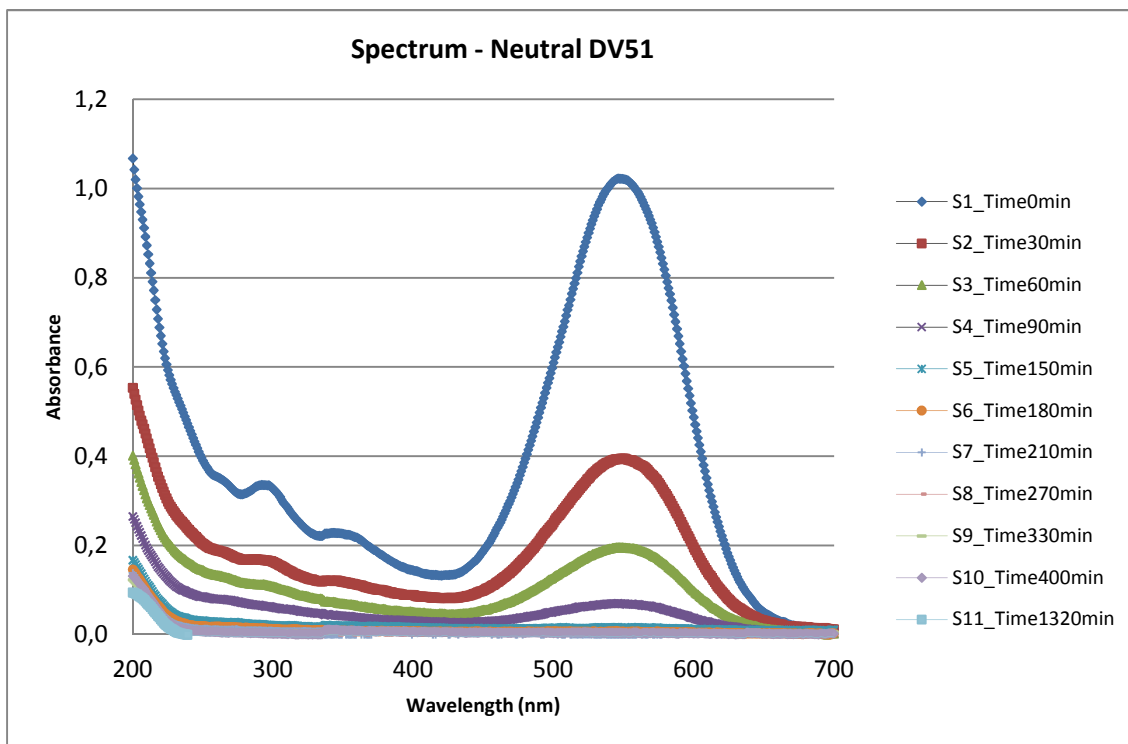
SAMPLE	S1	S2	S3	S4	S5	S6	S7	S8	S9	S10
Time (min)	0	60	120	180	240	300	360	420	480	1440
Absorbance at λ_{max}	1,084	0,989	0,937	0,864	0,803	0,731	0,689	0,636	0,597	0,195
Concentration (mg/l)	23,67	21,59	20,44	18,85	17,50	15,94	15,02	13,84	12,99	4,18
$\ln(C_0/C)$	0,000	0,092	0,147	0,228	0,302	0,395	0,455	0,537	0,600	1,734



DIRECT VIOLET 51

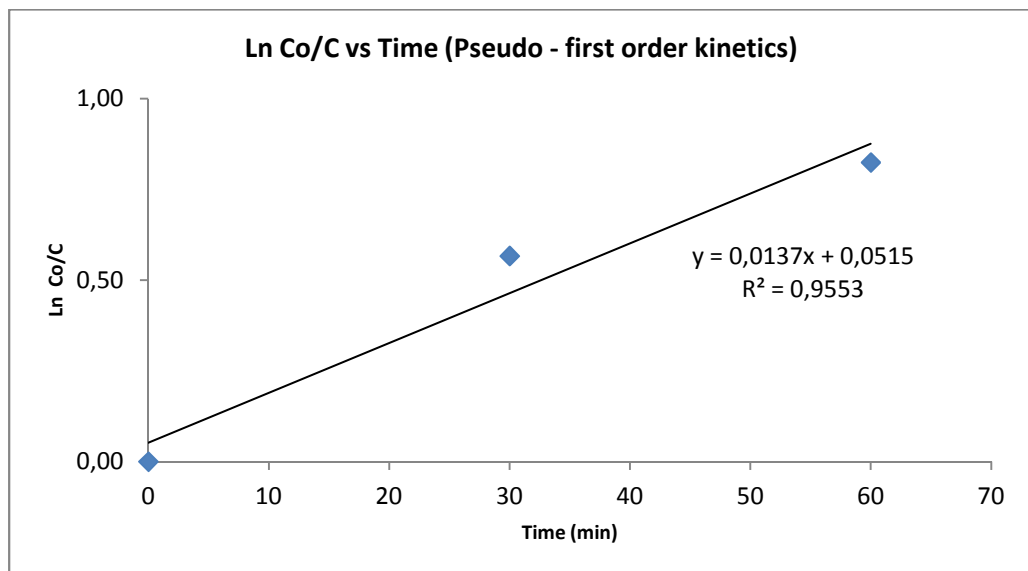
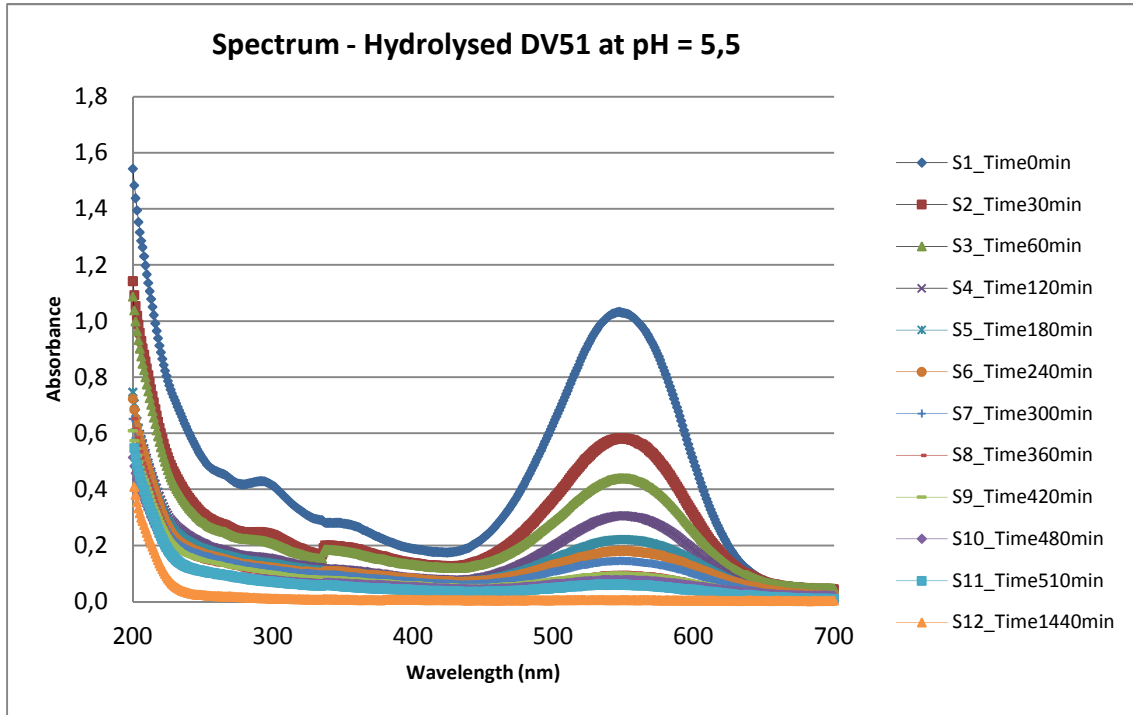
NEUTRAL DV51

SAMPLE	S1	S2	S3	S4	S5	S6	S7	S8	S9	S10	S11
Time (min)	0	30	60	90	150	180	210	270	330	400	1320
Absorbance at λ_{max}	1,023	0,394	0,196	0,070	0,017	0,008	0,001	0,001	0,006	0,004	-0,004
Concentration (mg/l)	21,40	7,68	3,38	0,64	-0,53	-0,73	-0,88	-0,87	-0,76	-0,79	-0,97
Ln (C ₀ /C)	0,000	1,024	1,846	3,512	-	-	-	-	-	-	-



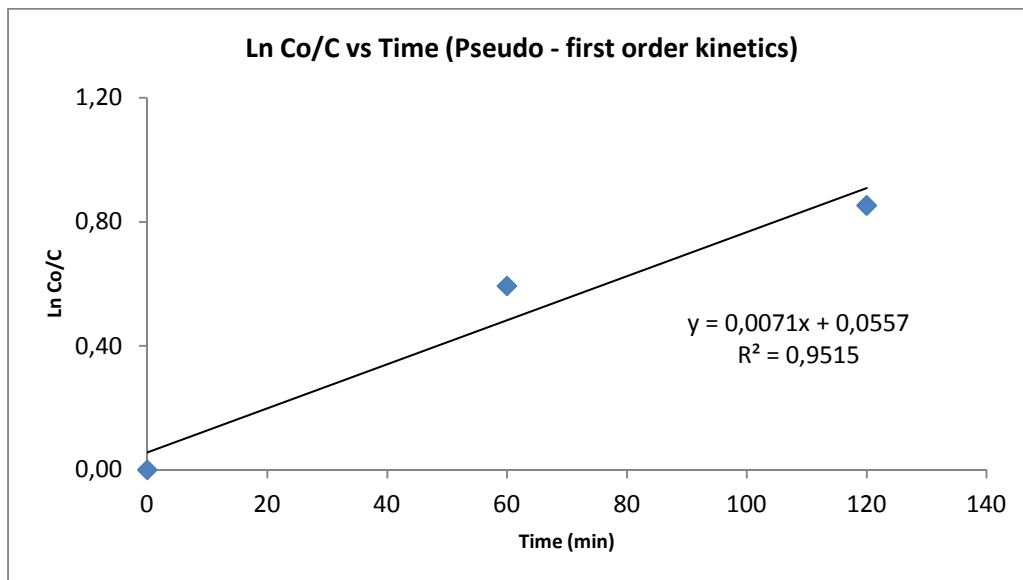
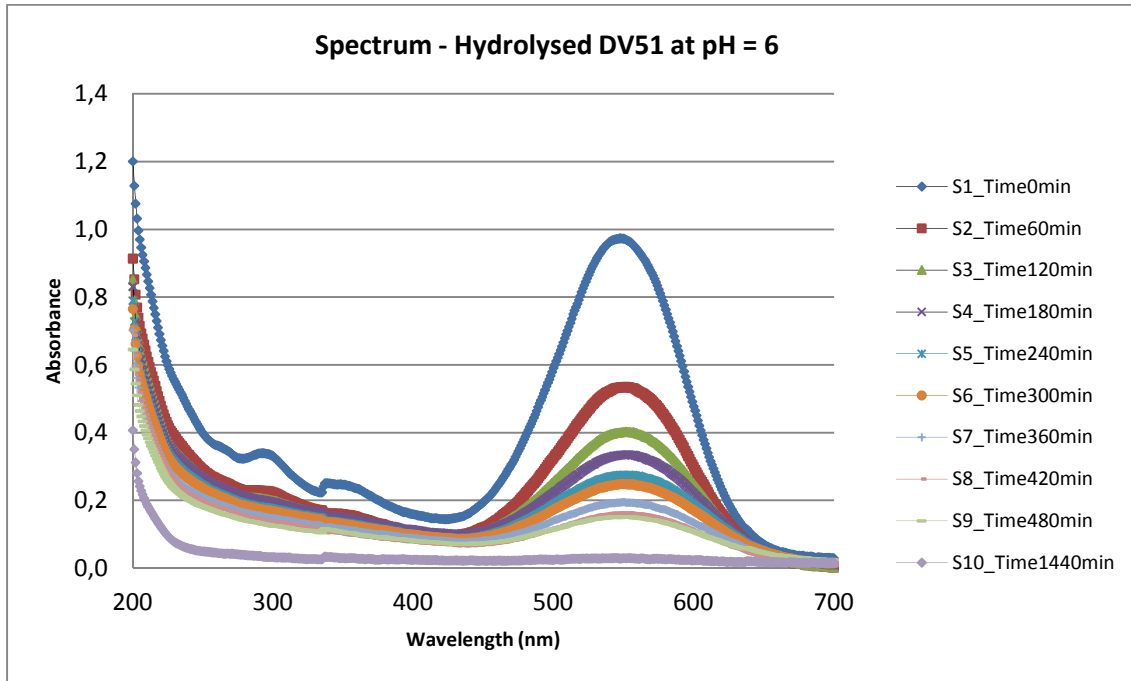
HYDROLYSED DV51 AT PH = 5,5

SAMPLE	S1	S2	S3	S4	S5	S6	S7	S8	S9	S10	S11	S12
Time (min)	0	30	60	120	180	240	300	360	420	480	510	1440
Absorbance at λ_{max}	1,033	0,569	0,431	0,298	0,217	0,178	0,143	0,102	0,099	0,077	0,059	0,006
Concentration (mg/l)	23,07	13,09	10,11	7,27	5,52	4,68	3,93	3,05	2,97	2,51	2,14	0,98
Ln (C ₀ /C)	0,000	0,567	0,825	1,155	1,430	1,594	1,769	2,0243	2,049	2,218	2,378	3,160



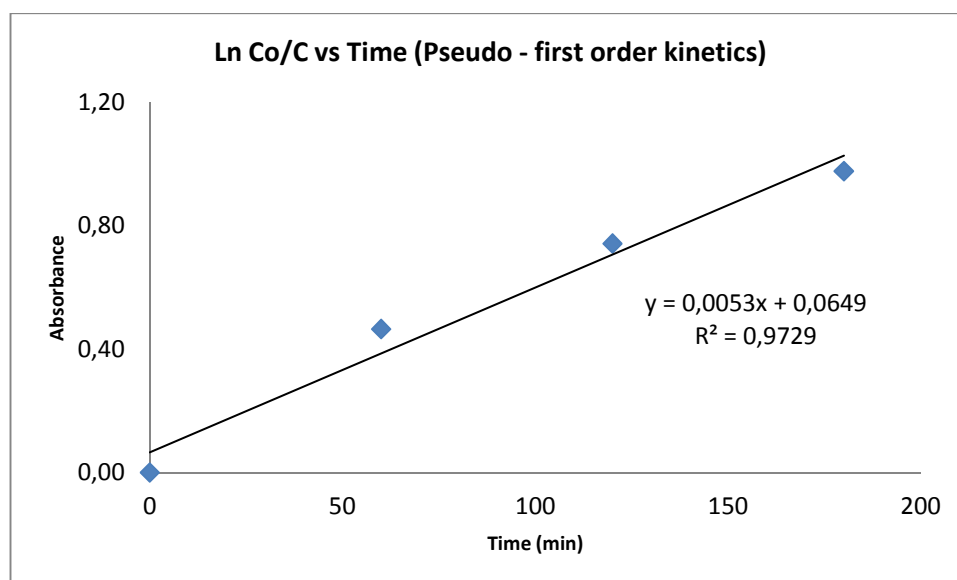
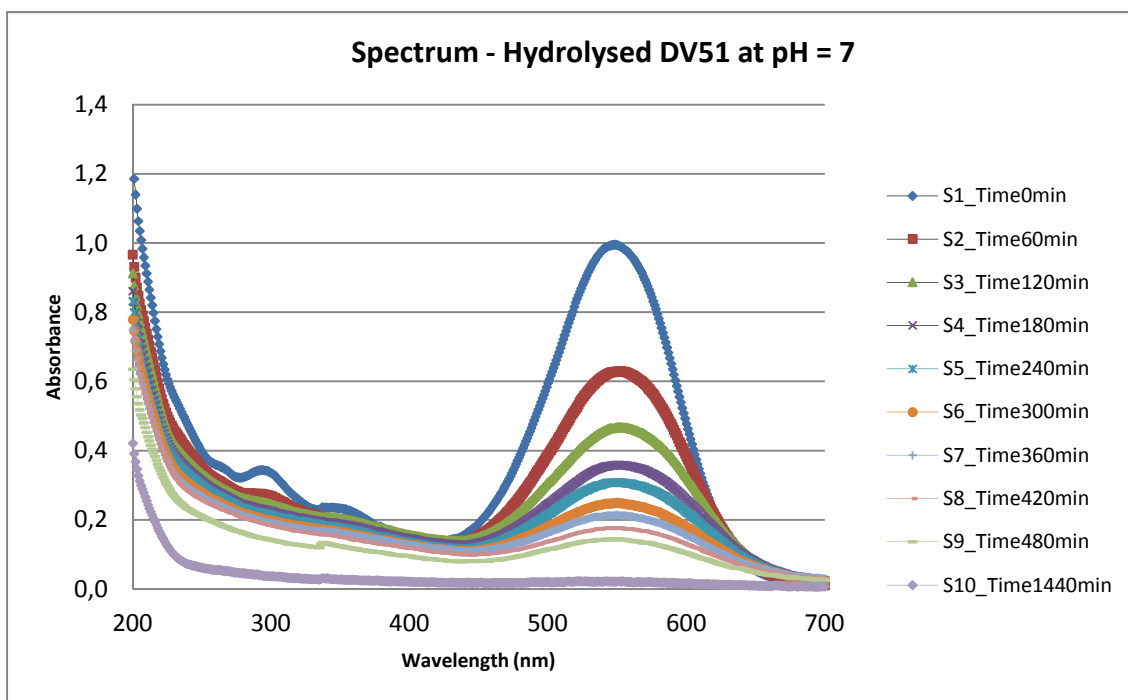
HYDROLYSED DV51 AT PH = 6

SAMPLE	S1	S2	S3	S4	S5	S6	S7	S8	S9	S10
Time (min)	0	60	120	180	240	300	360	420	480	1440
Absorbance at λ_{max}	0,9741	0,5202	0,3921	0,3259	0,2679	0,2421	0,1897	0,1599	0,1493	0,0295
Concentration (mg/l)	21,80	12,04	9,29	7,86	6,62	6,06	4,93	4,29	4,06	1,49
$\ln(C_0/C)$	0,0000	0,5937	0,8535	1,0199	1,1927	1,2803	1,4860	1,6251	1,6797	2,6845



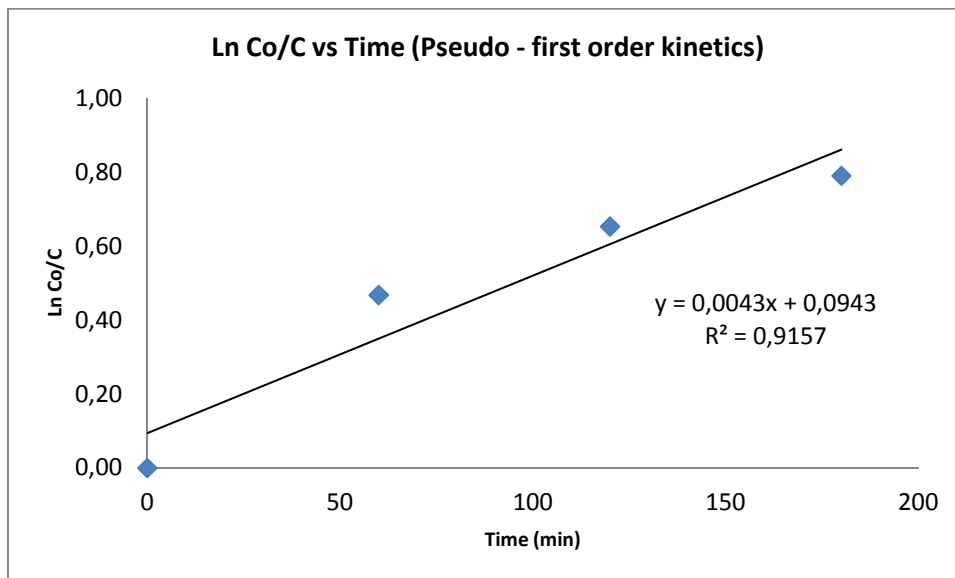
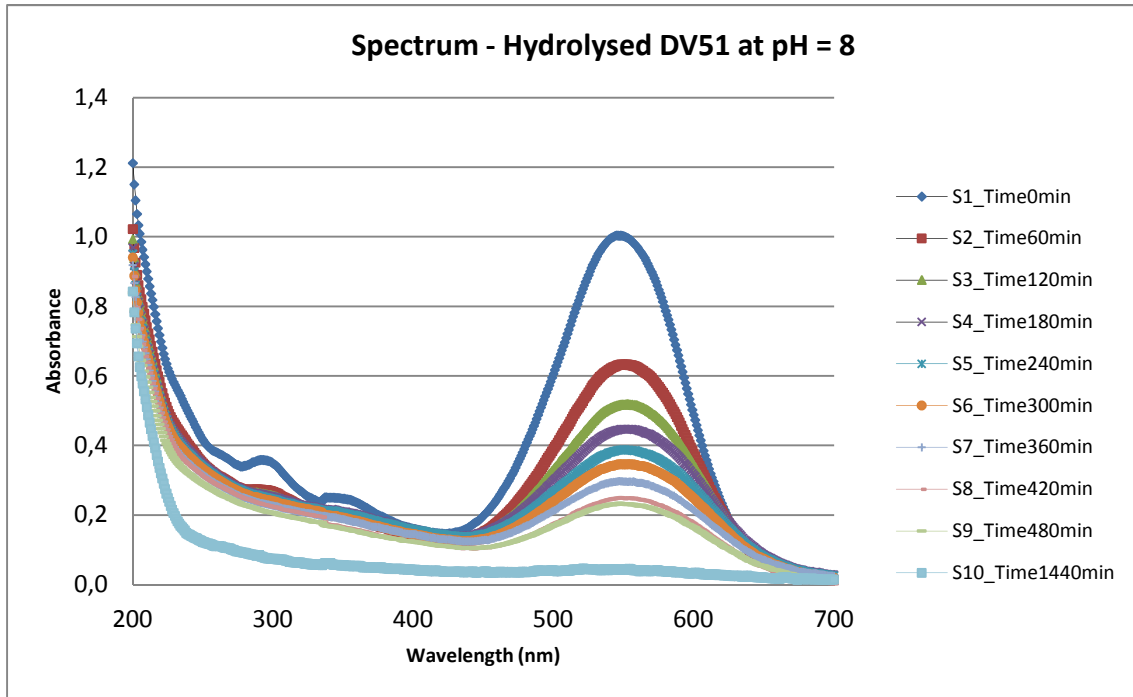
HYDROLYSED DV51 AT PH = 7

SAMPLE	S1	S2	S3	S4	S5	S6	S7	S8	S9	S10
Time (min)	0	60	120	180	240	300	360	420	480	1440
Absorbance at λ_{max}	0,995	0,610	0,453	0,350	0,301	0,243	0,209	0,174	0,143	0,022
Concentration (mg/l)	22,25	13,97	10,59	8,37	7,32	6,09	5,35	4,60	3,92	1,32
Ln (C ₀ /C)	0,000	0,465	0,743	0,978	1,112	1,296	1,423	1,576	1,737	2,828



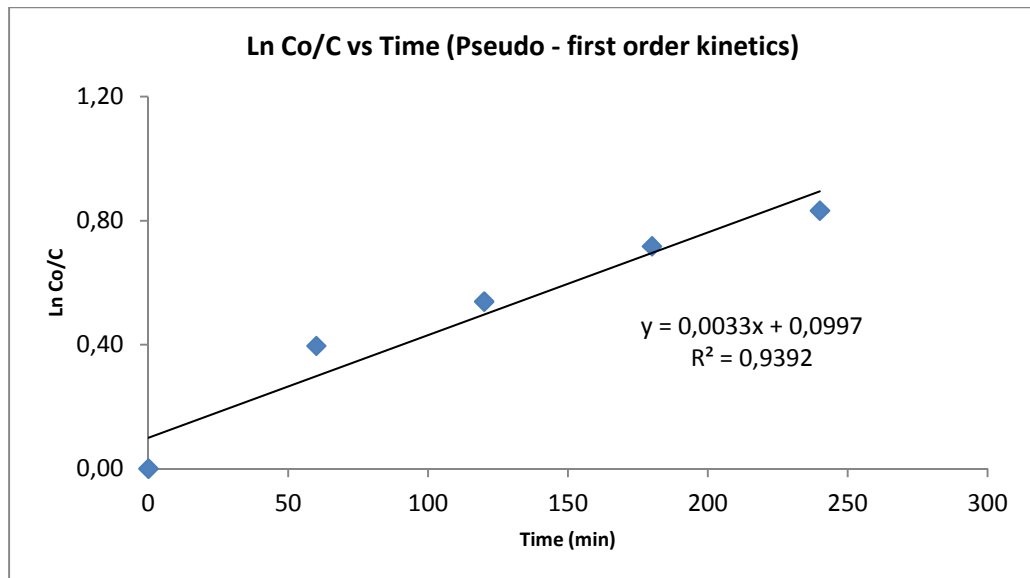
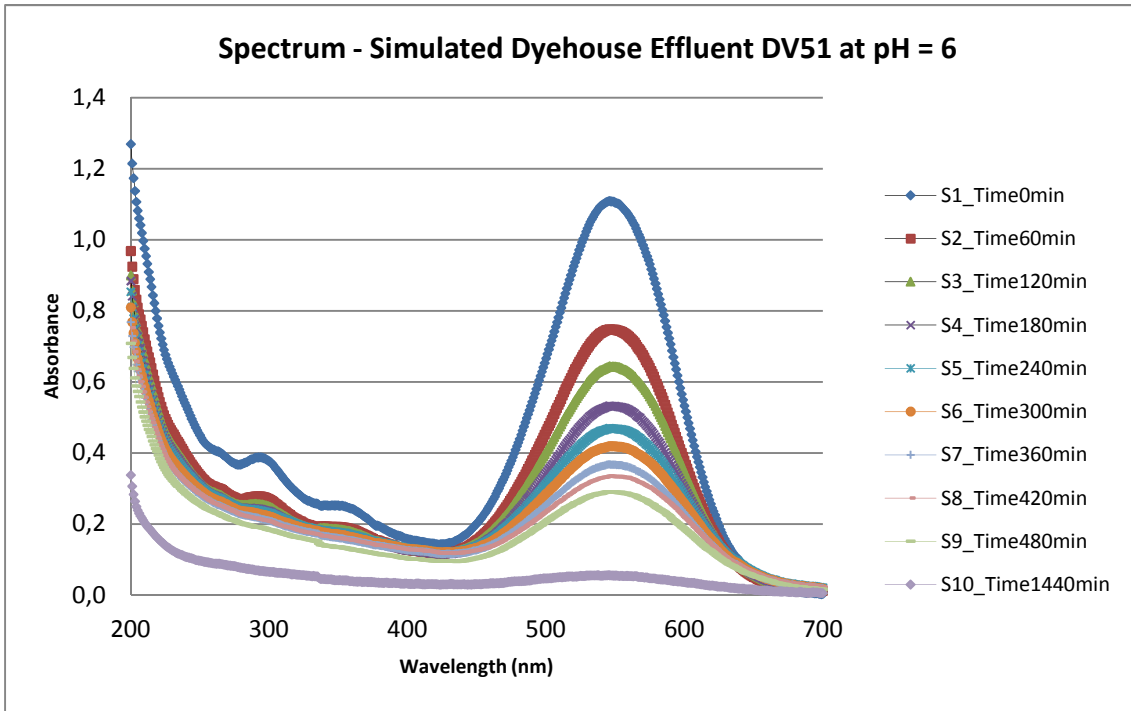
HYDROLYSED DV51 AT PH = 8

SAMPLE	S1	S2	S3	S4	S5	S6	S7	S8	S9	S10
Time (min)	0	60	120	180	240	300	360	420	480	1440
Absorbance at λ_{max}	1,003	0,614	0,503	0,434	0,376	0,337	0,292	0,245	0,229	0,087
Concentration (mg/l)	22,43	14,05	11,68	10,18	8,94	8,11	7,13	6,12	5,77	2,73
$\ln(C_0/C)$	0,000	0,468	0,653	0,790	0,920	1,018	1,146	1,299	1,357	2,107



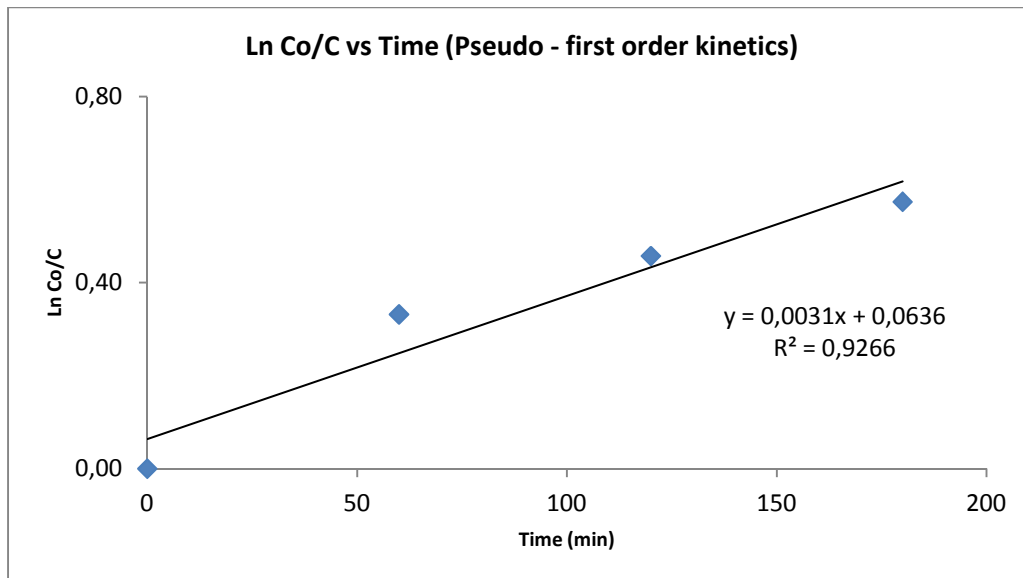
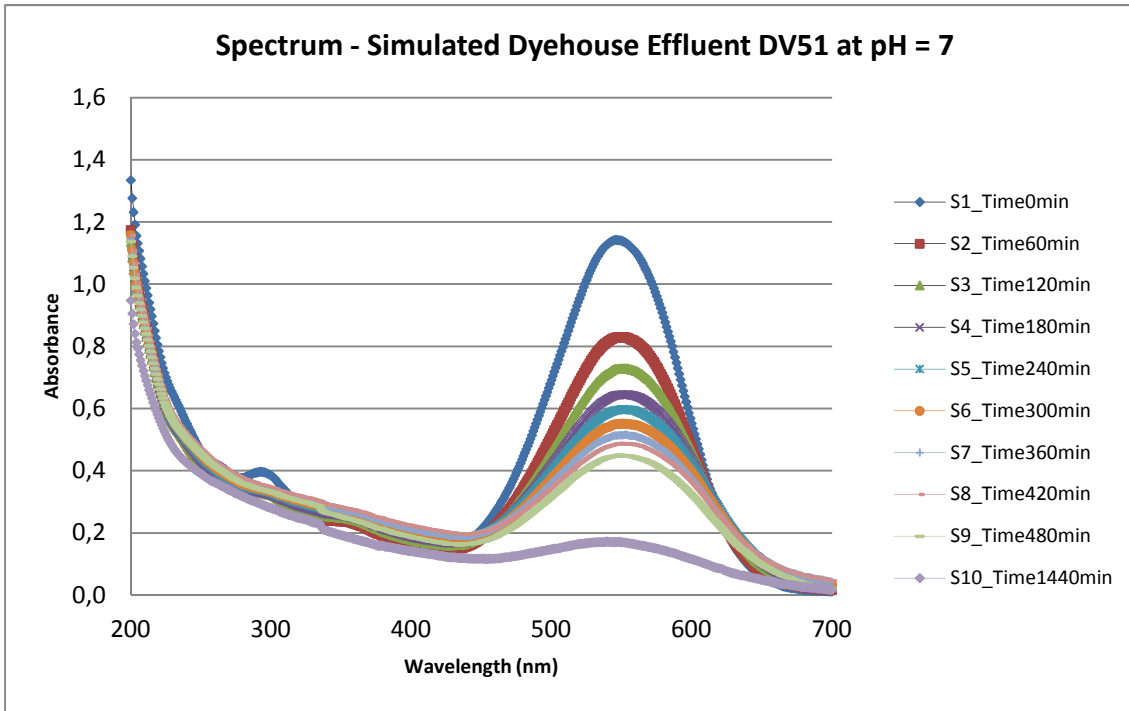
SIMULATED DYEHOUSE EFFLUENT DV51 AT PH = 6

SAMPLE	S1	S2	S3	S4	S5	S6	S7	S8	S9	S10
Time (min)	0	60	120	180	240	300	360	420	480	1440
Absorbance at λ_{max}	1,108	0,733	0,629	0,520	0,459	0,411	0,360	0,329	0,286	0,056
Concentration (mg/l)	24,69	16,61	14,40	12,05	10,74	9,69	8,60	7,94	7,01	2,06
Ln (C_0/C)	0,000	0,396	0,539	0,718	0,833	0,935	1,054	1,134	1,259	2,484



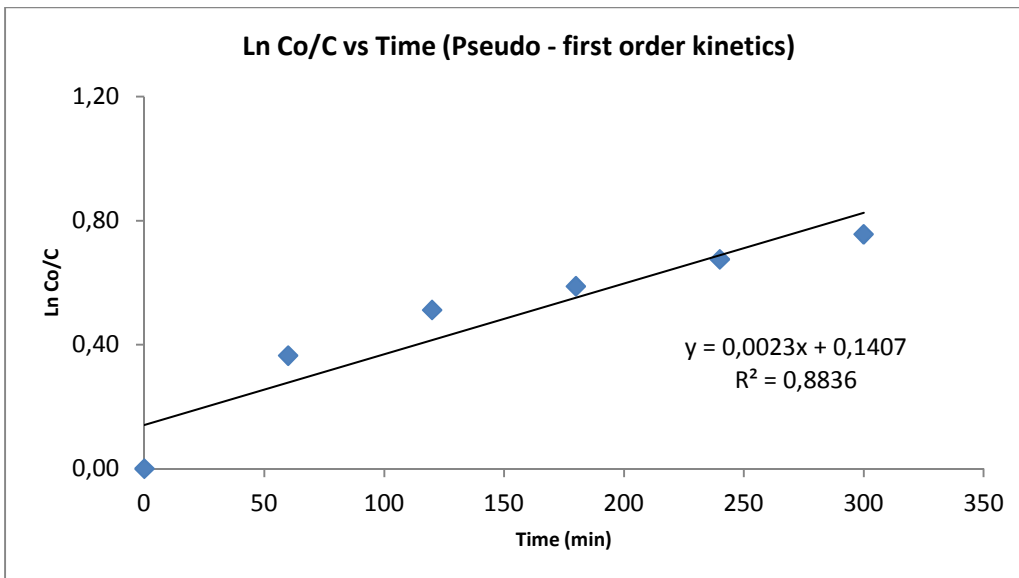
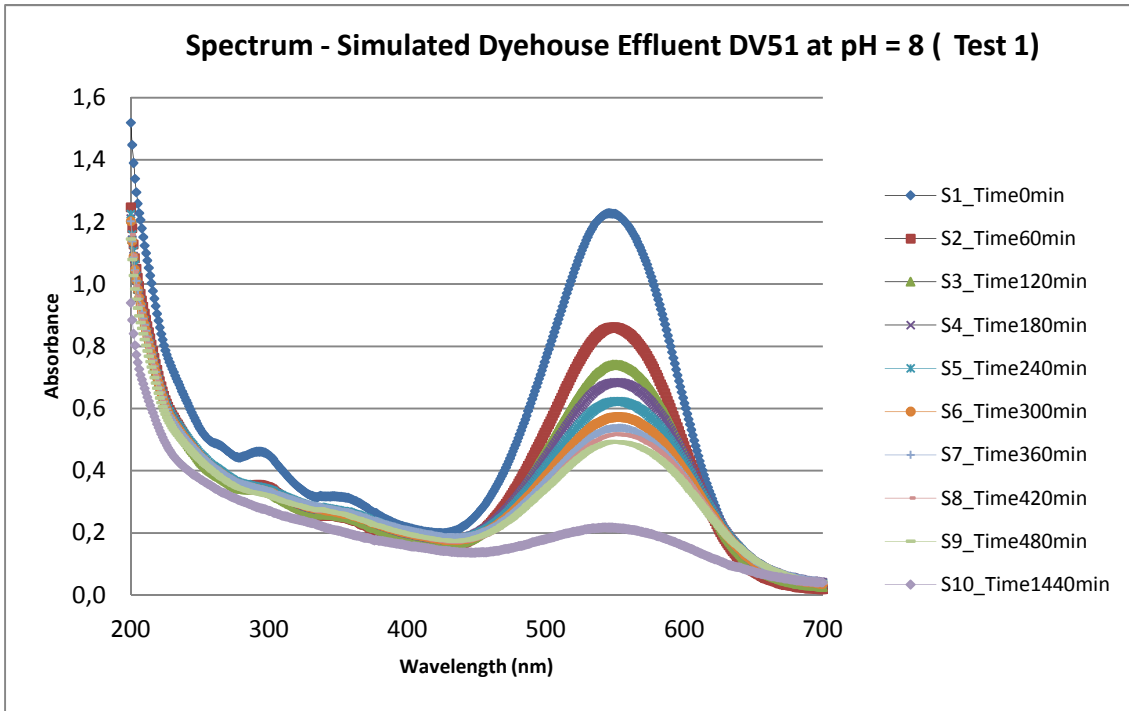
SIMULATED DYEHOUSE EFFLUENT DV51 AT PH = 7

SAMPLE	S1	S2	S3	S4	S5	S6	S7	S8	S9	S10
Time (min)	0	60	120	180	240	300	360	420	480	1440
Absorbance at λ_{max}	1,142	0,808	0,708	0,626	0,580	0,538	0,502	0,478	0,439	0,172
Concentration (mg/l)	25,42	18,24	16,08	14,31	13,33	12,41	11,65	11,12	10,31	4,54
$\ln(C_0/C)$	0,000	0,332	0,458	0,574	0,645	0,717	0,779	0,826	0,902	1,722



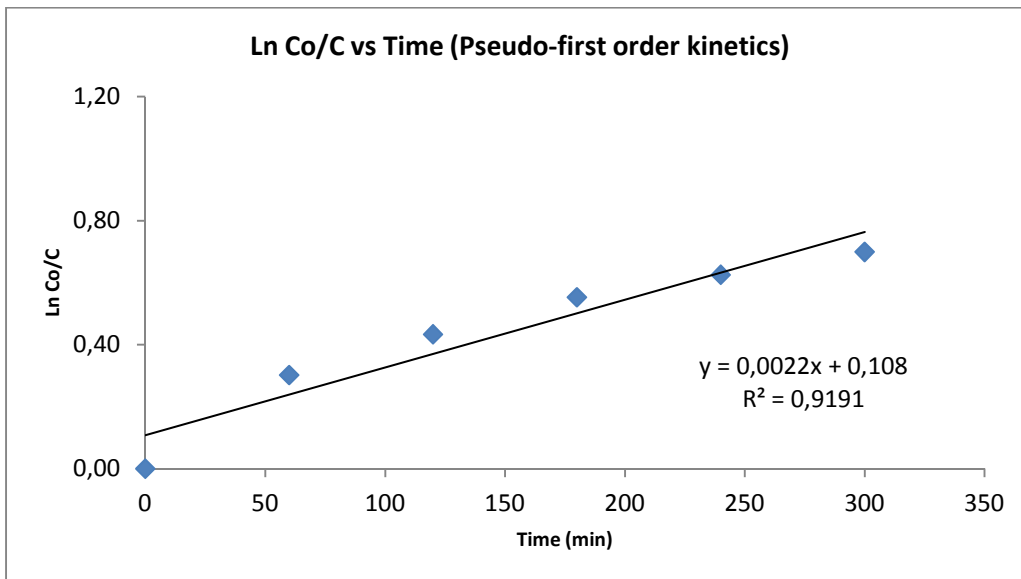
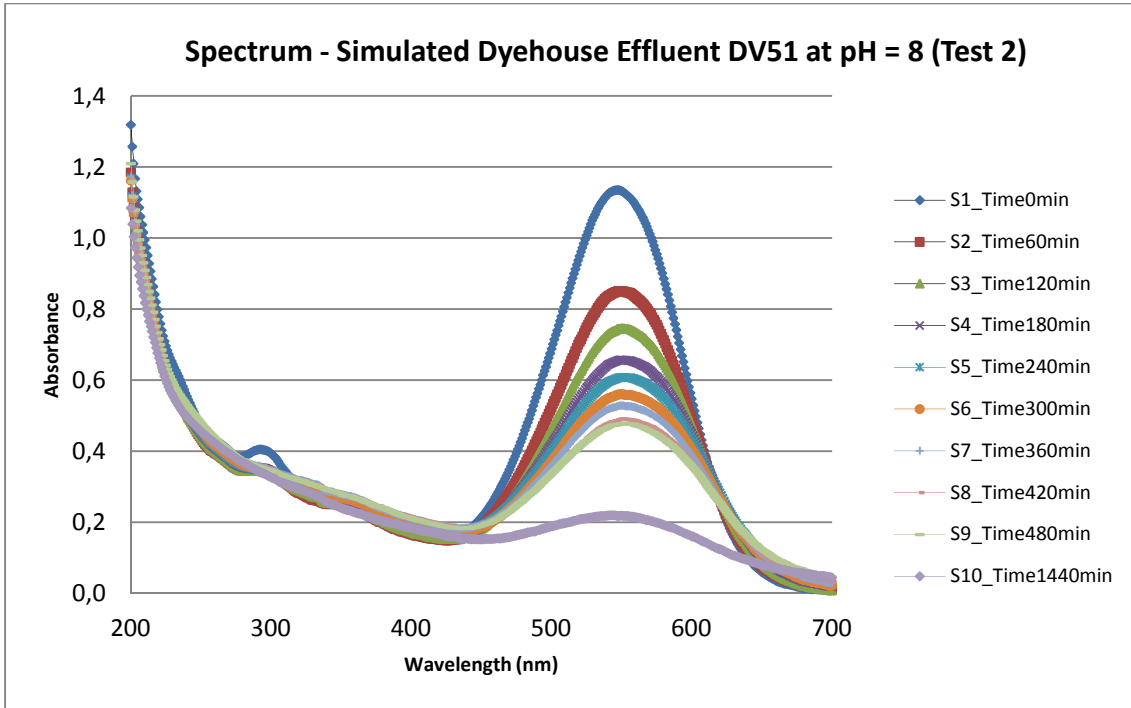
SIMULATED DYEHOUSE EFFLUENT DV51 AT PH = 8 (Test 1)

SAMPLE	S1	S2	S3	S4	S5	S6	S7	S8	S9	S10
Time (min)	0	60	120	180	240	300	360	420	480	1440
Absorbance at λ_{max}	1,228	0,840	0,719	0,664	0,605	0,555	0,522	0,504	0,481	0,217
Concentration (mg/l)	27,26	18,92	16,33	15,13	13,87	12,79	12,08	11,70	11,20	5,51
Ln (C ₀ /C)	0,000	0,365	0,512	0,589	0,676	0,757	0,813	0,846	0,889	1,598



SIMULATED DYEHOUSE EFFLUENT DV51 AT PH = 8 (Test 2)

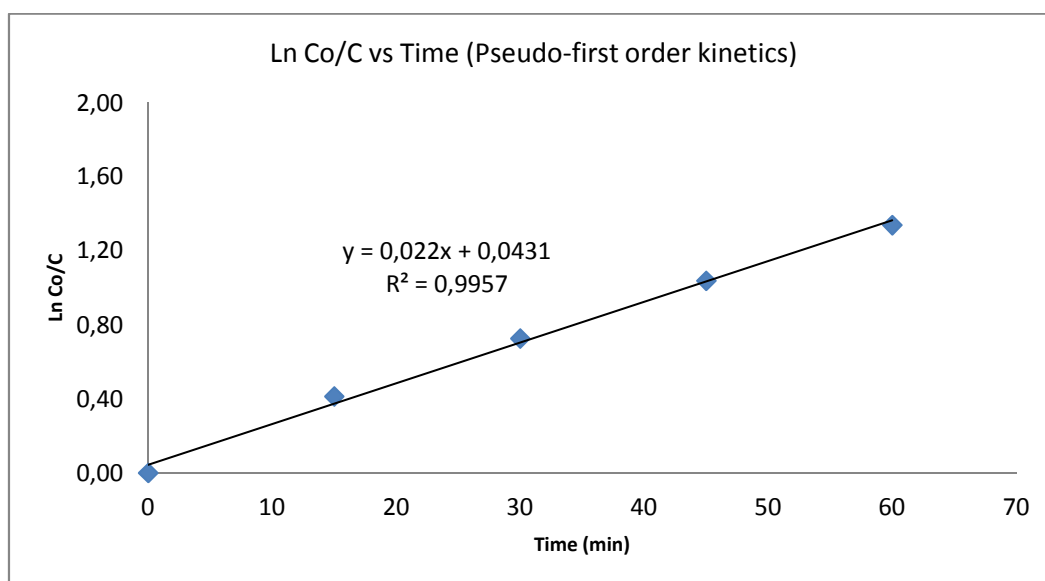
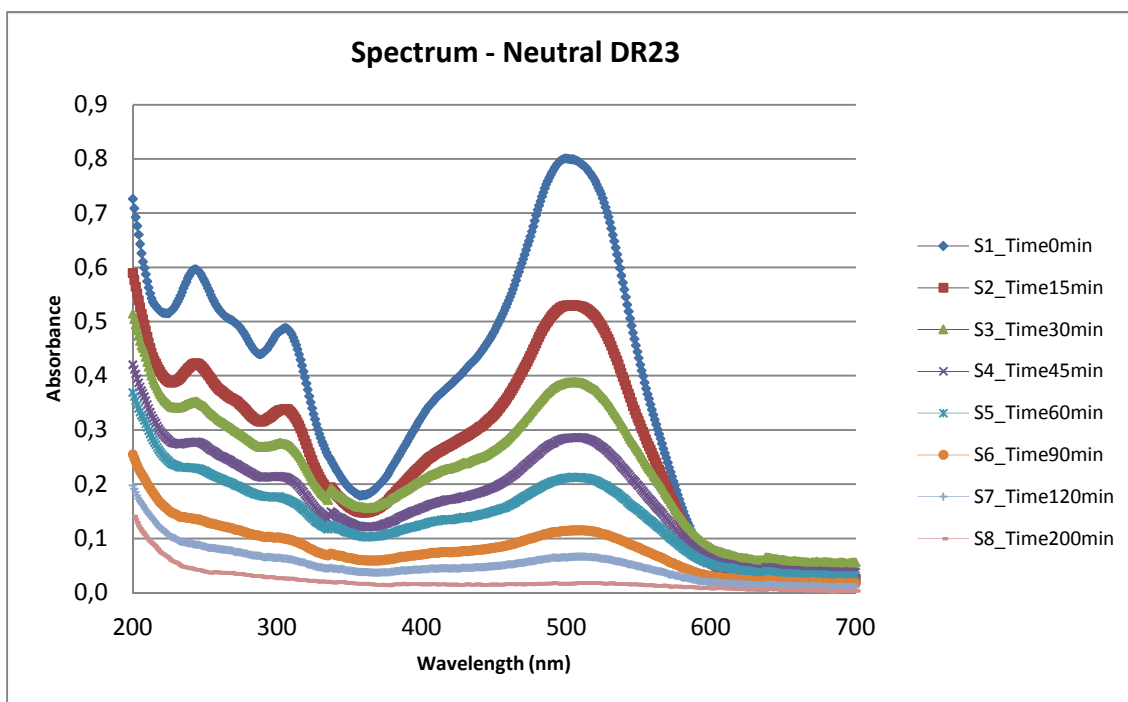
SAMPLE	S1	S2	S3	S4	S5	S6	S7	S8	S9	S10
Time (min)	0	60	120	180	240	300	360	420	480	1440
Absorbance at λ_{max}	1,135	0,829	0,722	0,636	0,589	0,544	0,514	0,477	0,464	0,218
Concentration (mg/l)	25,26	18,68	16,38	14,53	13,51	12,55	11,90	11,12	10,82	5,54
Ln (C ₀ /C)	0,000	0,302	0,434	0,553	0,626	0,699	0,753	0,821	0,848	1,517



DIRECT RED 23

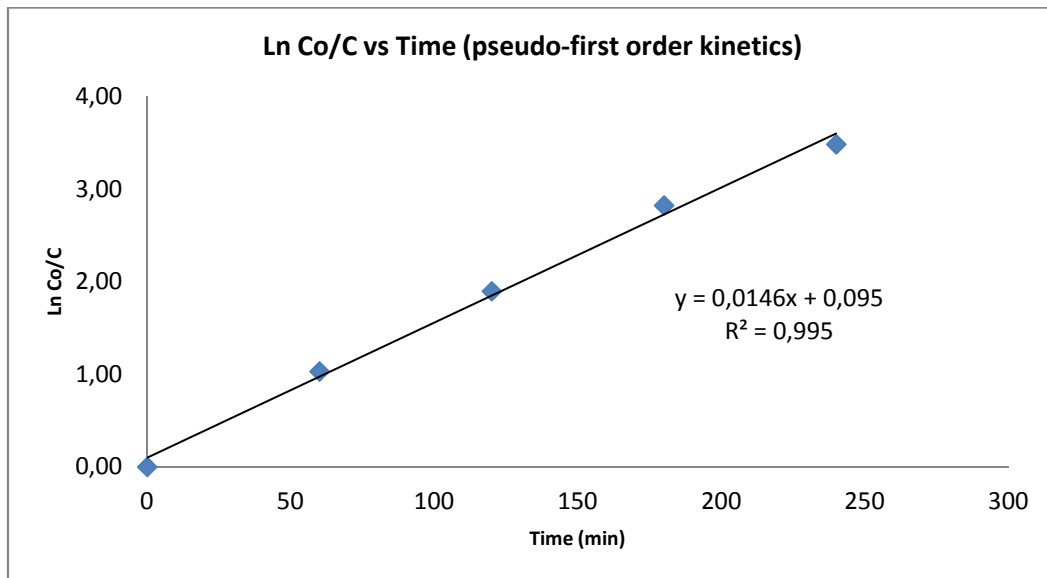
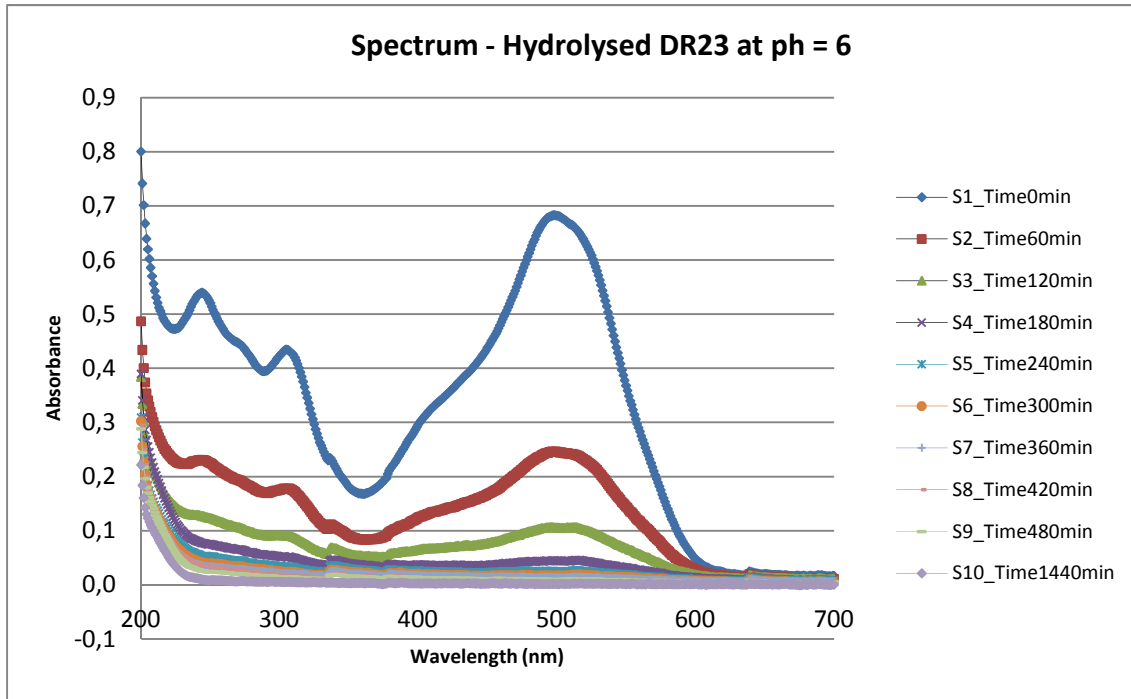
NEUTRAL DR23

SAMPLE	S1	S2	S3	S4	S5	S6	S7	S8
Time (min)	0	15	30	45	60	90	120	200
Absorbance at λ_{max}	0,799	0,530	0,389	0,286	0,213	0,115	0,066	0,017
Concentration (mg/l)	24,83	16,41	12,00	8,78	6,50	3,44	1,91	0,38
Ln (C ₀ /C)	0,000	0,414	0,728	1,039	1,340	1,976	2,563	4,168



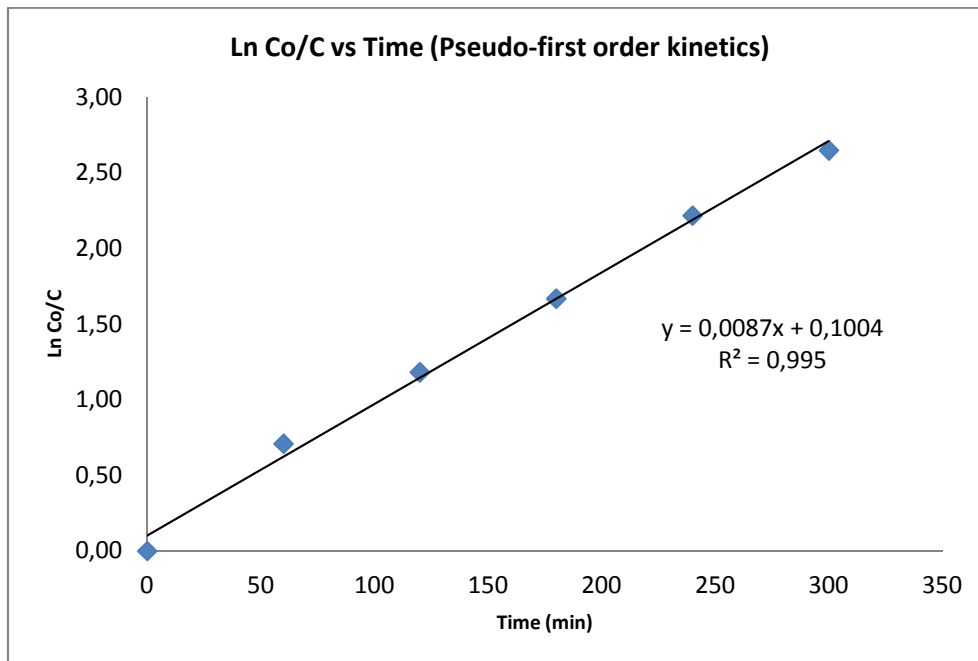
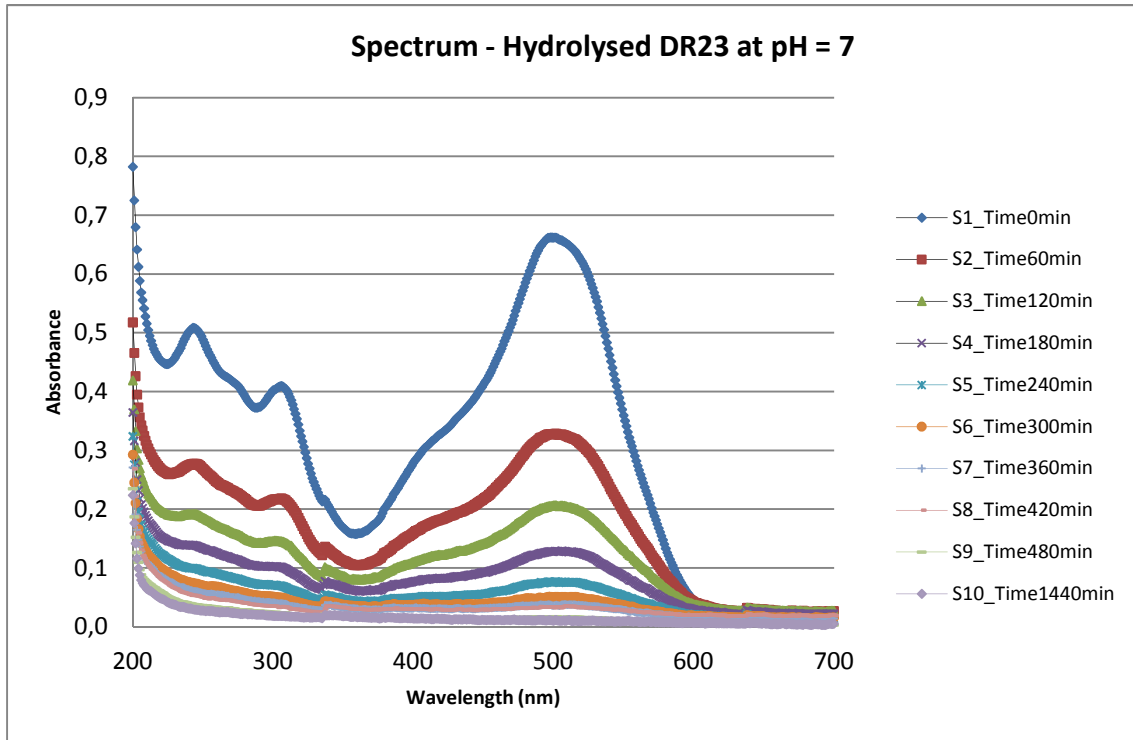
HYDROLYSED DR23 AT PH = 6

SAMPLE	S1	S2	S3	S4	S5	S6	S7	S8	S9	S10
Time (min)	0	60	120	180	240	300	360	420	480	1440
Absorbance at λ_{max}	0,679	0,245	0,106	0,045	0,025	0,017	0,014	0,011	0,009	0,002
Concentration (mg/l)	21,08	7,51	3,15	1,25	0,64	0,40	0,29	0,19	0,16	-0,07
Ln (C ₀ /C)	0,000	1,032	1,900	2,828	3,489	3,973	4,284	4,689	4,865	-



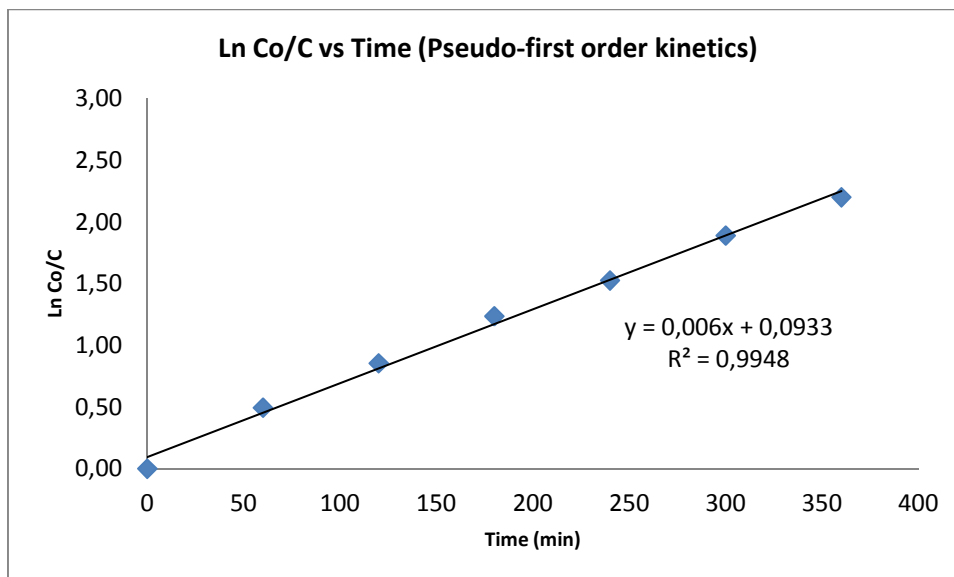
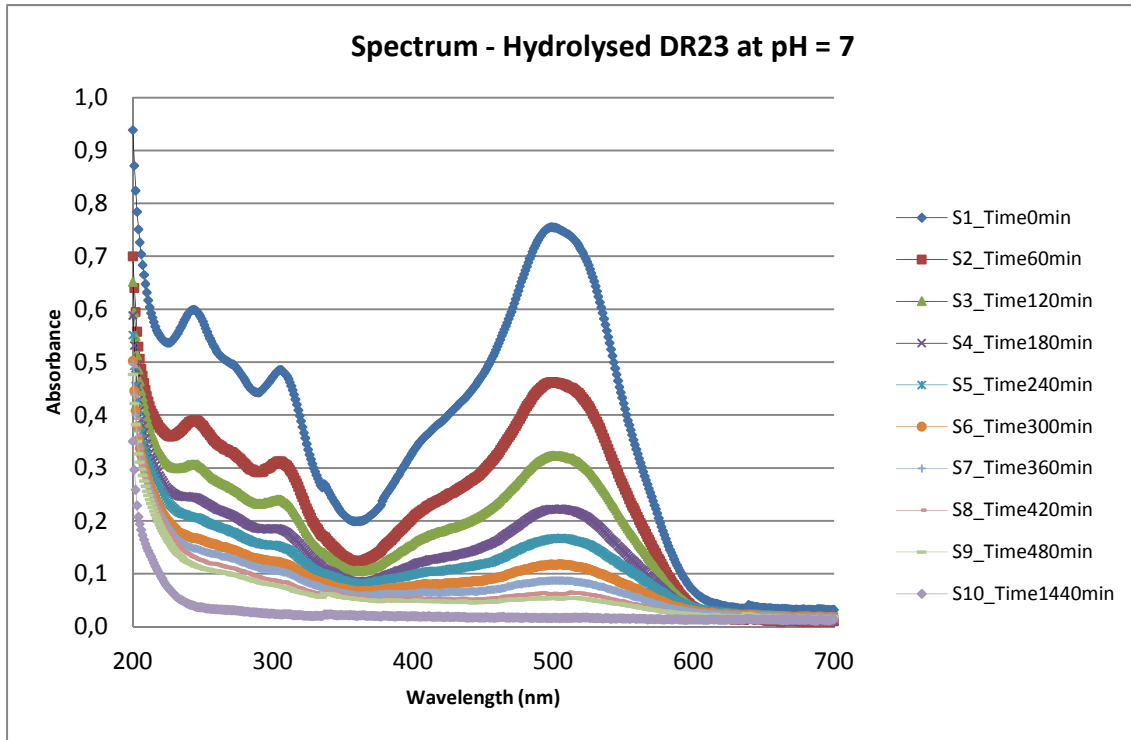
HYDROLYSED DR23 AT PH = 7

SAMPLE	S1	S2	S3	S4	S5	S6	S7	S8	S9	S10
Time (min)	0	60	120	180	240	300	360	420	480	1440
Absorbance at λ_{max}	0,660	0,327	0,206	0,128	0,076	0,051	0,037	0,034	0,017	0,011
Concentration (mg/l)	20,49	10,08	6,28	3,87	2,23	1,45	1,01	0,90	0,37	0,19
Ln (C ₀ /C)	0,000	0,709	1,182	1,668	2,218	2,649	3,014	3,122	4,001	4,694



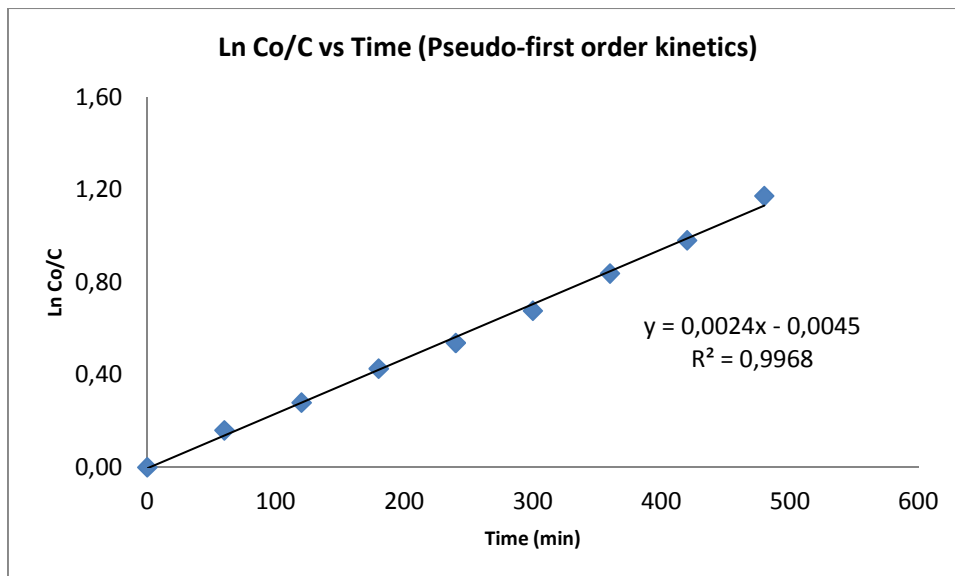
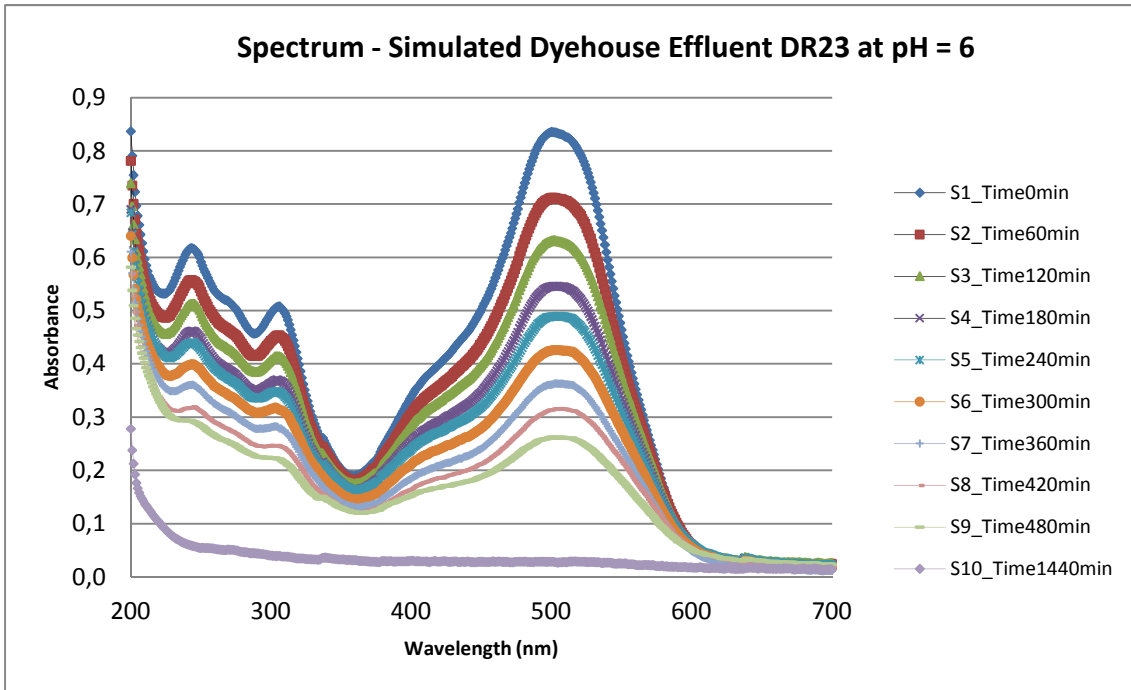
HYDROLYSED DR23 AT PH = 8

SAMPLE	S1	S2	S3	S4	S5	S6	S7	S8	S9	S10
Time (min)	0	60	120	180	240	300	360	420	480	1440
Absorbance at λ_{max}	0,753	0,461	0,323	0,222	0,167	0,118	0,087	0,062	0,054	0,017
Concentration (mg/l)	23,39	14,27	9,95	6,79	5,08	3,53	2,59	1,80	1,54	0,38
Ln (C ₀ /C)	0,000	0,494	0,855	1,237	1,527	1,891	2,202	2,566	2,720	4,117



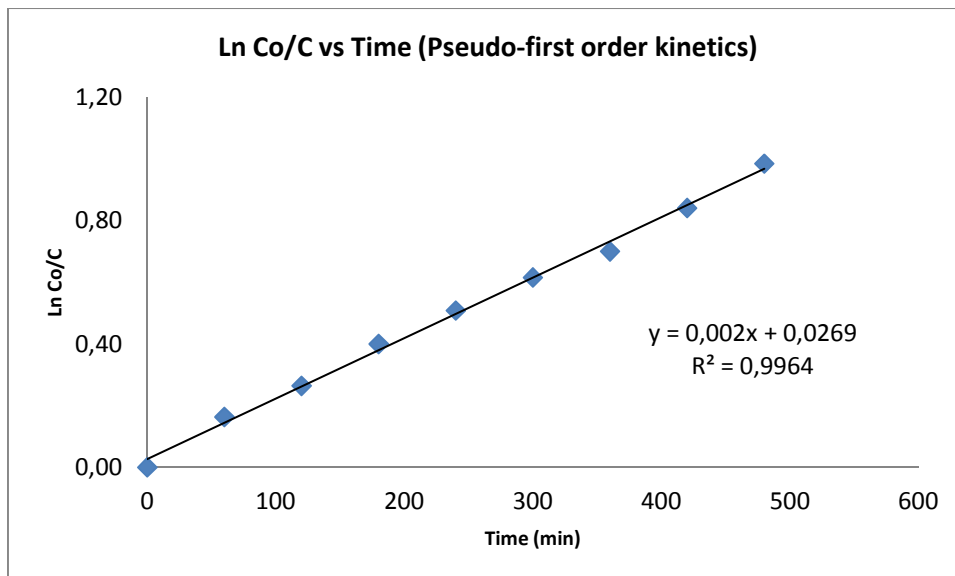
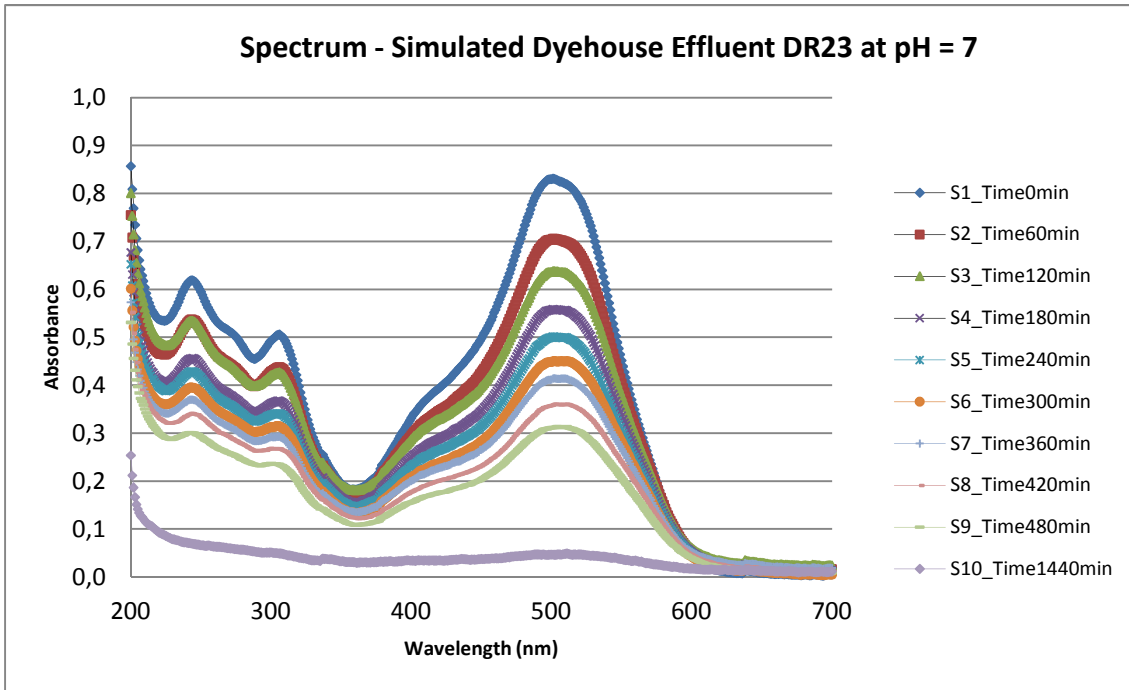
SIMULATED DYEHOUSE EFFLUENT DR23 AT PH = 6

SAMPLE	S1	S2	S3	S4	S5	S6	S7	S8	S9	S10
Time (min)										
Absorbance at λ_{max}										
Concentration (mg/l)										
Ln (C ₀ /C)										



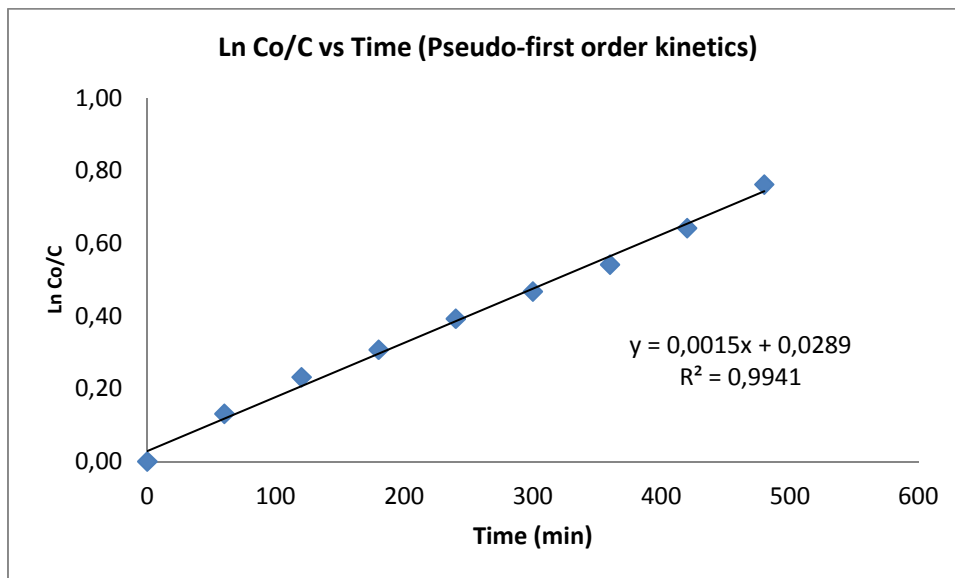
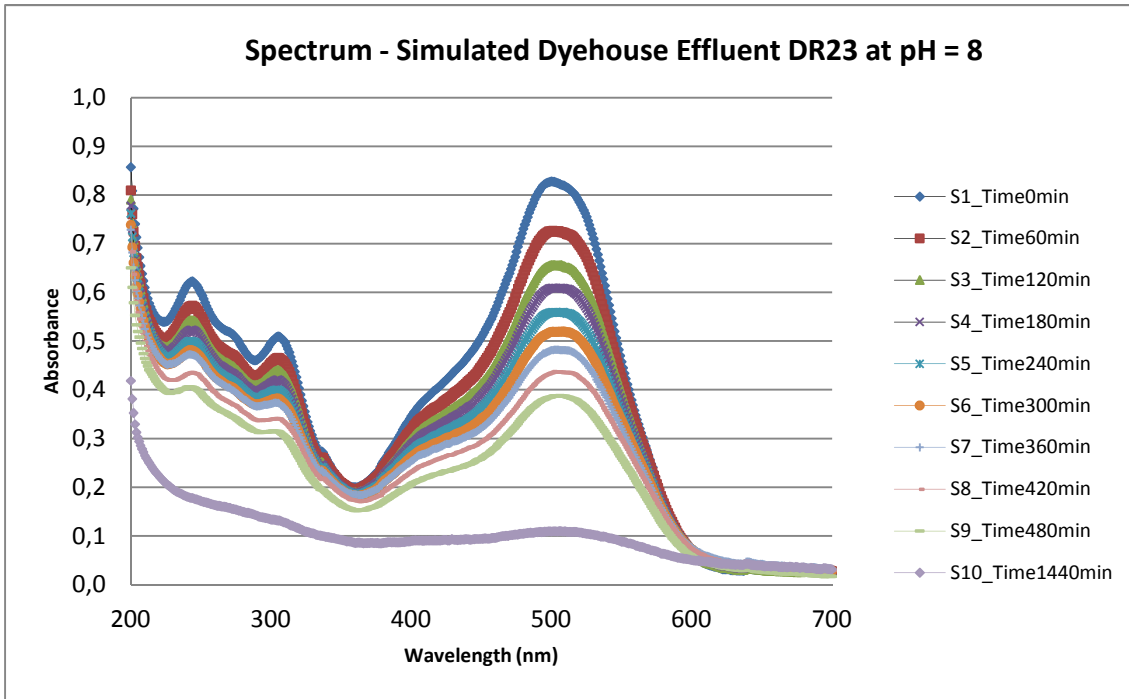
SIMULATED DYEHOUSE EFFLUENT DR23 AT PH = 7

SAMPLE	S1	S2	S3	S4	S5	S6	S7	S8	S9	S10
Time (min)	0	60	120	180	240	300	360	420	480	1440
Absorbance at λ_{max}	0,829	0,705	0,638	0,557	0,501	0,450	0,414	0,360	0,313	0,047
Concentration (mg/l)	25,78	21,89	19,78	17,27	15,50	13,92	12,79	11,11	9,62	1,31
Ln (C ₀ /C)	0,000	0,163	0,265	0,400	0,509	0,616	0,701	0,841	0,985	2,979



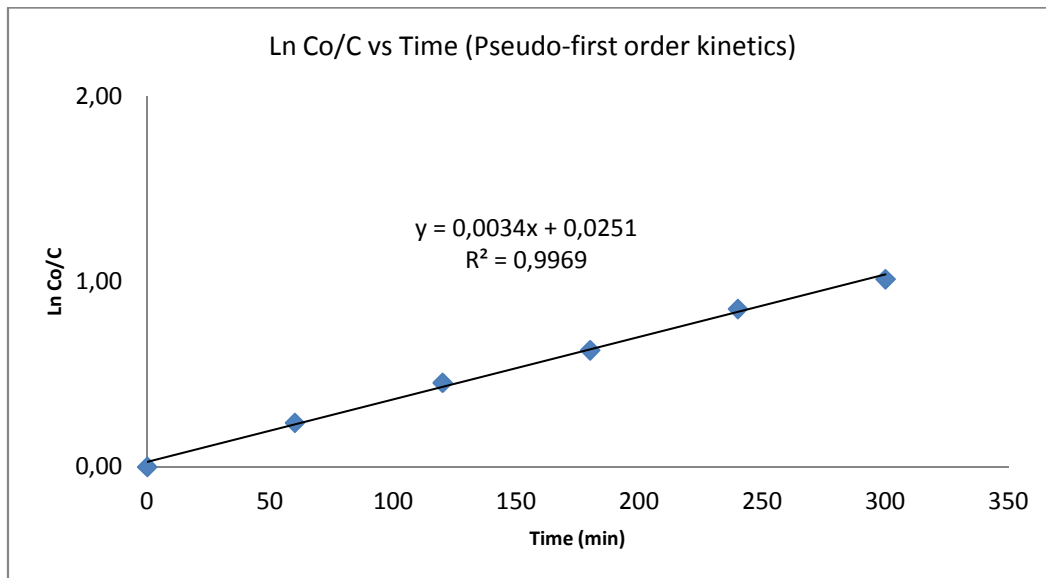
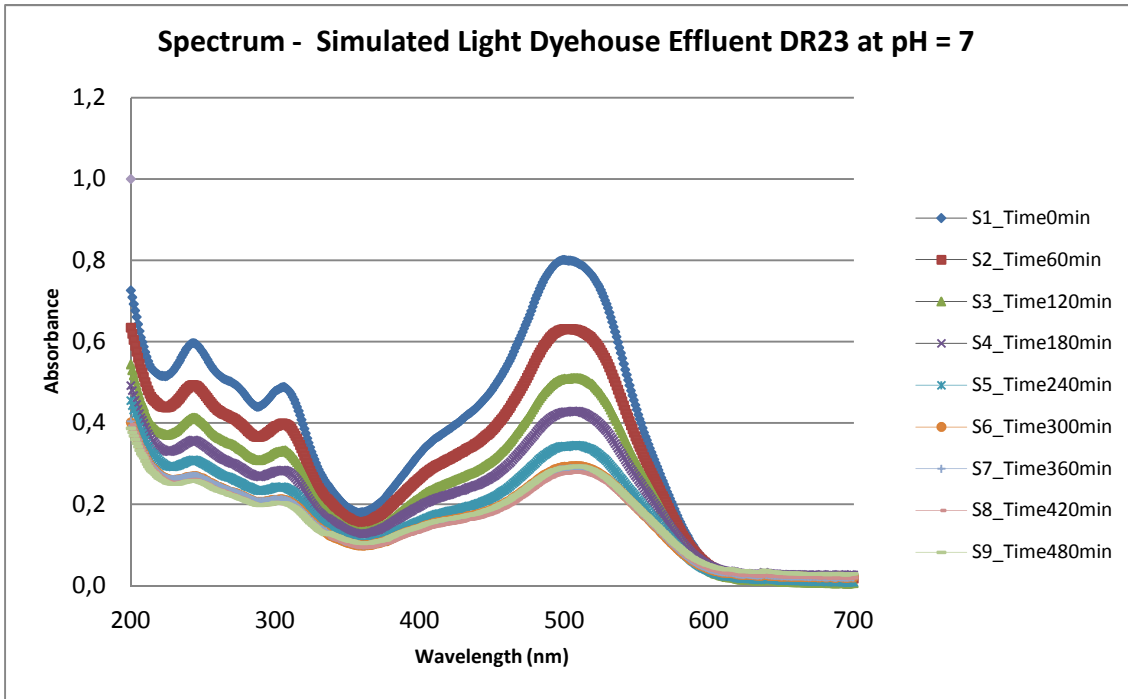
SIMULATED DYEHOUSE EFFLUENT DR23 AT PH = 8

SAMPLE	S1	S2	S3	S4	S5	S6	S7	S8	S9	S10
Time (min)	0	60	120	180	240	300	360	420	480	1440
Absorbance at λ_{max}	0,826	0,725	0,656	0,609	0,559	0,519	0,483	0,437	0,388	0,110
Concentration (mg/l)	25,68	22,52	20,36	18,88	17,34	16,09	14,94	13,51	11,98	3,29
$\ln(C_0/C)$	0,000	0,131	0,232	0,307	0,393	0,468	0,542	0,642	0,762	2,054



LIGHT SIMULATED DYEHOUSE EFFLUENT DR23 AT PH = 7

SAMPLE	S1	S2	S3	S4	S5	S6	S7	S8	S9
Time (min)	0	60	120	180	240	300	360	420	480
Absorbance at λ_{max}	0,799	0,631	0,509	0,427	0,343	0,293	0,287	0,278	0,291
Concentration (mg/l)	24,83	19,57	15,76	13,21	10,57	9,00	8,83	8,54	8,93
$\ln(C_0/C)$	0,000	0,238	0,455	0,631	0,854	1,015	1,034	1,068	1,022



ANNEX V: Kinetic results

DYE	NAME	k_{app} (min ⁻¹)	% ADSORPTION
DY50	DY50	0,0496	100
	DY50H at pH = 6	0,0042	99,83
	DY50H at pH = 7	0,0027	98,83
	DY50H at pH = 8	0,0031	99,67
	DY50SDE at pH = 6	0,0022	98,28
	DY50SDE at pH = 7 (Test 1)	0,0017	98,19
	DY50SDE at pH = 7 (Test 2)	0,0024	100
	DY50SDE at pH = 8	0,0019	93,27
DR81	DR81	0,0421	100
	DR81H at pH = 5,5	0,0092	99,39
	DR81H at pH = 6	0,0068	98,74
	DR81H at pH = 7	0,0033	91,49
	DR81H at pH = 8	0,0018	94,69
	DR81SDE at pH = 6	0,0014	87,32
	DR81SDE at pH = 8	0,0013	82,34
DV51	DV51	0,0308	100
	DV51H at pH = 5,5	0,0137	95,76
	DV51H at pH = 6	0,0071	93,17
	DV51H at pH = 7	0,0053	94,08
	DV51H at pH = 8	0,0043	87,63
	DV51SDE at pH = 6	0,0033	91,65
	DV51SDE at pH = 7	0,0031	82,13
	DV51SDE at pH = 8 (Test 1)	0,0023	79,77
DV51SDE at pH = 8 (Test 2)	0,0022	78,05	
DR23	DR23	0,022	100
	DR23H at pH = 6	0,0137	100
	DR23H at pH = 7	0,0093	99,08
	DR23H at pH = 8	0,0066	98,37
	DR23SLDE at pH = 7	0,0033	98,5
	DR23SDE at pH = 6	0,0024	97,24
	DR23SDE at pH = 7	0,0022	94,92
	DR23SDE at pH = 8	0,0017	87,17

ANNEX VI: COT Results

DYE	NAME	TOC _{INITIAL} (mg/l)	TOC _{FINAL} (mg/l)	% TOC Removal
DY50	DY50	4,821	1,648	65,82
	DY50H at pH = 6	5,018	1,358	72,94
	DY50H at pH = 7	4,932	3,831	22,32
	DY50H at pH = 8	5,100	4,586	10,08
	DY50SDE at pH = 6	5,211	1,205	76,88
	DY50SDE at pH = 7 (Test 1)	4,358	3,606	85,93
	DY50SDE at pH = 7 (Test 2)	5,669	1,330	76,54
	DY50SDE at pH = 8	5,660	2,610	53,89
DR81	DR81	7,320	2,726	62,76
	DR81H at pH = 5,5	8,569	0,399	95,34
	DR81H at pH = 6	8,079	1,392	82,77
	DR81H at pH = 7	7,896	2,542	67,81
	DR81H at pH = 8	6,961	3,363	51,69
	DR81SDE at pH = 6	7,416	4,020	45,79
	DR81SDE at pH = 8	7,918	5,736	27,56
DV51	DV51	4,431	1,342	69,71
	DV51H at pH = 5,5	7,101	3,204	54,88
	DV51H at pH = 6	6,912	2,196	68,23
	DV51H at pH = 7	6,821	8,370	-22,71
	DV51H at pH = 8	3,488	4,080	-16,97
	DV51SDE at pH = 6	4,394	3,455	21,37
	DV51SDE at pH = 7	3,006	5,647	-87,86
	DV51SDE at pH = 8 (Test 1)	3,070	5,061	-64,85
DV51SDE at pH = 8 (Test 2)	3,533	5,379	-52,25	
DR23	DR23	3,446	1,382	59,90
	DR23H at pH = 6	5,612	1,020	81,82
	DR23H at pH = 7	3,991	1,042	73,89
	DR23H at pH = 8	5,130	2,024	60,55
	DR23SLDE at pH = 7	4,879	1,996	59,09
	DR23SDE at pH = 6	4,709	2,511	46,68
	DR23SDE at pH = 7	5,268	2,556	51,48
	DR23SDE at pH = 8	4,902	3,837	21,73

ANNEX VII: Ammonium and nitrates results

DYE	NAME	AMMONIUM (μmol/l)	NITRATES (μmol/l)	TOTAL IONS(μmol/l)	EXPECTED IONS(μmol/l)
DR23	DR23	5,36	7,85	13,21	92,16
	DR23H at pH = 6	9,21	4,42	13,63	92,16
	DR23H at pH = 7	3,14		3,14	92,16
	DR23H at pH = 8	4,66		4,66	92,16
	DR23SLDE at pH = 7	13,33		13,33	92,16
	DR23SDE at pH = 6	6,48		6,48	92,16
	DR23SDE at pH = 7	6,88		6,88	92,16
	DR23SDE at pH = 8	10,78		10,78	92,16
DV51	DV51	13,76	8,89	22,64	34,70
	DV51H at pH = 5,5	19,12	10,78	29,90	34,70
	DV51H at pH = 6	4,46	6,43	10,90	34,70
	DV51H at pH = 7	11,59	5,73	17,31	34,70
	DV51H at pH = 8	36,88		36,88	34,70
	DV51SDE at pH = 6	11,99		11,99	34,70
	DV51SDE at pH = 7	42,44		42,44	34,70
	DV51SDE at pH = 8 (Test 1)	35,97		35,97	34,70
	DV51SDE at pH = 8 (Test 2)	37,63		37,63	34,70
DY50	DY50	1,88	10,04	11,92	52,26
	DY50H at pH = 6	2,11	4,86	6,97	52,26
	DY50H at pH = 7	2,33	6,03	8,36	52,26
	DY50H at pH = 8	1,72	9,39	11,11	52,26
	DY50SDE at pH = 6	0,94		0,94	52,26
	DY50SDE at pH = 7 (Test 1)	2,11		2,11	52,26
	DY50SDE at pH = 7 (Test 2)	2,48		2,48	52,26
	DY50SDE at pH = 8	2,37		2,37	52,26
DR81	DR81	1,44	8,77	10,21	37,00
	DR81H at pH = 5,5	5,17		5,17	37,00
	DR81H at pH = 6	1,92		1,92	37,00
	DR81H at pH = 7	5,93		5,93	37,00
	DR81H at pH = 8	10,02		10,02	37,00
	DR81SDE at pH = 6	22,94		22,94	37,00
	DR81SDE at pH = 8	45,88		45,88	37,00

Data for comparison of plants for germination toxicity tests

	DY50		DR81		DV51		DR23	
TYPE OF SEED	L Init (cm)	L Fin (cm)						
Lettuce	4,3	4,52	4,06	3,95	3,44	4,03	4,07	4,23
Tomatoe	1,44	1,62	1,13	1,08	1,23	1,4	0,87	1,05
Cucumber	3,71	2,4	2,4	4,32	3,12	2,8	2,4	2,1
Watercress	8,16	8,73	8,73	6,29	6,46	6,8	5,99	6,4
Radish	8,07	9,06	9,06	7,51	7,04	7,8	6,57	7,3
Millet	0	0	0	0	0	0	0	0

L Init (cm): average seed length of initial samples.

L Fin (cm): average seed length of final samples.

	DY50		DR81		DV51		DR23	
TYPE OF SEED	Ngerm Init	Ngerm Fin						
Lettuce	11	11	12	12	12	12	12	12
Tomatoe	11	11	12	12	11	11	11	11
Cucumber	10	10	12	12	11	11	9	10
Watercress	12	12	12	12	12	12	12	12
Radish	11	12	10	11	12	12	12	12
Millet	0	0	11	11	0	0	0	0

Ngerm Init: number of germinated seeds in initial samples.

Ngerm Fin: number of germinated seeds in final samples.

ANNEX IX: Toxicity test results

SAMPLE	TYPE	L _{rad} (cm)	L _{hip} (cm)	L _{seed}	N ^o germ	RT	AG	%T _{REMOVAL}	GI
Pure Water EVIAN		1,57	2,67	4,24	12		1		1,00
Salt Water EVIAN		0,61	1,31	1,92	9		0,75		0,31
Pure Water VITTEL		1,43	2,41	3,84	12		1		1,00
Salt Water VITTEL		0,83	1,41	2,24	10		0,83		0,49
DY50	INITIAL	1,69	2,61	4,30	11	14,39	0,92	55,00	0,84
DY50	FINAL	1,67	2,85	4,52	11	6,47	0,92		0,88
DY50H at pH = 6	INITIAL	1,63	2,57	4,20	12	17,99	1	32,00	0,89
DY50H at pH = 6	FINAL	1,82	2,54	4,36	12	12,23	1		0,93
DY50H at pH = 7	INITIAL	1,35	2,50	3,85	12	30,58	1	51,79	0,82
DY50H at pH = 7	FINAL	1,72	2,42	4,14	12	20,14	1		0,88
DY50H at pH = 8	INITIAL	1,37	2,43	3,80	12	32,37	1	30,00	0,81
DY50H at pH = 8	FINAL	1,63	2,44	4,07	12	22,66	1		0,87
DY50SDE at pH = 6	INITIAL	1,33	2,80	4,13	11	20,50	0,92	38,60	0,81
DY50SDE at pH = 6	FINAL	1,33	3,02	4,35	12	12,59	1		0,93
DY50SDE at pH = 7	INITIAL	1,15	2,89	4,04	11	23,74	0,92	-25,76	0,79
DY50SDE at pH = 7	FINAL	1,03	2,84	3,87	12	29,86	1		0,82
DY50SDE at pH = 8	INITIAL	0,89	2,59	3,48	11	43,88	0,92	68,85	0,68
DY50SDE at pH = 8	FINAL	1,54	2,78	4,32	12	13,67	1		0,92
DR81	INITIAL	1,48	2,58	4,06	12	23,02	1	-17,19	0,86
DR81	FINAL	1,26	2,69	3,95	12	26,98	1		0,84
DR81H at pH = 6	INITIAL	1,30	2,39	3,69	12	36,33	1	19,80	0,79
DR81H at pH = 6	FINAL	1,49	2,40	3,89	12	29,14	1		0,83
DR81H at pH = 7	INITIAL	1,30	2,68	3,98	11	25,90	0,92	33,33	0,78
DR81H at pH = 7	FINAL	1,62	2,60	4,22	12	17,27	1		0,90
DR81H at pH = 8	INITIAL	1,15	2,39	3,54	12	41,73	1	35,34	0,75
DR81H at pH = 8	FINAL	1,48	2,47	3,95	12	26,98	1		0,84
DR81SDE at pH = 6	INITIAL	1,45	2,22	3,67	12	37,05	1	74,76	0,78
DR81SDE at pH = 6	FINAL	1,83	2,61	4,44	12	9,35	1		0,94
DR81SDE at pH = 8	INITIAL	1,41	2,37	3,78	12	33,09	1	51,09	0,80
DR81SDE at pH = 8	FINAL	1,55	2,70	4,25	12	16,19	1		0,90
DV51	INITIAL	1,20	2,24	3,44	12	45,32	1	46,83	0,73
DV51	FINAL	1,63	2,40	4,03	12	24,10	1		0,86
DV51H at pH = 6	INITIAL	1,47	2,43	3,90	12	28,78	1	41,25	0,83
DV51H at pH = 6	FINAL	1,78	2,45	4,23	12	16,91	1		0,90
DV51H at pH = 7	INITIAL	1,52	2,41	3,93	11	27,70	0,92	24,68	0,77
DV51H at pH = 7	FINAL	1,79	2,33	4,12	12	20,86	1		0,88
DV51H at pH = 8	INITIAL	1,50	2,43	3,93	11	27,70	0,92	42,86	0,77
DV51H at pH = 8	FINAL	1,76	2,50	4,26	12	15,83	1		0,91
DV51SDE at pH = 6	INITIAL	1,39	2,41	3,80	12	32,37	1	46,67	0,81
DV51SDE at pH = 6	FINAL	1,62	2,60	4,22	12	17,27	1		0,90
DV51SDE at pH = 7	INITIAL	1,32	2,23	3,55	11	41,37	0,92	73,04	0,69
DV51SDE at pH = 7	FINAL	1,72	2,67	4,39	12	11,15	1		0,93
DV51SDE at pH = 8	INITIAL	1,32	2,53	3,85	11	30,58	0,92	36,47	0,75
DV51SDE at pH = 8	FINAL	1,52	2,64	4,16	12	19,42	1		0,89
DR23	INITIAL	1,43	2,64	4,07	12	22,66	1	34,92	0,87
DR23	FINAL	1,46	2,83	4,29	12	14,75	1		0,91
DR23H at pH = 6	INITIAL	1,61	2,41	4,02	12	24,46	1	5,88	0,86
DR23H at pH = 6	FINAL	1,53	2,53	4,06	12	23,02	1		0,86
DR23H at pH = 7	INITIAL	1,47	2,58	4,05	12	23,38	1	95,38	0,86
DR23H at pH = 7	FINAL	1,71	2,96	4,67	12	1,08	1		0,99
DR23H at pH = 8	INITIAL	1,43	2,60	4,03	11	24,10	0,92	46,27	0,79
DR23H at pH = 8	FINAL	1,68	2,66	4,34	12	12,95	1		0,92
DR23SDE at pH = 6	INITIAL	1,27	1,95	3,22	12	53,24	1	43,92	0,69
DR23SDE at pH = 6	FINAL	1,53	2,34	3,87	12	29,86	1		0,82
DR23SDE at pH = 7	INITIAL	1,45	2,17	3,62	12	38,85	1	55,56	0,77
DR23SDE at pH = 7	FINAL	1,49	2,73	4,22	12	17,27	1		0,90
DR23SDE at pH = 8	INITIAL	1,31	1,95	3,26	12	51,80	1	42,36	0,69
DR23SDE at pH = 8	FINAL	1,59	2,28	3,87	12	29,86	1		0,82

